The Dissertation Committee for Nicholas D. Laws
certifies that this is the approved version of the following dissertation:

A Bilevel Modeling Methodology to Optimize the Value of Distributed Energy Resources in Electric Transmission and Distribution Systems

Committee:

Michael E. Webber, Supervisor

Dongmei Chen, Co-Supervisor

Joseph Beaman

Dragan Djurdjanovic

Adam Warren

A Bilevel Modeling Methodology to Optimize the Value of Distributed Energy Resources in Electric Transmission and Distribution Systems

by

Nicholas D. Laws

DISSERTATION

Presented to the Faculty of the Graduate School of

The University of Texas at Austin

in Partial Fulfillment

of the Requirements

for the Degree of

DOCTOR OF PHILOSOPHY

The University of Texas at Austin

December 2023

Acknowledgments

First and foremost I would like to acknowledge my wife Rachel Laws for her unwavering support in this arduous PhD process.

My proposed work truly stands on the shoulders of giants from NREL, leveraging over a decade of research and development related to the REopt platform by the likes of: Dr. Andy Walker, Dr. Kate Anderson, Dylan Cutler, Dan Olis, and Emma Elgqvist. At NREL, I would also like to acknowledge Dr. Adam Warren, Dylan Cutler, and especially Kate Anderson for supporting my growth as a research engineer at NREL. I am also grateful to Hallie Dunham and Dylan Cutler for providing valuable feedback and contributions to the development of the methodology of Research Objective Two.

I am specially grateful to Dr. Michael Webber for welcoming me into the his research group, as well as his salient advice. I also owe a great debt of gratitude to Dr. Maggie Chen; without her advice and instruction my research would be less impactful. Without Dr. Grani Hanasusanto's expertise Research Objective One would not have been possible. And, I would like to thank the whole Webber Energy Group, especially Sarah De Berry-Caperton and Dr. Isabella Gee.

A Bilevel Modeling Methodology to Optimize the Value of Distributed Energy Resources in Electric Transmission and Distribution Systems

Nicholas D. Laws, Ph.D.
The University of Texas at Austin, 2023

Supervisor: Michael E. Webber
Co-Supervisor: Dongmei Chen

The transition of electricity generation from a centralized structure to a more distributed framework in grids across the globe calls for new methods to appropriately value the services that distributed energy resources (DER) can provide. Current methods for valuing DER services account for the grid operator perspective but typically ignore DER owner objectives and constraints. The goal of this dissertation is to develop new methods for valuing distributed energy resources in electricity transmission and distribution systems, with a particular focus on accounting for multiple perspectives. This goal is achieved by developing a new linearization technique for bilevel optimization problems that allows modeling energy system optimization problems at scales that matter. The linearization technique is leveraged to develop a new framework for valuing distributed energy resources in transmission and distribution systems. The proposed framework allows for competing perspectives to be modeled. Furthermore, a new method for creating synthetic electricity price scenarios is developed and its value demonstrated in a stochastic optimization framework.

The current model for valuing electricity generation in deregulated energy markets determines prices from an optimal power flow problem whose objective is to

maximize the social welfare. This work develops a general framework for determining the spatiotemporal value of DER that includes DER owner objectives in concert with maximizing the social welfare. The framework is built in a bilevel program that allows for incorporation of any optimal power flow model as well as replacing the social welfare objective with any value function, such as the objective of a profit-oriented DER aggregator. Special attention is placed on linearizing bilinear products of dispatch and price variables such that the framework can scale to large network models.

The general framework is leveraged to develop a method to assess the techno-economic potential of DER for distribution system upgrade deferrals. The state-of-the-art for valuing DER for distribution system upgrade deferrals is advanced by accounting for DER owner objectives and constraints in concert with system operator goals and constraints. A use-case shows how the framework can be leveraged to value DER for non-wires alternatives. Comparing life cycle costs over 20 years for the system planner, the results show that by valuing DER for non-wires alternatives the DSO can avoid upgrading most of the overloaded components as well as achieve a net present value of nearly $3M relative to the cost of the traditional upgrades. The results also show that the DSO can achieve an additional $1M in net present value when valuing privately owned DER relative to a scenario with utility owned batteries.

Finally, recognizing the need for better representation of the uncertainty in electricity market prices in energy system models, a novel method for generating realistic, synthetic electricity prices is developed. Several weaknesses in the state-of-the-art for stochastic price generation methods are addressed: (1) better characterization of daily and weekly trends is achieved by replacing the mean-reversion component of the stochastic differential equation with an autoregressive integrated moving average

process; (2) the conditional probability of consecutive price-spikes, or "jumps", is captured for the first time by replacing the traditional Poisson process with a generalized point process inspired by brain neuron models; and (3) a more realistic model variance is achieved by replacing the static empirical variance with a Markov process. The new methodology allows researchers and practitioners to evaluate bidding strategies for DER in electricity markets. In addition to accurately modeling historical trends, market behavior that has not been observed can be created by tuning model parameters. The method is exercised with electricity prices from the US ERCOT market and a use-case example is provided for bidding an energy storage unit into the ERCOT market. The results show that accounting for price uncertainty via the synthetic time-series can increase market profits by as much as 47% over a bidding strategy that relies on a deterministic price forecast.

Table of Contents

List of Tables

List of Figures

Acronyms

ARIMA   auto-regressive integrated moving average

BESS   battery energy storage systems
BTM   behind-the-meter

DER   distributed energy resources
DLMP   distributed locational marginal pricing
DSO   distribution system operator

ERCOT   Electric Reliability Council of Texas

FERC   Federal Energy Regulatory Committee

IEEE   Institute of Electrical and Electronics Engineers

LMP   locational marginal pricing

NWA   non-wires alternatives

PV   photovoltaic

SDE   stochastic differential equation

Chapter 1

Introduction

1.1 Overview

The over-arching objective of this dissertation is to develop methods for the optimal integration of distributed energy resources (DER) into electric transmission and distribution systems. Examples of DER include community solar photovoltaic (PV) generators as well as residential rooftop PV systems; grid-interactive energy storage including controllable electric vehicle charging infrastructure; and dispatchable building loads such as aggregated smart thermostats. Current models for optimal grid planning and operations take a single perspective, typically minimizing the total cost of operations for the grid operator. This work advances the state-of-the art for power system planning and operations by developing scalable methods for *multi-perspective* optimization of power systems. A general linearization technique for bilevel optimization programs is developed to make problems at scales that matter tractable. Leveraging the linearization technique, a new bilevel optimization framework is developed for incorporating DER owner perspectives into power system planning tools, thereby allowing power system planners to find least-cost solutions that incentivize DER integration that benefits the system as well as DER investors. Lastly, a new method for generating realistic, stochastic electricity price time-series is developed to improve the representation of price uncertainty in power system models.

1.2 Motivation

With electric vehicle adoption and load electrification accelerating and expected to grow significantly in the coming decade electricity system planners operators are facing a rapidly changing load. Additionally, new government actions like Federal Energy Regulatory Committee (FERC) Order 2222 and the Inflation Reduction Act are encouraging investment in DER, which further challenge the traditionally centralized electricity system model. How to model DER and grid-interactive loads in planning and operational frameworks remains an open question; modeling them poorly can leave us with expensive decisions that we regret as well as discourage cost-efficient operations. However, by leveraging advanced energy system modeling methods such as those developed in this thesis, transmission and distribution system operators can optimally plan, control, and value distributed energy resources, including flexible loads.

Since the restructuring of electricity markets began in the early 1980s [1] and the introduction of locational marginal pricing into large scale power markets in the 1990s researchers have investigated electricity market design optimization problems. From a market participant point-of-view one of the most critical terms in a problem is the price signal (typically in $/MWh) from the market operator multiplied by the energy delivered (MWh) by the participant, which together represent the participant's income in a bulk energy market. When both the price signal and energy delivered are decision variables in a mathematical program then the problem becomes bilinear.

In many electricity markets the price signal to market participants (or generators) is determined as the marginal price of the load balance constraint at any given network node at any given time step. The objective of the market model is to minimize the total cost of energy, which is a proxy for maximizing the social welfare. In

electricity market models the social welfare is typically determined as the benefit to demand minus the total cost of generation. Demand benefits are not captured in practice, though they might include values for reliability or the social cost of carbon for example. The constraints of the market model typically represent an approximation to the power flow equations and take generator cost functions as input.

Equilibrium models allow simulating the electricity market and participant behavior by including the power flow constraints and multiple, competing objective functions. Bilevel or Stackelberg Game formulations are common in electricity market models that include participant objectives, which are typically to maximize profits. The literature has provided a few use-case specific examples for linearizing the bilinear terms of concern, but has not addressed the general conditions necessary for the linearization. **In Research Objective 1 a general method for linearizing the bilinear terms of the price signal and energy delivered is presented, which facilitates the development of a general framework for determining the spatiotemporal value of DER that accounts for DER owner and system operator objectives.** To my knowledge the proposed framework is the first to develop a compensation mechanism for grid support from DER that includes the DER owner perspective while accounting for the social welfare.

DER owned by retail customers, or behind-the-meter (BTM) DER, are expected to drive \$110 billion of investment in the US over 2020-2024, primarily driven by PV rooftop panel systems, adding over 70 GW of capacity for a total expected capacity of 387 GW in 2025 [2].[1] Furthermore, BTM storage energy capacity is expected to grow from 0.7 GWh to 6.2 GWh in 2025, primarily in the form of lithium-ion batteries [2]. An emerging, high value proposition for DER is distribution system up-

---

[1]As of March 2020 the US electricity grid had a total capacity of 1,200 GW [3].

grade deferral by leveraging DER for non-wires alternatives (NWA). Since Federal Energy Regulatory Commission (FERC) Order 1000 [4] bulk power markets have seen widespread acceptance that strategically located generators can provide NWA to traditional "wires" updgrades, such as replacing overly burdened lines or transformers with higher capacity components. With the growing adoption of DER many have argued that customer-sited DER can also provide NWA for distribution system upgrades [5]. However, most distribution system operators (DSO), which are responsible for the long-term planning and short-term operation of the distribution system, do not have a way to value the benefits of DER [6].

Used intelligently, DER can support voltage management, relieve capacity constrained lines or transformers, and avoid power back-feed while increasing hosting capacity. The state-of-the-art for evaluating DER as NWA for distribution system upgrades assumes that customer-sited DER will provide the utility's required services when called upon – and does not account for the DER owner perspective, where the customer may be using the DER to reduce her/his utility bill [7] or increase their energy resilience by meeting critical loads during grid outages [8]. Figure 1.1 shows how the DER owner and distribution system values are stacked, in addition to the transmission system values that DER can offer. **A method to assess the techno-economic potential of DER for NWA, or distribution system upgrade deferrals, is the topic of Research Objective 2 (RO2).**

Since the introduction of FERC Order 2222 in late 2020 transmission system operators and regional transmission organizations have started the process of integrating DER into wholesale electricity markets [9]. Whether DER is owned by third-parties or grid operators, a primary value stream for DER comes from buying and/or selling energy in wholesale electricity markets (energy storage systems
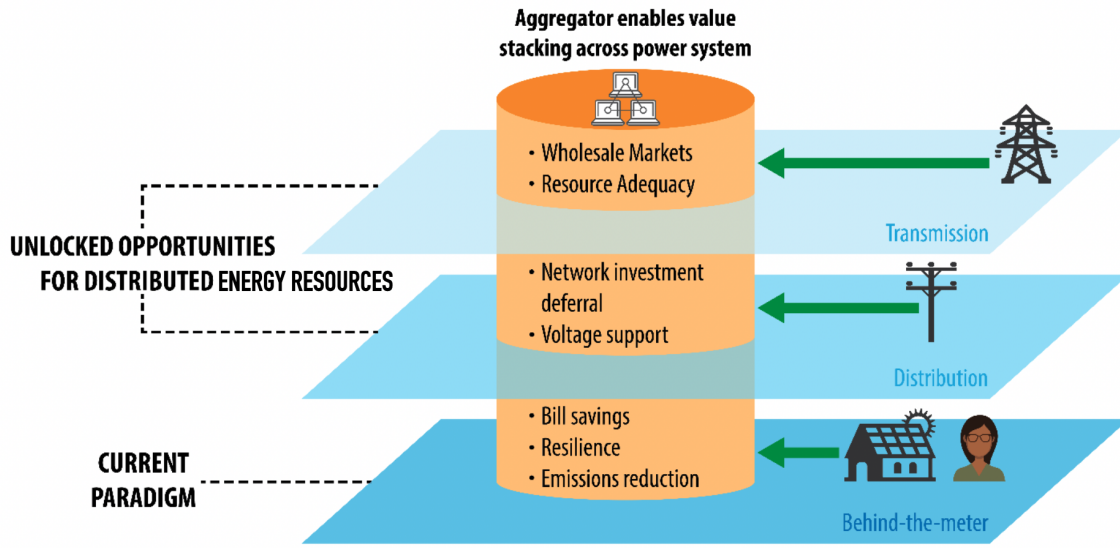
Figure 1.1: The value stack of distributed energy resource (DER) aggregations: the current paradigm only accounts for DER owner value but many other value streams are possible when considering the value that DER can provide for power distribution and transmission system operators. ©NREL.

can do both). Electricity market prices exhibit significant stochasticity and therefore make it difficult to quantify the value that could be achieved with DER in wholesale electricity markets. In recognition of this issue, **a method to generate realistic synthetic electricity market price scenarios is the topic of Research Objective 3 (RO3).**

1.3   Research Objectives

The three research objectives of this work are centered around creating win-win solutions for DER owners and power system operators. First, a general method for linearizing bilinear products of price and dispatch variables is developed to facilitate the solution of large scale bilevel optimization problems. The bilevel framework allows one to account for competing objective functions, forming a Stackelberg Game [10], in which an optimal compromise price signal can be determined. The result of Research

Objective 1 is a general framework for maximizing the social welfare of DER in power systems.

Second, the result of Research Objective 1 is leveraged in Research Objective 2 to size and locate DER in a distribution grid for non-wire alternatives to system upgrades, while accounting for DER owner objectives and constraints. According to a 2018 report from the Rocky Mountain Institute, leveraging DER for non-wire alternatives in the U.S. will unlock an additional $17 billion in system benefits through 2030 [11]. This work seeks to account for both sides of the meter for valuing grid support services from DER, and in doing so will fill a gap in the published literature.

Third, in recognition of the need to account for uncertainty in a primary DER value stream for both system operators and third-party DER owners, Research Objective 3 presents a method to generate synthetic, yet realistic electricity market prices. An example use-case shows how the methodology for generating prices can be leveraged in a stochastic optimization framework for bidding DER into day-ahead and real-time electricity markets.

In summary, the over-arching objective of this work is to develop win-win solutions for the integration of DER into modern electricity grids by accounting for both system operator objectives and DER owner objectives. The specific objectives are to:

RO1 develop a general framework for determining the spatiotemporal value of DER that includes DER owner costs and constraints while maximizing the social welfare;

RO2 develop a method to assess the techno-economic potential of DER for distribution system upgrade deferrals;

RO3 and develop a method to generate realistic synthetic electricity market price scenarios.

This dissertation begins with the relevant background of the three research objectives via the Literature Review in Chapter 2. Next, a chapter is devoted to each research objective. Chapters 3, 4, and 5 provide the theory behind each method and demonstrate their value with use-case examples. Finally, Chapter 6 summarizes the results of the research and closes with suggestions for future research directions.

Chapter 2

Literature Review

The literature review is divided into subsections aligned with the Research Objectives.

2.1 Literature related RO1: To develop a general framework for determining the spatiotemporal value of DER that includes DER owner costs and constraints while maximizing the social welfare

To co-optimize the benefits of distributed energy resources (DER) for DER owners and electricity grid operators one must account for two crucial decisions: the DER owner's decision of how to use their system, also known as the dispatch decision; and the system operator's decision of how to value a service provided by DER, also known as the price decision. The product of these two decisions determines both the DER owner income and the system operator's cost of purchasing a service from a DER owner. Currently, in deregulated wholesale energy markets, the dispatch of bulk power generators and the value of the energy provided are determined from

---

Some sections of this chapter were adapted from the peer-reviewed publication [12]. The majority of the paper's research and writing were completed by the author of this dissertation. The co-author contributed via theoretical development and editing. Some sections of this chapter were also adapted from the journal article: [13]. The majority of this paper's research, analysis, and writing were completed by the author of this dissertation. The co-authors contributed to the background and conclusions. Some sections of this chapter were also adapted from the technical report: [14]. The majority of this paper's research, analysis, and writing were completed by the author of this dissertation. The co-authors contributed to the literature review, editing, writing, and technical development.

some variation of an economic dispatch problem, where the value is known as the "locational marginal price".

The theory and practice of locational marginal pricing (LMP) in electricity markets, also known as optimal spot pricing, began in the early 1980s [15, 16] (motivated by [17] in 1971). Locational marginal pricing is used in many deregulated wholesale electricity markets today and was first implemented in Chile and UK in the 1980s with many more countries following in the 1990s [18]. The premise of optimal spot pricing is built upon an offer-based optimal power flow model. The objective of the model is to maximize the social welfare function, which includes the value of electricity usage (demand benefit) minus the total cost of generation. The problem is subject to energy balance constraints and the network constraints. The energy balance constraints require that the demand is met by generation at each node in the network in each time step[1]. It can be shown that when each generator's offer is equal to its marginal cost of generation then the Lagrange multipliers of the energy balance constraints are the optimal spot prices that simultaneously maximize the social welfare and the generators' profits [15].

The theory of LMP has naturally been extended to electricity distribution systems and follows the same framework as the transmission system model [19, 20, 21]. However, distributed locational marginal pricing (DLMP) has not been implemented outside of academia due to the lack of the communication infrastructure necessary to coordinate such a market, among other factors such as scalability of the models required to determine DLMP.

Both LMP and DLMP models assume that market participants are compensated using the Lagrange multiplier of the load balance constraint in some power flow

---

[1]The network constraints are equivalent to Kirchoff's Voltage and Current Laws.

model. Lagrange multipliers are also known as shadow prices and as *dual variables*. For demonstrative purposes, let λ_j be the price or dual variable at node j and let p_j be the optimal power injected by the market participant at node j. Then the income for the j-th market participant is $\lambda_j p_j$. Because any *single* level mathematical program cannot simultaneously include primal variables (such as p_j) and dual variables, the bilinear $\lambda_j p_j$ term for a market participant's income (or the market operator's cost of purchasing p_j from DER at node j) cannot be modeled in the power flow model used to determine λ_j. Therefore, a single power flow model cannot directly capture the price-responsiveness of DER owners.

Equilibrium models, on the other hand, allow modeling the electricity market and participant behavior by including the power flow constraints and multiple, competing objective functions. Bilevel or Stackelberg Game formulations are common in electricity market models that include participant objectives, which are typically to maximize profits, i.e. the income $\lambda_j p_j$ minus a cost of generation $c_j p_j$, where c_j represents a cost per unit of energy. The general bilevel problem is intractable but when the lower level problem is linear then the upper and lower level problems can be combined into a tractable single level problem [22]. However, to co-optimize the price signal λ_j for the market operator and DER owners, bilinear terms of price and dispatch decision variables are required. Fortunately, some researchers have been able to find problem specific methods to linearize these bilinear terms [23, 24, 25, 26].

Ruiz *et al.* 2009 [23] is the earliest known example to demonstrate that bilinear terms for market price and participant dispatch can be linearized. Their model places the market participant in the upper level, which chooses its offer curve for energy generation, while the lower level models the electricity market given the other participants' offer curves. Fernandez-Blanco *et al.* 2016 [24] is the first to find a

linearization for the same bilinear terms (products of lower level primal and dual variables) in the upper level of a bilevel program for revenue adequacy constraints. More recently, Naebi *et al.* 2020 [27] forms a bilevel problem to optimize the bidding strategy of a microgrid owner in a day ahead market. The upper level minimizes operating costs from the microgrid owner's perspective with the product of its exported power and the dual variable of the lower level, linear power flow load balance in its objective. (In other words, the microgrid operator knows its impact on the market price). The lower level minimizes the system operator's cost, including the payment to the microgrid owner, subject to linear power flow constraints. Xu *et al.* 2020 [28] proposes a bilevel model in which the upper level represents a coalition of PV system owners that can sell excess power to the grid or to other consumers. The upper level objective contains a bilinear product of the price to charge consumers and the level of excess PV production to be sold. The lower level objective is the sum of the PV owners' cost functions, which contain the benefit of selling excess PV and the cost of consuming grid power. The bilinear product of price and dispatch variables is linearized by setting the lower level primal objective equal to the dual objective. Additional problem specific examples of the linearization technique can be found in [25] and [26].

Each of the aforementioned examples presents problem-specific examples of how the bilinear products of shadow prices and dual variables can be linearized in bilevel problems using Strong Duality Theorem [29]. This thesis presents a general method for linearizing the bilinear terms of interest and determines the exact conditions under which the bilinear terms can be linearized in general bilevel problems. The method is implemented in an open source *Julia* module for mathematical programming that allows researchers to write their bilevel problems in an intuitive fashion ([30], which extends [31]). After showing the linearization method I present some

simple and complex use-case examples to demonstrate the value of the linearization method for power system planning research questions. In the complex use-case, with a power flow model, I show that the linearization method makes otherwise intractable problems solvable in a matter of minutes. Using the open source module other researchers can take advantage of the linearization method for any bilevel problem with bilinear products of shadow prices and dispatch variables of interest.

As part of Research Objective 1, a general method for linearizing bilinear products of lower level primal and dual variables in the upper level of bilevel optimization problems will be developed. The linearization method is especially relevant for modeling large scale energy distribution systems with many stakeholders and is therefore applicable to a growing number of problems as energy markets expand and adapt to new regulations such as FERC Order 2222 [10] and the increasing adoption of distributed energy resources [11]. By publishing the general linearization method it is hoped that more use cases will be discovered for the linearization technique beyond energy market models. Additionally, the linearization method (detailed in Section 3) is leveraged in Research Objective 2.

2.2 Literature related to RO2: To develop a method to assess the techno-economic potential of DER for distribution system upgrade deferrals

Early evaluations of DER for non-wires alternatives compared costs and benefits of known DER capacities and locations against capacity upgrade costs [32]. A common theme in the literature for valuing DER as non-wires alternatives accounted for the single perspective of the distribution system operator (DSO). For example, Contreras-Ocana *et al.* developed a model that puts DER costs and benefits in competition with upgrade deferrals from a single perspective, at a single location (substation

12

or transformer) with forecasted overloads [33]. By neglecting power flow constraints they were able to account for many types of DER including energy efficiency investments. However, without a network model the DER are presumably installed at the single, overloaded location.

The valuable work by Andrianesis *et al.* demonstrates how to determine a locational marginal value (LMV) of DER in a three step process, where the value of DER is determined relative to the locational marginal cost of traditional system upgrades [7]. The method in [7] also only accounts for the DSO perspective, implicitly assuming that DER will behave in a manner that best suits the system operator's cost function and constraints. Furthermore, it is assumed that the LMV is sufficient to motivate DER investment and that the LMV will not motivate behavior that leads to greater operating costs or the need for additional system upgrades.

The work by Garcia-Santacruz *et al.* is perhaps the first to account for both the DSO and DER owner perspectives when valuing DER for non-wires alternatives [34]. The DSO perspective is represented by minimizing energy losses in a relaxed branch flow model [35]. The DER owner perspective is represented by maximizing a DER utilization factor, i.e. minimizing the amount of energy curtailed. The system losses and DER utilization factors are combined in a single cost function with weighting factors that must be selected by the planner. To make their problem tractable, only 24 hours of loading is modeled, which prevents representation of the full value proposition of DER.

The work in [36] employs a bilevel model to account for the competing perspectives of the DSO and DER owners. Their work looks at planning electric vehicle (EV) charging stations within a distribution network. However, their approach does not include a value signal from the DSO to DER owners and requires that all cost

coefficients are known. They modeled 48 hours of load in each of the four years modeled and used a Genetic Algorithm (GA) to solve the bilevel problem. Similar work on EV charging station integration employed a multi-objective function and a GA to produce a pareto set of solutions, but also does not include any value signal from the DSO [37].

The work in [38] uses a tri-level model and a novel solution technique to optimize system planner and DER owner objectives. However their method also does not include any value signal from the DSO.

The recent work by Kabirifar *et al.* leverages a bilevel model for distribution system planning while accounting for DER investor decisions [39]. By placing the power flow model in the lower level problem (and using a linear power flow approximation) they include distribution locational marginal prices as compensation to DER investors, whose net present cost is constrained to be less than zero (i.e. profit) in the upper level. The upper level minimizes the system capital and operating costs; while the lower level minimizes the total cost of power in a distribution market. Their framework requires knowledge of DER price bids for every time step in the planning horizon, as well as requires that the power flow model is a linear approximation.

The method presented in this dissertation also uses a bilevel model to represent the DSO and DER perspectives. The proposed framework for valuing DER as non-wires alternatives allows system planners to determine the minimum compensation required to motivate DER investment that minimizes the DSO's cost function. The framework does not require knowledge of DER owner bidding functions nor does it require a linear power flow model. The framework determines a co-optimal, spatiotemporal price signal that simultaneously minimizes DSO costs while guaranteeing the DER owners' financial returns. No ad-hoc weighting factors of the competing ob-

jectives are required. The proposed framework can be used to determine the optimal locations and capacities of both utility-owned and third-party-owned DER subject to power flow constraints, which is demonstrated with a use-case example. The example uses a year of hourly loads, which accounts for the full value proposition of DER for non-wires alternatives.

2.3 Literature related to RO3: To develop a method to generate realistic synthetic electricity market price scenarios

In their comprehensive review of electricity price forecasting [40], Weron identifies five main categories of price forecasting: multi-agent (including game theoretic and production cost models), fundamental/structural models, reduced-form quantitative/stochastic models, statistical or econometric models, and artificial intelligence-based models. Additionally, Weron notes that many of the approaches fall into a "hybrid" category where two or more categories are combined. The developed price model is a hybrid of reduced-form stochastic and statistical models.

The jump-diffusion model is a special case of a general stochastic differential equation. The jump-diffusion model draws heavily from risk management finance literature on price dynamics and derivatives [40]. Mean-reversion, spot price spikes, and non-normality characteristics observed in stock markets are even more pronounced in electricity markets [41]. Electricity markets are unique in that the commodity being traded cannot be easily stored for long periods of time. This constraint creates a system that is highly reactive to small changes in supply and demand. Electricity is traded on a spot market, which is based on day-ahead prices [42]. Trading based on day-ahead prices allows the system operator to verify that supply will meet demand in the next market period.

Weron et al. uses two separate approaches to model the "jumpy" character of spot prices in electricity markets [42]. One approach adds a jump term to a mean-reverting diffusion-type stochastic differential equation (SDE), with the assumption that a negative jump always follows a positive one. This approach reflects the authors' observation that spikes usually only last one day. The second approach, which can handle spikes that last multiple time steps, uses a Markov chain with two states: a base state and a spike state. Each state is modeled by an independent price process, one mean-reverting and one log-normal. Both spike models are fit to data from which an annual sinusoidal term and a week-long moving average term have been subtracted. A key contribution to the mean-reverting jump diffusion approach comes from Cartea and Figueroa [41]. In contrast to Weron et al. [42], only weekly periodicity is removed from the price data (by subtracting the mean of data corresponding to the same day of the week). Deterministic annual seasonality is modeled with a time-varying mean reversion equilibrium. Cartea and Figueroa demonstrate that stripping spikes from electricity price data improves the result of a normality test dramatically, which makes a jump-diffusion approach applicable [41].

Geman and Roncoroni [43] propose a similar model to Cartea and Figueroa [41] with two main differences. First, instead of assuming that every positive jump is followed by a downward jump, they introduce a jump sign that is dependent on the current price (+1 if below a threshold, -1 if above). Second, they introduce a separate threshold above which the probability of a spike increases. Benth et al. compares the mean-reverting jump-diffusion model in Cartea, and Figueroa [41] to the threshold variation in [43], and a third approach previously proposed by Benth et al. [44]. The latter is a multi-factor model made up of a superposition of Ornstein-Uhlenbeck processes. Hayfavi and Talasli [45] propose an alternative multifactor model combining deterministic seasonality terms, Brownian motion, and three jump processes. One is

16

an Ornstein-Uhlenbeck type process that reverts in the next time step after a jump, another is an Ornstein-Uhlenbeck process with slower mean reversion that takes a few time steps, and the third is a pure jump process that captures long term jump effects.

Weron proposes the idea of non-homogenous Poisson processes in [46], but is not able to fully apply this method due to lack of data to fit the model. The non-homogeneous approach considers arrival rates indexed on time of year and does not consider how spike probability also depends on prices in preceding hours, which is an important dependency in day-ahead pricing.

Borovkova and Schmeck [47] present another jump-diffusion variation that employs stochastic time change, which transforms the price distribution to be closer to Gaussian using the "activity rate". They build from prior research demonstrating a positive correlation between demand and the occurrence of price spikes and use temperature (as a proxy for demand) as the driving factor in the activity rate for the stochastic time change. The resulting model captures similar key characteristics as the jump-diffusion models described above (e.g., seasonality, mean reversion, and spikes) and uses the stochastic time change to incorporate exogenous variables such as temperature as a proxy for electricity demand.

Most of the literature described above has focused on forecasting of daily average spot prices rather than hourly day-ahead or sub-hourly real-time pricing. A review article by Lago et al. summarizing state-of-the-art algorithms in day-ahead price forecasting [48] identified that most of the recent research has primarily been in statistical models and deep learning models. Lago et al. note that the leading statistical models are generally autoregressive yet utilize least absolute shrinkage and selection operator (LASSO) or elastic nets for model estimation and feature selection

17

tools (e.g., the LASSO Estimated AutoRegressive model) and employ variance stabilizing tools. The leading deep learning models generally fall into the category of deep neural network, recurrent neural network, or convolution network with multiple levels and long short-term memory components [48]. While many of these models have shown promising improvements in point forecast accuracy, they are not focused on generating stochastic price scenarios and capturing the total uncertainty in the market. The proposed model combines recent learnings from the statistical model space into a hybrid model with the reduced-form stochastic approach.

Finally, while the literature review is focused on price forecasting, note that the work herein does not aim to create a better forecast of hourly pricing. Rather this work develops a methodology for capturing the uncertainty inherent in the market, generating thousands of potential realizations of future prices, and applying those synthetic price scenarios to bidding models. There is a dearth of adequate data for testing bidding approaches where the underlying time series exhibit high periodicity and heavy tails. Even with the increased collection and curation of large time series datasets, any available datasets that have these qualities are of limited use for testing, calibrating, and vetting time series models [49]. It is imperative that time series modeling and forecasting approaches use diverse training/testing data to be generalizable to future data realizations, especially as market conditions shift [49] [50].

Chapter 3

A general framework for determining the spatiotemporal value of DER that includes DER owner costs and constraints while maximizing the social welfare

By leveraging recent advances in bilevel programming and developing a general linearization method for bilinear products of primal dispatch decisions and dual price variables a general framework is developed for determining the spatiotemporal value of DER that includes DER owner costs and constraints while maximizing the social welfare.

As part of Research Objective 1 a general method for linearizing bilinear terms of dual and primal variables in a bilevel program is developed. The method also accounts for linearizing bilinear products of upper and lower level primal variables in the lower level objective. These bilinear terms represent the product of the price signal selected by the upper level market operator and the dispatch variable selected by the lower level DER owner. This method is applied in Research Objective 2, which demonstrates the usefulness of the linearization method for appropriately valuing DER for social welfare maximization.

This chapter was adapted from the journal article [12]. The majority of this paper's research, analysis, and writing were completed by the author of this dissertation. The majority of the paper's research and writing were completed by the author of this dissertation. The co-author contributed via theoretical development and editing.

By modeling the optimal power flow problem in a bilevel framework one is able to account for the objectives and constraints of DER owners in an electricity market. Typically, it is assumed that the dispatch decisions of power generators are made by the market coordinator or system operator, rather than the generator owners. This is a valid assumption in bulk power transmission markets where generator owners seek only to maximize profits. However, it is not appropriate to assume that DER owners, (especially residential DER owners), will fully surrender control of their DER to a centralized dispatcher.

3.1   Methodology

The general framework consists of a bilevel problem with bilinear terms in the upper and lower level objectives and linear lower level constraints:

$$\min_{\boldsymbol{x} \in \mathcal{R}^M, \boldsymbol{y} \in \mathcal{R}^N} \; f(\boldsymbol{x}, \boldsymbol{y}) + \boldsymbol{\lambda}^{\mathsf{T}} \boldsymbol{A} \boldsymbol{y} \tag{3.1a}$$

$$\text{s.t. } g(\boldsymbol{x}, \boldsymbol{y}) \le 0, \tag{3.1b}$$

$$\boldsymbol{y} \in \arg\min_{\boldsymbol{y} \in \mathcal{R}^N} \; \boldsymbol{c}^{\mathsf{T}} \boldsymbol{y} + \boldsymbol{x}^{\mathsf{T}} \boldsymbol{B} \boldsymbol{y} \tag{3.1c}$$

$$\text{s.t.} \qquad \underline{\boldsymbol{y}} \le \boldsymbol{y} \quad (\underline{\boldsymbol{\mu}}) \tag{3.1d}$$

$$\boldsymbol{y} \le \overline{\boldsymbol{y}} \quad (\overline{\boldsymbol{\mu}}) \tag{3.1e}$$

$$\boldsymbol{U}\boldsymbol{x} + \boldsymbol{V}\boldsymbol{y} = \boldsymbol{w} \quad (\boldsymbol{\lambda}). \tag{3.1f}$$

Table 3.1 summarizes the terms in Equation 3.1. Note that the linearization method developed in this work is also valid for bilinear terms of $\boldsymbol{\lambda}$ and $\boldsymbol{y}$ in the upper level constraints, but they are not shown for clarity.

Table 3.1: Sets, indices, parameters, and decision variables for Equation 3.1, the general bilevel framework.

Decision Variables

$\boldsymbol{x} \in \mathcal{R}^M$	upper level, primal decision variables
$\boldsymbol{y} \in \mathcal{R}^N$	lower level, primal decision variables
$\boldsymbol{\lambda} \in \mathcal{R}^J$	lower level, dual variables for equality constraints
$\overline{\boldsymbol{\mu}} \in \mathcal{R}^N_+$	lower level, non-negative, dual variables for upper bounds
$\underline{\boldsymbol{\mu}} \in \mathcal{R}^N_+$	lower level, non-negative, dual variables for lower bounds

Parameters

$\boldsymbol{c} \in \mathcal{R}^N$	lower level cost coefficients for lower level decisions $\boldsymbol{y}$
$\boldsymbol{U} \in \mathcal{R}^{J \times M}$	lower level equality constraint coefficients for upper level decisions x
$\boldsymbol{V} \in \mathcal{R}^{J \times N}$	lower level equality constraint coefficients for lower level decisions $\boldsymbol{y}$
$\boldsymbol{w} \in \mathcal{R}^J$	lower level equality constraints right-hand-side
$\overline{\boldsymbol{y}} \in \mathcal{R}^N$	upper bounds for lower level, primal decision variables
$\underline{\boldsymbol{y}} \in \mathcal{R}^N$	lower bounds for lower level, primal decision variables
$\boldsymbol{A} \in \mathcal{R}^{J \times N}$	upper level coefficients for bilinear terms of lower level primal and dual variables
$\boldsymbol{B} \in \mathcal{R}^{M \times N}$	lower level coefficients for bilinear terms of lower level primal and upper level primal variables

Sets and Indices

$\mathcal{A}$	$\{(j,n) \in \mathcal{J} \times \mathcal{N} : A_{jn} \neq 0\}$
$\mathcal{A}_\mathcal{J}$	$\{j \in \mathcal{J} : \exists n \in \mathcal{N} \text{ such that } A_{jn} \neq 0\}$
$\mathcal{A}_\mathcal{N}$	$\{n \in \mathcal{N} : \exists j \in \mathcal{J} \text{ such that } A_{jn} \neq 0\}$
$\mathcal{J}$	$1, 2, \ldots, J$, $|\mathcal{J}| = $ number of lower level equality constraints
$\mathcal{J}_j \subseteq \mathcal{J}$	indices of lower level equality constraints connected to constraint j via non-zero values of $\boldsymbol{V}$, i.e. the constraints that share variables with constraint j and the constraints that share variables with those constraints (and so on recursively as described in Algorithm 1).
$\mathcal{J}_\cup$	$\bigcup_{j \in \mathcal{A}_\mathcal{J}} \mathcal{J}_j$
$\mathcal{M}$	$1, 2, \ldots, M$, $|\mathcal{M}| = $ number of upper level variables
$\mathcal{N}$	$1, 2, \ldots, N$, $|\mathcal{N}| = $ number of lower level variables
$\mathcal{N}_n \subseteq \mathcal{N}$	indices of lower level variables connected to variable y_n via non-zero values of $\boldsymbol{V}$
$\mathcal{N}_\cup$	$\bigcup_{n \in \mathcal{A}_\mathcal{N}} \mathcal{N}_n$
$\mathcal{AB}_\mathcal{N}$	$\{n \in \mathcal{A}_\mathcal{N} : \exists m \in \mathcal{M} \text{ such that } B_{mn} \neq 0\}$
$\mathcal{AB}$	$\{(j,n) \in \mathcal{A} : \exists m \in \mathcal{M} \text{ such that } B_{mn} \neq 0\}$
$\varnothing$	The empty set
$\mathcal{Z}$	The set of integers

In the upper level objective (3.1a) the system operator or DER aggregator seeks to minimize its cost function f (which might include the cost of wholesale power

purchased at the feeder for example) plus the payments made to DER owners, represented by $\boldsymbol{\lambda}^{\mathsf{T}}\boldsymbol{A}\boldsymbol{y}$. By minimizing the total cost of power in the network the system operator maximizes the social welfare. The $\boldsymbol{A}$ matrix selects the appropriate lower level dual variables $\boldsymbol{\lambda}$ from the DER owner power balance constraints and the lower level primal variables $\boldsymbol{y}$ for the power injected by each DER owner. The constraint set (3.1b) represents Kirchoff's Voltage and Current Laws, or an approximation as appropriate.

The lower level objective (3.1c) represents a linear cost function for all DER owners (capturing investment and operating costs for example) and a bilinear term $\boldsymbol{x}^{\mathsf{T}}\boldsymbol{B}\boldsymbol{y}$ for the income from selling DER services to the upper level. The $\boldsymbol{B}$ matrix selects the price signal decisions from the upper level and the power export decisions from the lower level. Constraints (3.1d) and (3.1e) represent the lower and upper bounds on the lower level decisions, with the dual variables shown in parantheses. These constraints might represent comfort bounds on temperature decision variables for example. Constraints (4.1e) include all of the lower level operational constraints including each node's power balance constraint, which can be separate from the upper level's optimal power flow load balance in (3.1b). For example, the upper level load balance will include line flows into and out of each node, where as the lower level load balance only accounts for the load balance behind the meter.

The linearization algorithm is applicable when the upper level and/or the lower level problems are non-linear in constraints or objectives. However, the lower level constraints that include the lower level variables from the upper level bilinear terms must be linear to get an exact linearization of the upper level bilinear terms. Futhermore, we assume that the lower level problem is linear in its decision variables (given the upper level decisions) so that we can replace the lower level with its Karush

Kuhn Tucker conditions to show single level problem equivalents to the non-linear bilevel problems of interest.

We begin by assuming that the upper level variables $\boldsymbol{x}$ are integer such that any product of integer $\boldsymbol{x}$ and the continuous variables $\boldsymbol{y}$ or $\boldsymbol{\lambda}$ can be made linear using binary expansion [51][1]. In the sequel we relax the integer assumption to account for continuous upper level $\boldsymbol{x}$ variables in the bilinear products, which requires stricter conditions than the integer $\boldsymbol{x}$ case for the exact linearization.

3.1.1 Linearization Method with Integer Upper Level Variables

To linearize any $\lambda_j y_n$ term one must combine the lower level primal and dual constraints. The dual formulation of the lower level problem is shown below for reference.

$$\max_{\overline{\boldsymbol{\mu}}, \underline{\boldsymbol{\mu}} \in \mathcal{R}_+^N, \boldsymbol{\lambda} \in \mathcal{R}^J} \underline{\boldsymbol{y}}^T \underline{\boldsymbol{\mu}} - \overline{\boldsymbol{y}}^T \overline{\boldsymbol{\mu}} + (\boldsymbol{w} - \boldsymbol{U}\boldsymbol{x})^T \boldsymbol{\lambda} \tag{3.2a}$$

$$\text{s.t.} \quad \boldsymbol{V}^T \boldsymbol{\lambda} = \boldsymbol{c} + \overline{\boldsymbol{\mu}} - \underline{\boldsymbol{\mu}} + \boldsymbol{B}^T x \tag{3.2b}$$

The first step is to multiply the lower level primal constraints (4.1e) by $\boldsymbol{\lambda}$ component-wise:

$$\boldsymbol{V}\boldsymbol{y} \circ \boldsymbol{\lambda} = \boldsymbol{w} \circ \boldsymbol{\lambda} - \boldsymbol{U}\boldsymbol{x} \circ \boldsymbol{\lambda} \tag{3.3}$$

where $\circ$ denotes the Hadamard product.[2]

Second, the dual constraints (3.2b) are multiplied with $\boldsymbol{y}$ as follows:

$$(\boldsymbol{V}^\intercal \boldsymbol{\lambda}) \circ \boldsymbol{y} = \boldsymbol{c} \circ \boldsymbol{y} + \overline{\boldsymbol{\mu}} \circ \boldsymbol{y} - \underline{\boldsymbol{\mu}} \circ \boldsymbol{y} + (\boldsymbol{B}^\intercal \boldsymbol{x}) \circ \boldsymbol{y}. \tag{3.4}$$

---

[1]It is important to note that in some cases good bounds, which are necessary for the "big M" constraints used to linearize the product of integer and continuous variables, cannot be found [52].

[2]Note that one can also multiply each of the primal constraints by each of the components of $\boldsymbol{\lambda}$ to get J^2 equations. However, in practice the bilinear terms that appear in the upper level problem are bilinear in y_n and λ_j, where λ_j is the Lagrange multiplier of the constraint that involves y_n.

Note that any $\bar{\mu}_n y_n$ can be linearized because of the upper bound

$$y_n \le \bar{y}_n. \tag{3.5}$$

The complementary slackness condition for (3.5) allows one to linearize $\bar{\mu}_n y_n$:

$$\bar{\mu}_n y_n = \bar{\mu}_n \bar{y}_n. \tag{3.6}$$

A similar result follows for any $\underline{\mu}_n y_n$. Combining the last result with the complementary slackness conditions gives:

$$(\boldsymbol{V}^{\mathsf{T}} \boldsymbol{\lambda}) \circ \boldsymbol{y} = \boldsymbol{c} \circ \boldsymbol{y} + \bar{\boldsymbol{\mu}} \circ \bar{\boldsymbol{y}} - \underline{\boldsymbol{\mu}} \circ \underline{\boldsymbol{y}} + (\boldsymbol{B}^{\mathsf{T}} \boldsymbol{x}) \circ \boldsymbol{y}. \tag{3.7}$$

Equations (3.3) and (3.7) are then combined to produce a system of equations with the bilinear products of $\boldsymbol{\lambda}$ and $\boldsymbol{y}$ as the unknowns. In the following we show how to solve for a specific $\lambda_j V_{jn} y_n$.

Let the ith row of (3.3) be defined as (P_i), which can be written:

$$(P_i) : \lambda_i V_{in} y_n = w_i \lambda_i - \lambda_i \sum_{k \in \mathcal{N} \backslash \{n\}} V_{ik} y_k - \lambda_i \sum_{m \in \mathcal{M}} U_{im} x_m \tag{3.8}$$

And, let the kth row of (3.7) be defined as (D_k), which can be written:

$$(D_k) : y_k \sum_{i \in \mathcal{J}} V_{ik} \lambda_i = c_k y_k + \bar{\mu}_k \bar{y}_k - \underline{\mu}_k \underline{y}_k + y_k \sum_{m \in \mathcal{M}} B_{mk} x_m \tag{3.9}$$

Note that the choice of P for (P_i) and D for (D_k) are intentional: P is for *primal* constraints and D is for *dual* constraints.

Algorithm 1 outlines the procedure for determining the minimum set of the (P_i) and (D_k) equations needed to linearize a given $\lambda_j y_n$ term. Note that the algorithm refers to the indices of (P_i) as rows and (D_k) as columns because the sums over V_{jk} in (3.8) and (3.9) are over the rows and columns of $\boldsymbol{V}$ respectively.

24

The first step of Algorithm 1 is to check if V_{jn} is the only non-zero value in the nth column of $\boldsymbol{V}$: in this case (D_n) provides the exact linearization of $\lambda_j y_n$ (and (P_i) is unnecessary):

$$y_n \lambda_j = \frac{1}{V_{jn}} \left(c_n y_n + \overline{\mu}_n \overline{y}_n - \underline{\mu}_n \underline{y}_n + y_n \sum_{m \in \mathcal{M}} B_{mn} x_m \right) \tag{3.10}$$

Note that (3.10) only applies under the condition that y_n is in a single lower level primal constraint. Additionally, the bilinear products of y_n and x_m in (3.10) can be linearized since we are assuming that $\boldsymbol{x}$ is integer in this section.

In the second step of Algorithm 1 the first primal equation (P_j) is added to the set of row indices that will be returned at the end of the algorithm (where j is an input). Additionally, for all the non-zero values in the jth row of $\boldsymbol{V}$, except V_{jn}, the indices of the dual equations (D_k) are added to the set of column indices. In mathematical terms, this step is taking (P_j):

$$\lambda_j V_{jn} y_n = w_j \lambda_j - \lambda_j \sum_{k \in \mathcal{N} \setminus \{n\}} V_{jk} y_k - \lambda_j \sum_{m \in \mathcal{M}} U_{jm} x_m \tag{3.11}$$

and all of the (D_k) equations for $k \in \mathcal{N} \setminus \{n\}$ in order to replace the bilinear terms of λ_j and y_k on the right-hand-side of (3.11). Each (D_k) equation can add more bilinear terms of $\boldsymbol{\lambda}$ and $\boldsymbol{y}$ and so step three of Algorithm 1 adds additional equations if necessary.

In the third and final step of Algorithm 1 a recursive function, Algorithm 2, is used to search the array $\boldsymbol{V}$ for non-zero, "connected" values. We use the term "connected" to indicate that one could draw horizontal and vertical paths through $\boldsymbol{V}$ to connect non-zero entries to the first entry of interest V_{jn}, starting with a horizontal line each time. A horizontal line adds a (P_i) equation and a vertical line adds a (D_k) equation. The indices of the rows and columns are collected until a sufficient amount of equations are obtained to linearize the $\lambda_j y_n$ term in the upper level objective.

25

Note that Algorithm 2 is similar to — but not the same as — finding the blocks of a block-diagonal matrix. The difference is that Algorithm 2 does not necessarily find *all* of the non-zero values in a block. In other words, one does not need all of the (P_i) and (D_k) equations that may be available; one only needs as many equations as unknowns (where the unknowns are products of $\boldsymbol{\lambda}$ and $\boldsymbol{y}$ entries). Algorithm 2 has

---

Algorithm 1: Minimum set of equations to linearize $\lambda_j y_n$

    input : The 2D array V; and the integers (j, n) of non-zero V_{jn}.
    output: Indices of (P_i) and (D_k) necessary to linearize a $\lambda_j y_n$ term.
    1. **if** $V_{j'n} = 0 \ \forall j' \in \mathcal{J} \setminus \{j\}$ **then**
       | **return** $\{\},\{n\}$ (only need D_n)
    end
    2. Initialize arrays of integers for the rows and columns:
        $\mathcal{J}_j = \{j\}$
        cols_to_check $= \{k \in \mathcal{N} \setminus \{n\} : V_{jk} \neq 0\}$
        $\mathcal{N}_n = \text{copy(cols\_to\_check)}$
    3. Recursive search to find all connections
    foreach k *in cols_to_check* **do**
        rows, *cols* = recursive_array_search(V, j, k, {}, {})
        $\mathcal{J}_j \leftarrow \mathcal{J}_j \cup rows$
        $\mathcal{N}_n \leftarrow \mathcal{N}_n \cup cols$
    end
    return $\mathcal{J}_j, \mathcal{N}_n$

---

some conditions under which it returns an error: these errors occur when the search has indicated that redundant row or column indices should be appended to the final vectors. Mathematically, these errors indicate that there are more unknowns than equations and thus the system of equations is underdetermined.

Let the indices of (P_i) and (D_k) returned from Algorithm 1 for a given $(j, n) \in$

Algorithm 2: recursive_array_search

input : The 2D array V; integers row j and column k; and two vectors of integers to append to: *rows* and *cols*.

output: Two vectors of integers for the non-zero entries of V connected to row j and column k.

$rs = \{\, j' \in \mathcal{J} \setminus \{j\} : V_{j'k} \neq 0 \,\}$

if $rs \cap rows \neq \emptyset$ **then**
  | **return** error: redundant row
end

$rows \leftarrow rows \cup rs$

foreach $r \in rs$ **do**
  | $cs = \{\, k' \in \mathcal{N} \setminus \{k\} : V_{rk'} \neq 0 \,\}$
  | **if** $\{cs \cap cols\} \neq \emptyset$ **then**
  | | **return** error: redundant column
  | **end**
  | $cols \leftarrow cols \cup cs$
  | **foreach** $c \in cs$ **do**
  | | recursive_array_search(V, r, c, *rows*, *cols*)
  | **end**
end

return *rows*, *cols*

$\mathcal{A}$ pair be defined as $\mathcal{J}_j$ and $\mathcal{N}_n$ respectively. The exact linearization of $\lambda_j y_n$ is:

$$
\lambda_j y_n = \frac{1}{V_{jn}} \left[\sum_{j' \in \mathcal{J}_j} \left(w_{j'} \lambda_{j'} - \lambda_{j'} \sum_{m \in \mathcal{M}} U_{j'm} x_m \right) \right.
$$
$$
- \sum_{n' \in \mathcal{N}_n} \left(c_{n'} y_{n'} + \overline{\mu}_{n'} \overline{y}_{n'} - \underline{\mu}_{n'} \underline{y}_{n'} \right.
$$
$$
\left. \left. + y_{n'} \sum_{m \in \mathcal{M}} B_{mn'} x_m \right) \right],
$$

(3.12)

which is simply a combination of (3.8) and (3.9) for all of the non-zero values of $\boldsymbol{V}$ connected to $\lambda_j y_n$, as demonstrated with the examples in Appendix B.

Finally, using the result (3.12) the mixed integer linear form of (3.1) is:

$$
\min_{\boldsymbol{x}, \boldsymbol{y}, \boldsymbol{\lambda}, \overline{\boldsymbol{\mu}}, \underline{\boldsymbol{\mu}}} \; f(\boldsymbol{x}, \boldsymbol{y})
$$
$$
+ \sum_{(j,n) \in \mathcal{A}} \frac{A_{jn}}{V_{jn}} \left[\sum_{j' \in \mathcal{J}_j} \left(w_{j'} \lambda_{j'} - \lambda_{j'} \sum_{m \in \mathcal{M}} U_{j'm} x_m \right) \right.
$$
$$
- \sum_{n' \in \mathcal{N}_n} \left(c_{n'} y_{n'} + \overline{\mu}_{n'} \overline{y}_{n'} - \underline{\mu}_{n'} \underline{y}_{n'} \right.
$$
$$
\left. \left. + y_{n'} \sum_{m \in \mathcal{M}} B_{mn'} x_m \right) \right]
$$

(3.13a)

$$
\text{s.t. } g(\boldsymbol{x}, \boldsymbol{y}) \leq 0, \tag{3.13b}
$$

$$
\boldsymbol{c} + \boldsymbol{B}^{\mathsf{T}} \boldsymbol{x} + \boldsymbol{V}^{\mathsf{T}} \boldsymbol{\lambda} + \overline{\boldsymbol{\mu}} - \underline{\boldsymbol{\mu}} = \boldsymbol{0} \tag{3.13c}
$$

$$
\underline{\boldsymbol{y}} \leq \boldsymbol{y} \leq \overline{\boldsymbol{y}} \tag{3.13d}
$$

$$
\boldsymbol{U}\boldsymbol{x} + \boldsymbol{V}\boldsymbol{y} = \boldsymbol{w} \tag{3.13e}
$$

$$
\overline{\boldsymbol{\mu}} \perp (\boldsymbol{y} - \overline{\boldsymbol{y}}) \tag{3.13f}
$$

$$
\underline{\boldsymbol{\mu}} \perp (\underline{\boldsymbol{y}} - \boldsymbol{y}) \tag{3.13g}
$$

where the lower level problem has been replaced with the Karush Kuhn Tucker (KKT) conditions and the complementary constraints can be modeled as special order sets or using the "big M" method from [53]. Note that this section assumes that the $\boldsymbol{x}$

variables are integer and therefore the products of x_m and y_n or λ_j can be linearized using binary expansion [51].

It is important to note that finding valid values for the "big M" can be difficult [54]. The open source package in which the linearization method presented in this paper is implemented includes the options to use big M (Fortuny-McCarl) constraints, special order sets, or indicator constraints to linearize the complementary conditions used to integrate the lower level problem into the upper level. The latter two methods do not require defining bounds for the dual variables, but may be more difficult to solve than the "big M" method.

3.1.2 Linearization Method with Continuous Upper Level Variables

In Section 5.1 we assumed that $\boldsymbol{x}$ are integer such that all of the products of x_m and y_n or products of x_m and λ_j can be linearized using binary expansion [51]. Here we show the conditions under which a $\lambda_j y_n$ term can be linearized when the upper level variables $\boldsymbol{x}$ are continuous.

The conditions are divided into two groups with one group less restrictive than the other. The first group of conditions is less restrictive but does not allow lower level variables $\boldsymbol{y}$ to be bilinear in both the upper level problem with $\boldsymbol{\lambda}$ and the lower objective with $\boldsymbol{x}$. In mathematical terms this is when $\mathcal{AB} = \emptyset$, where $\mathcal{AB} \triangleq \{(j, n) \in \mathcal{A} : \exists m \in \mathcal{M} \text{ such that } B_{mn} \neq 0\}$.

The second group of conditions allows a problem to be linearized when bilinear products of $\lambda_j y_n$ are in the upper level *and* bilinear products of $x_m y_n$ are in the lower level objective for a given n. These types of problems are particularly relevant to energy system market models, in which the upper and lower level bilinear products together represent a zero-sum game. Demonstrative examples are provided in Section

3.2, in which the upper level products of $\lambda_j y_n$ represent payments to distributed generator owners and the lower level products of $x_m y_n$ represent generator owner income.

3.1.2.1 Conditions when $\mathcal{AB} = \emptyset$

Recall that the Algorithms 1 and 2 provide the sets $\mathcal{J}_j$ for each λ_j in the upper level objective. Let $\mathcal{J}_\cup \triangleq \bigcup_{j \in \mathcal{A}_\mathcal{J}} \mathcal{J}_j$, which includes the indices of all the lower level constraints that are connected (via non-zero values of $\boldsymbol{V}$) to the λ_j terms in the upper level objective. Therefore, in order to eliminate all bilinear terms of the form $\lambda_j U_{jm} x_m$ in (3.13a) the following condition must be met:

Condition 1. $U_{jm} = 0 \; \forall j \in \mathcal{J}_\cup, \; \forall m \in \mathcal{M}$

Similar to Condition 1, let $\mathcal{N}_\cup \triangleq \bigcup_{n \in \mathcal{A}_\mathcal{N}} \mathcal{N}_n$, then one could assume that

Condition 2. $B_{mn} = 0 \; \forall m \in \mathcal{M}, \; \forall n \in \mathcal{N}_\cup$

to eliminate all bilinear terms of the form $x_m B_{mn} y_n$ from (3.13a). Under Conditions

1 and 2 the mixed integer result for (3.1) is

$$
\min_{\boldsymbol{x},\boldsymbol{y},\boldsymbol{\lambda},\overline{\boldsymbol{\mu}},\underline{\boldsymbol{\mu}}} f(\boldsymbol{x},\boldsymbol{y}) + \sum_{(j,n)\in\mathcal{A}} \frac{A_{jn}}{V_{jn}} \left[\sum_{j'\in\mathcal{J}_j} (w_{j'}\lambda_{j'}) \right. \tag{3.14a}
$$
$$
\left. - \sum_{n'\in\mathcal{N}_n} \left(c_{n'}y_{n'} + \overline{\mu}_{n'}\overline{y}_{n'} - \underline{\mu}_{n'}\underline{y}_{n'} \right) \right]
$$
$$
\text{s.t. } g(\boldsymbol{x},\boldsymbol{y}) \le 0, \tag{3.14b}
$$
$$
\boldsymbol{c} + \boldsymbol{B}^{\mathsf{T}}\boldsymbol{x} + \boldsymbol{V}^{\mathsf{T}}\boldsymbol{\lambda} + \overline{\boldsymbol{\mu}} - \underline{\boldsymbol{\mu}} = \boldsymbol{0} \tag{3.14c}
$$
$$
\underline{\boldsymbol{y}} \le \boldsymbol{y} \le \overline{\boldsymbol{y}} \tag{3.14d}
$$
$$
\boldsymbol{U}\boldsymbol{x} + \boldsymbol{V}\boldsymbol{y} = \boldsymbol{w} \tag{3.14e}
$$
$$
\overline{\boldsymbol{\mu}} \perp (\boldsymbol{y} - \overline{\boldsymbol{y}}) \tag{3.14f}
$$
$$
\underline{\boldsymbol{\mu}} \perp (\underline{\boldsymbol{y}} - \boldsymbol{y}) \tag{3.14g}
$$

3.1.2.2 Conditions when $\mathcal{A}\mathcal{B} \ne \varnothing$

The case when Condition 2 is violated and Problem (3.1) has bilinear terms in the upper and lower level objectives of the form $\lambda_j A_{jn} y_n$ and $x_m B_{mn} y_n$, (where $A_{jn} \ne 0$ and $B_{mn} \ne 0$), for some n is particularly relevant to energy system market models. For example, take the case where $A_{jn} = 1$ and $B_{mn} = -1$ for some particular m, j, and n. Let y_n represent a lower level generator dispatch decision. Then λ_j represents the marginal cost of the dispatch decision y_n as well as the upper level's cost of purchasing power from the lower level. And $-x_m y_n$ in the lower level objective is the lower level's income for the generation y_n using the price signal x_m. Section 3.2 provides an example of such a scenario. Thus it is useful to investigate the linearization of problems when $\mathcal{A}\mathcal{B} \ne \varnothing$ (i.e. when Condition 2 is violated).

The problem of interest has the following structure:

$$\min_{\boldsymbol{x},\boldsymbol{y}} f(\boldsymbol{x},\boldsymbol{y}) + \sum_{(j,n)\in\mathcal{A}} \lambda_j A_{jn} y_n \tag{3.15a}$$

$$\text{s.t. } g(\boldsymbol{x},\boldsymbol{y}) \leq 0 \tag{3.15b}$$

$$\boldsymbol{y} \in \arg\min_{\boldsymbol{y}} \ \boldsymbol{c}^\mathsf{T}\boldsymbol{y} + \sum_{m\in\mathcal{M}}\sum_{n\in\mathcal{A}_\mathcal{N}} x_m B_{mn} y_n$$
$$+ \sum_{m\in\mathcal{M}}\sum_{n\in\mathcal{N}\setminus(\mathcal{A}_\mathcal{N}\cup\mathcal{N}_\cup)} x_m B_{mn} y_n \tag{3.15c}$$

$$\text{s.t. } \quad \underline{\boldsymbol{y}} \leq \boldsymbol{y} \quad (\underline{\boldsymbol{\mu}}) \tag{3.15d}$$

$$\boldsymbol{y} \leq \overline{\boldsymbol{y}} \quad (\overline{\boldsymbol{\mu}}) \tag{3.15e}$$

$$\sum_{n\in\mathcal{N}} V_{jn} y_n = w_j \quad (\lambda_j), \quad \forall j \in \mathcal{J}_\cup \tag{3.15f}$$

$$\sum_{m\in\mathcal{M}} U_{jm} x_m + \sum_{n\in\mathcal{N}} V_{jn} y_n = w_j \quad (\lambda_j),$$
$$\forall j \in \mathcal{J} \setminus \mathcal{J}_\cup. \tag{3.15g}$$

Note that the products of $\boldsymbol{x}$ and $\boldsymbol{y}$ in the lower level objective (3.15c) are linearized when the lower level problem is replaced with the KKT conditions. And the set of y_n for all $n \in \mathcal{N} \setminus (\mathcal{A}_\mathcal{N} \cup \mathcal{N}_\cup)$ in the last sum of (3.15c) are the values of $\boldsymbol{y}$ that are *not* in the upper level objective nor connected to the $y_n, n \in \mathcal{A}_\mathcal{N}$, in the upper level objective. Recall that the connected indices are provided by Algorithm 1 and captured in $\mathcal{N}_\cup$. We will show shortly that the connected y_n values must not be in the lower level objective with $\boldsymbol{x}$ terms to prevent $y_n x_m$ terms from showing up in the (D_k) equations needed to linearize the $\lambda_j y_n$ in the upper level objective. Also, Condition 1 is reflected in (3.15f).

Now, applying Condition 1 to (3.12) gives

$$\lambda_j y_n = \frac{1}{V_{jn}} \left[\sum_{j'\in\mathcal{J}_j} w_{j'}\lambda_{j'} - \sum_{n'\in\mathcal{N}_n} \left(c_{n'} y_{n'} + \overline{\mu}_{n'}\overline{y}_{n'} \right. \right.$$
$$\left. \left. -\underline{\mu}_{n'}\underline{y}_{n'} + y_{n'} \sum_{m\in\mathcal{M}} B_{mn'} x_m \right) \right], \quad \forall(j,n) \in \mathcal{A}. \tag{3.16}$$

32

We wish to eliminate the $y_{n'} B_{mn'} x_m$ terms when $\mathcal{AB} \neq \emptyset$. Recall that the $y_{n'} B_{mn'} x_m$ terms in (3.12) and (3.16) come from the (D_k) equations with $B_{mk} \neq 0$, and that the (D_k) equations for all $k \in \mathcal{N}_\cup$ are necessary to linearize the upper level $\lambda_j A_{jk} y_k$ terms.

Let us assume that a less restrictive version of Condition 2 holds:

Condition 2′. $B_{mn} = 0 \ \forall m \in \mathcal{M}, \ \forall n \in \mathcal{N}_\cup \setminus \mathcal{A}_\mathcal{N}$

Condition 2′ implies that none of the lower level variables *connected* to the $\lambda_j A_{jn} y_n$ terms (provided by Algorithm 1) are in the lower level objective with $y_n B_{mn} x_m$ terms, except the lower level variables in the upper level objective ($y_n \ \forall n \in \mathcal{A}_\mathcal{N}$). Applying Condition 2′ to (3.16) gives:

$$
\lambda_j y_n = \frac{1}{V_{jn}} \left[\sum_{j' \in \mathcal{J}_j} w_{j'} \lambda_{j'} \right.
$$
$$
- \sum_{n' \in \mathcal{N}_n \setminus \mathcal{A}_\mathcal{N}} \left(c_{n'} y_{n'} + \overline{\mu}_{n'} \overline{y}_{n'} - \underline{\mu}_{n'} \underline{y}_{n'} \right)
$$
$$
- \sum_{n' \in \mathcal{N}_n \cap \mathcal{A}_\mathcal{N}} \left(c_{n'} y_{n'} + \overline{\mu}_{n'} \overline{y}_{n'} - \underline{\mu}_{n'} \underline{y}_{n'} \right.
$$
$$
\left. \left. + y_{n'} \sum_{m \in \mathcal{M}} B_{mn'} x_m \right) \right], \ \forall (j, n) \in \mathcal{A}. \quad (3.17)
$$

Let us also assume that Condition 3 holds:

Condition 3. $\mathcal{A}_\mathcal{N} \setminus \{n\} \subseteq \mathcal{N}_n \ \forall n \in \mathcal{A}_\mathcal{N}$

$$
\Rightarrow \mathcal{N}_n \cap \mathcal{A}_\mathcal{N} = \mathcal{A}_\mathcal{N} \setminus \{n\} \ \forall n \in \mathcal{A}_\mathcal{N}
$$

Condition 3 implies that the $y_n \ \forall n \in \mathcal{A}_\mathcal{N}$ variables of interest are connected to each other via non-zero values of $\boldsymbol{V}$. Section 3.2.2 provides an example problem, in which the $y_n \ \forall n \in \mathcal{A}_\mathcal{N}$ are indexed on time and connected to each other via another

time-indexed variable in each equality constraint that is restricted to be no more than a certain value across all time.

Condition 3 allow us to rewrite (3.17) as

$$\lambda_j y_n = \frac{1}{V_{jn}} \left[\sum_{j' \in \mathcal{J}_j} w_{j'} \lambda_{j'} \right.$$
$$- \sum_{n' \in \mathcal{N}_n \setminus \mathcal{A}_\mathcal{N}} \left(c_{n'} y_{n'} + \overline{\mu}_{n'} \overline{y}_{n'} - \underline{\mu}_{n'} \underline{y}_{n'} \right)$$
$$- \sum_{n' \in \mathcal{A}_\mathcal{N} \setminus \{n\}} \left(c_{n'} y_{n'} + \overline{\mu}_{n'} \overline{y}_{n'} - \underline{\mu}_{n'} \underline{y}_{n'} \right.$$
$$\left. \left. + y_{n'} \sum_{m \in \mathcal{M}} B_{mn'} x_m \right) \right], \ \forall (j, n) \in \mathcal{A}. \quad (3.18)$$

Applying (3.9) to the last summation in (3.18) gives:

$$\lambda_j y_n = \frac{1}{V_{jn}} \left[\sum_{j' \in \mathcal{J}_j} w_{j'} \lambda_{j'} \right.$$
$$- \sum_{n' \in \mathcal{N}_n \setminus \mathcal{A}_\mathcal{N}} \left(c_{n'} y_{n'} + \overline{\mu}_{n'} \overline{y}_{n'} - \underline{\mu}_{n'} \underline{y}_{n'} \right)$$
$$\left. - \sum_{n' \in \mathcal{A}_\mathcal{N} \setminus \{n\}} \left(y_{n'} \sum_{j' \in \mathcal{J}} V_{j'n'} \lambda_{j'} \right) \right], \ \forall (j, n) \in \mathcal{A}, \quad (3.19)$$

This step is key to eliminating the bilinear $y_{n'} B_{mn'} x_m$ terms when $\mathcal{AB} \neq \varnothing$. The next steps are to impose conditions that allow us to move the last summation in (3.19) to the left hand side to get a single sum of terms over the set $\mathcal{A}$.

Let us assume that Condition 4 holds:

Condition 4. $V_{j'n} = 0 \ \forall j' \in \mathcal{J} \setminus \{j\}, \ \forall (j, n) \in \mathcal{A}$.

Condition 4 is equivalent to each y_n for all $n \in \mathcal{A}_\mathcal{N}$ being in only one lower level constraint. Condition 4 implies that

$$y_k \sum_{j' \in \mathcal{J}} V_{j'k} \lambda_{j'} = \lambda_j V_{jk} y_k, \ \forall (j, k) \in \mathcal{A} \quad (3.20)$$

34

Note that Condition 4 requires that Step 1 of the Algorithm be skipped. The revised algorithm for Conditions 1, 2′, 3, and 4 is shown in Algorithm 3.

Algorithm 3: Minimum set of equations to linearize $\lambda_j y_n$ under Conditions 1, 2′, 3, and 4

    input : The 2D array V; and the integers (j, n) of non-zero V_{jn}.
    output: Indices of (P_i) and (D_k) necessary to linearize a $\lambda_j y_n$ term.

1. Initialize arrays of integers:
    $\mathcal{J}_j = \{j\}$
    cols_to_check $= \{k \in \mathcal{N} \setminus \{n\} : V_{jk} \neq 0\}$
    $\mathcal{N}_n = \text{copy}(\text{cols\_to\_check})$

2. Recursive search to find all connections
foreach k *in cols_to_check* **do**
    $rows, cols = \text{recursive\_array\_search}(V, j, k, \{\}, \{\})$
    $\mathcal{J}_j \leftarrow \mathcal{J}_j \cup rows$
    $\mathcal{N}_n \leftarrow \mathcal{N}_n \cup cols$
end
return $\mathcal{J}_j$, $\mathcal{N}_n$

Condition 4 allows us to write (3.19) as

$$
\lambda_j y_n = \frac{1}{V_{jn}} \left[\sum_{j' \in \mathcal{J}_j} w_{j'} \lambda_{j'} \right.
$$
$$
- \sum_{n' \in \mathcal{N}_n \setminus \mathcal{A}_\mathcal{N}} \left(c_{n'} y_{n'} + \overline{\mu}_{n'} \overline{y}_{n'} - \underline{\mu}_{n'} \underline{y}_{n'} \right)
$$
$$
\left. - \sum_{(j',n') \in \mathcal{A} \setminus \{(j,n)\}} \left(y_{n'} V_{j'n'} \lambda_{j'} \right) \right], \quad \forall (j,n) \in \mathcal{A}, \quad (3.21)
$$

Rearranging (3.21) gives:

$$
\sum_{(j',n') \in \mathcal{A}} \lambda_{j'} V_{j'n'} y_{n'} = \sum_{j' \in \mathcal{J}_j} w_{j'} \lambda_{j'}
$$
$$
- \sum_{n' \in \mathcal{N}_n \setminus \mathcal{A}_\mathcal{N}} \left(c_{n'} y_{n'} + \overline{\mu}_{n'} \overline{y}_{n'} - \underline{\mu}_{n'} \underline{y}_{n'} \right), \quad \forall (j,n) \in \mathcal{A}. \quad (3.22)
$$

Note that since (3.22) is valid for all $(j, n) \in \mathcal{A}$ it implies that $\mathcal{N}_n$ are equal for all $n \in \mathcal{A}_\mathcal{N}$ and that $\mathcal{J}_j$ are equal for all $j \in \mathcal{A}_\mathcal{J}$.

35

Lastly, we see that to replace $\sum_{(j,n)\in\mathcal{A}} \lambda_j A_{jn} y_n$ with the last result for $\sum_{(j,n)\in\mathcal{A}} \lambda_j V_{jn} y_n$ we must require that the two sums are equal to a proportionality constant p:

Condition 5. $A_{jn} = pV_{jn} \ \forall (j,n) \in \mathcal{A}$

$$\Rightarrow \sum_{(j,n)\in\mathcal{A}} \lambda_j A_{jn} y_n = p \sum_{(j,n)\in\mathcal{A}} \lambda_j V_{jn} y_n.$$

With Condition 5 we can write (3.22) as:

$$\sum_{(j,n)\in\mathcal{A}} \lambda_j A_{jn} y_n = p \left[\sum_{j'\in\mathcal{J}_j} w_{j'} \lambda_{j'} \right.$$

$$\left. - \sum_{n'\in\mathcal{N}_n\backslash\mathcal{A}_\mathcal{N}} \left(c_{n'} y_{n'} + \overline{\mu}_{n'} \overline{y}_{n'} - \underline{\mu}_{n'} \underline{y}_{n'} \right) \right] \quad \forall (j,n) \in \mathcal{A}. \quad (3.23)$$

Substituting (3.23) into (3.1) and replacing the lower level with the KKT conditions, under Conditions 1, 2′, 3, 4 and 5 the mixed integer result is shown in (3.24). Note that any $(j,n) \in \mathcal{A}$ can be used in (3.24a) to define the sets $\mathcal{J}_j$ and $\mathcal{N}_n$.

$$\min_{\boldsymbol{x},\boldsymbol{y},\boldsymbol{\lambda},\overline{\boldsymbol{\mu}},\underline{\boldsymbol{\mu}}} \ f(\boldsymbol{x},\boldsymbol{y}) + p\left[\sum_{j'\in\mathcal{J}_j}(w_{j'}\lambda_{j'})\right.$$

$$\left. - \sum_{n'\in\mathcal{N}_n\backslash\mathcal{A}_{\mathcal{N}}}\left(c_{n'}y_{n'} + \overline{\mu}_{n'}\overline{y}_{n'} - \underline{\mu}_{n'}\underline{y}_{n'}\right)\right] \tag{3.24a}$$

$$\text{s.t. } g(\boldsymbol{x},\boldsymbol{y}) \le 0, \tag{3.24b}$$

$$\boldsymbol{c} + \boldsymbol{B}^{\mathsf{T}}\boldsymbol{x} + \boldsymbol{V}^{\mathsf{T}}\boldsymbol{\lambda} + \overline{\boldsymbol{\mu}} - \underline{\boldsymbol{\mu}} = \boldsymbol{0} \tag{3.24c}$$

$$\underline{\boldsymbol{y}} \le \boldsymbol{y} \tag{3.24d}$$

$$\boldsymbol{y} \le \overline{\boldsymbol{y}} \tag{3.24e}$$

$$\boldsymbol{U}\boldsymbol{x} + \boldsymbol{V}\boldsymbol{y} = \boldsymbol{w} \tag{3.24f}$$

$$\overline{\boldsymbol{\mu}} \perp (\boldsymbol{y} - \overline{\boldsymbol{y}}) \tag{3.24g}$$

$$\underline{\boldsymbol{\mu}} \perp (\underline{\boldsymbol{y}} - \boldsymbol{y}) \tag{3.24h}$$

To summarize all of the conditions under which (3.24) is valid:

- Condition 1: $U_{jm} = 0 \ \forall j \in \mathcal{J}_{\cup}, \ \forall m \in \mathcal{M}$

  – None of the connected constraints contain $\boldsymbol{x}$ terms.

- Condition 2': $B_{mn} = 0 \ \forall m \in \mathcal{M}, \ \forall n \in \mathcal{N}_{\cup} \setminus \mathcal{A}_{\mathcal{N}}$

  – None of the connected variables are multiplied with $\boldsymbol{x}$ in the lower level objective, except the $\boldsymbol{y}$ in the upper level objective that are multiplied with $\boldsymbol{\lambda}$.

- Condition 3: $\mathcal{A}_{\mathcal{N}} \setminus \{n\} \subseteq \mathcal{N}_n \ \forall n \in \mathcal{A}_{\mathcal{N}}$

  – Each of the y_n in the upper level objective are connected to each other via non-zero values of $\boldsymbol{V}$.

37

- Condition 4 $V_{j'n} = 0 \ \forall j' \in \mathcal{J} \setminus \{j\}, \ \forall j \in \mathcal{A}_{\mathcal{J}}$

    - Each of the y_n in the upper level objective are in only one lower level equality constraint.

- Condition 5 $A_{jn} = pV_{jn} \ \forall (j, n) \in \mathcal{A}$

    - All of the coefficients of the upper level $\lambda_j y_n$ terms are proportional to the corresponding coefficients in the lower level constraints to the same constant p.

The examples in Section 3.2 meet the Conditions 1, 2′, 3, 4 and 5. Both problems consist of an energy market model with a load balance constraint in the lower level, bilinear products in the upper level objective of lower level dispatch variables and the load balance dual variables, and bilinear products in the lower level objective of upper level price signal variables and the same lower level dispatch variables as in the upper level objective.

3.1.3 A note on separable lower level problems

It is important to note that the conditions required to linearize the bilinear products of shadow prices and primal variables can be applied to sub-matrices when the lower level problem is separable. For example, in a multi-follower Stackelberg game the lower level is likely to be separable, such as when modeling multiple distributed energy resource (DER) owners or grid customers. In these cases Conditions 3 and 5 should be checked against the blocks of $\boldsymbol{A}$ and $\boldsymbol{V}$ corresponding to each sub-problem. An example of a separable lower level problem is provided in Section 3.2

3.2 Use-case examples

It is important to note that the use of the linearization algorithm is not limited to the problem types shown in these examples. Indeed, the conditions required for the linearization algorithm are met in each of the references mentioned in Section 2.1. For example, other use cases include:

- optimizing generator offer curves in an energy market [23];

- applying generator revenue constraints in a market clearing process [24];

- and optimal profit sharing in a community microgrid [25].

3.2.1 Simple examples without time indices

The first use-case example shows a step-by-step linearization process for a scenario in which the upper level model minimizes the total cost of power with the option to purchase power from the bulk system or from customer owned DER. The lower level can choose to meet its demand from the grid at some retail rate or invest

in DER to lower its total cost.

$$\min_{\boldsymbol{x},\boldsymbol{y}} c_{\text{LMP}}x_0 + \lambda y_e \tag{3.25a}$$

$$\text{s.t. } x_0 + y_e - y_i - d_2 = 0 \tag{3.25b}$$

$$x_\lambda \geq 0 \tag{3.25c}$$

$$0 \leq y_e \perp y_i \geq 0 \tag{3.25d}$$

$$\boldsymbol{y} \in \arg\min_{\boldsymbol{y}} \ c_{\text{DER}}y_{\text{DER}} + c_i y_i - x_\lambda y_e \tag{3.25e}$$

$$\text{s.t. } y_i - y_e + y_{\text{DER}} = d_1 \quad (\lambda) \tag{3.25f}$$

$$\overline{y}_{\text{DER}} \geq y_{\text{DER}} \geq 0, \ (\overline{\mu}_{\text{DER}}, \underline{\mu}_{\text{DER}}) \tag{3.25g}$$

$$\overline{y}_e \geq y_e \geq 0 \ (\overline{\mu}_e, \underline{\mu}_e) \tag{3.25h}$$

$$\overline{y}_i \geq y_i \geq 0 \ (\overline{\mu}_i, \underline{\mu}_i). \tag{3.25i}$$

In example (3.25) the upper level (UL) can purchase power x_0 at the feeder head at the wholesale price c_{LMP} and/or from the lower level (LL) at a price of the UL's choosing. The UL chooses x_λ to set the LL's marginal cost of power λ when the LL chooses to export power y_e ("e" for export). The LL considers buying power y_i from grid at the retail rate c_i ("i" for import) and/or purchasing the DER capacity y_{DER} at the cost c_{DER} to meet its demand d_1. Constraint (3.25b) is the system load balance, which includes an uncontrollable demand d_2 (in practice this constraint is replaced with a power flow model). Constraint (3.25d) is the UL enforcement of no simultaneous export and import[3]. Constraint (3.25f) is the LL's load balance. The lower level dual variables, μ_{DER}, μ_e, and μ_i, are show in parentheses.

Let $\boldsymbol{y} \triangleq [y_e, y_i, y_{\text{DER}}]^\intercal$. The lower level has one equality constraint, making $\boldsymbol{V} = [-1 \ 1 \ 1]$. In this case we wish to linearize the product λy_e, making the indices of

---

[3]Allowing simultaneous power import and export would require two isolated meters: one measuring demand and one measuring DER production.

interest $j = 1$ for the first and only equality constraint in the lower level, and $n = 1$ because we put y_e in the first index of $\boldsymbol{y}$.

First, let us check the linearization conditions for this problem. Note that the set $\mathcal{AB}$ is not empty because we have a bilinear term in the upper and lower level objectives of the form $\lambda_j A_{jn} y_n$ and $x_m B_{mn} y_n$. Thus, we must check the Conditions 1, 2′, 3, 4, and 5. To check the conditions we need the sets $\mathcal{J}_\cup$, $\mathcal{N}_\cup$, $\mathcal{A}$ and their sub-sets $\mathcal{J}_j$, $\mathcal{N}_n$, $\mathcal{A}_\mathcal{N}$. With $\mathcal{N} = \{1, 2, 3\}$ for the three LL variables and $\mathcal{J} = \{1\}$ for the single LL constraint, we get:

- $\mathcal{A} = \{(j, n) \in \mathcal{J} \times \mathcal{N} : A_{jn} \neq 0\} = \{(1, 1)\}$

- $\mathcal{A}_\mathcal{N} = \{n \in \mathcal{N} : \exists j \in \mathcal{J} \text{ such that } A_{jn} \neq 0\} = \{1\}$

With only one pair of (j, n) in $\mathcal{A}$ we only need to call Algorithm 3 once with the values for $\boldsymbol{V}$, $j = 1$, and $n = 1$. Algorithm 3 first initializes $\mathcal{J}_1 = \{1\}$ and defines the cols_to_check as $\{2, 3\}$ because $V_{1,2}$ and $V_{1,3}$ are non-zero. The cols_to_check is copied to start the set $\mathcal{N}_1$ and then the recursive search is started. The recursive search loops over the values in cols_to_check and calls Algorithm 2, appending the results to the sets $\mathcal{J}_1$ and $\mathcal{N}_1$. In this case no new non-zero values are found (there is only one row in $\boldsymbol{V}$) and so Algorithm 2 returns the values that it was provided. Finally, Algorithm 3 returns the sets $\mathcal{J}_1 = \{1\}$ and $\mathcal{N}_1 = \{2, 3\}$.

Now, since we only have one pair of (j, n) in $\mathcal{A}$ the union sets $\mathcal{J}_\cup$ and $\mathcal{N}_\cup$ are equal to the sets $\mathcal{J}_1$ and $\mathcal{N}_1$ respectively. With the necessary sets defined we can use (3.23) to linearize the product of λ and y_e in the UL objective:

$$
\begin{aligned}
\lambda_e(-1)y_e &= d_1\lambda - (c_g y_{\text{DER}} + \overline{y}_{\text{DER}}\overline{\mu}_{\text{DER}} + c_i y_i + \overline{y}_i\overline{\mu}_i) \\
\Rightarrow \lambda y_e &= c_{\text{DER}} y_{\text{DER}} + \overline{y}_{\text{DER}}\overline{\mu}_{\text{DER}} + c_i y_i + \overline{y}_i\overline{\mu}_i - d_1\lambda.
\end{aligned}
\tag{3.26}
$$

With this last result, we replace the lower level problem in (3.25) with its KKT conditions to get the mixed integer linear program:

$$\min_{\boldsymbol{x},\boldsymbol{y}} c_{\text{LMP}}x_0 + c_{\text{DER}}y_{\text{DER}} + \overline{y}_{\text{DER}}\overline{\mu}_{\text{DER}} + c_i y_i + \overline{y}_i\overline{\mu}_i - d_1\lambda \tag{3.27a}$$

$$\text{s.t. } x_0 + y_e - y_i - d_2 = 0 \tag{3.27b}$$

$$x_\lambda \geq 0 \tag{3.27c}$$

$$0 \leq y_e \perp y_i \geq 0 \tag{3.27d}$$

$$y_i - y_e + y_{\text{DER}} = d_1 \quad (\lambda) \tag{3.27e}$$

$$y_{\text{DER}} \geq 0, y_e \geq 0, y_i \geq 0 \tag{3.27f}$$

$$-x_\lambda + \lambda - \mu_e = 0 \tag{3.27g}$$

$$c_i - \lambda - \mu_i = 0 \tag{3.27h}$$

$$c_{\text{DER}} - \lambda - \mu_{\text{DER}} = 0 \tag{3.27i}$$

$$0 \leq y_{\text{DER}} \perp \underline{\mu}_{\text{DER}} \geq 0 \tag{3.27j}$$

$$0 \leq y_e \perp \underline{\mu}_e \geq 0 \tag{3.27k}$$

$$0 \leq y_i \perp \underline{\mu}_i \geq 0 \tag{3.27l}$$

$$y_{\text{DER}} - \overline{y}_{\text{DER}} \perp \overline{\mu}_{\text{DER}} \geq 0 \tag{3.27m}$$

$$y_e - \overline{y}_e \perp \overline{\mu}_e \geq 0 \tag{3.27n}$$

$$y_i - \overline{y}_i \perp \overline{\mu}_i \geq 0 \tag{3.27o}$$

Example (3.25) (and its mixed-integer linear version (3.27)) is useful for showing how DER can benefit system operators. First, let us assume that the DER system has a relatively high cost of 10 $/MW when compared to the other cost values, which are $c_{\text{LMP}} = 1$ $/MW, $c_i = 1$ $/MW, $d_1 = 1$ MW, and $d_2 = 2$ MW. In this case it is not in the LL's interest to buy DER and so $y_{\text{DER}} = 0$ and the LL purchases all of its power $d_1 = 1$ from the grid. Also, the UL purchases all power from the bulk system

at $c_{\text{LMP}} = 1$ to meet the total demand $d_1 + d_2 = 3$ MW. Therefore, the UL's cost is $3 and the LL's cost is $1.

Now, let us assume that the DER system cost is equivalent to the other cost values at 1 $/MW. The LL can now meet its demand for equivalent costs from either the grid or from a DER system. However, it is in the UL's best interest for demand to be met by the LL's DER system because the UL can lower its total cost from $3 to $2 by paying the LL $2 for exporting excess DER power in to the grid to meet demand d_2 instead of meeting the total demand $d_1 + d_2$ from the bulk system. Therefore, the UL chooses $x_\lambda = 1$ $/MW, which incentivizes the LL to purchase $y_{\text{DER}} = 3$ MW. The LL meets its demand $d_1 = 1$ MW behind-the-meter and exports 2 MW, which meets demand $d_2 = 2$ MW (and $x_0 = 0$ MW). The LL's cost is $1 (the same as in the high DER cost scenario), but the UL reduces its cost from $3 to $2.

In summary, in this simple demonstration, only when the marginal cost of power from DER for the LL is less than (or equal to) retail rate will the LL purchase DER, which allows the UL to purchase excess power. When the LL can export excess power, and the UL can lower its total cost by purchasing DER exports, the UL will set the LL's marginal cost of power by choosing the minimum compensation rate to incentivize the LL to export the optimal amount of power that minimizes the total system cost of power. Note that in practice the decision variables are indexed on time; and, with solar PV as a DER option, there can be times when the LL has a zero marginal cost of power. Therefore, determining the DER solutions in practice are not as simple as comparing the cost coefficients.

3.2.2 Complex example with separable lower level problem

In this planning example we have a distribution system planner in the upper level that is considering purchasing battery energy storage systems for installation at

three different nodes in a distribution system in order to reduce its operating cost in a real-time energy market. The planner also accounts for purchasing exported PV power from customers and sending a time-of-use price signal to refrigerated warehouses with price-responsive cooling systems. The upper level model is shown in (3.28). Tables 3.3, 3.4, and 3.5 summarize the variables, parameters and sets in (3.28). The objective (3.28a) includes three components to minimize: (1) the cost of energy purchased on the bulk market at the feeder head; (2) the cost of energy purchased from distributed, customer-owned photovoltaic (PV) systems; and (3) the capital costs of battery systems. We assume an analysis period of 20 years and a discount rate of 5%. For the bulk market price $c_{\mathrm{LMP},t}$ we use the average hourly real-time market prices from Electric Reliability Council of Texas (ERCOT) over the year of 2019 [55]. A year of load is simulated at an hourly resolution by randomly assigning different U.S. Department of Energy Commercial Reference Building profiles to the load nodes [56]. The load nodes are defined in [7], from which we take the 38 node network model. Constraints (3.28c) – (3.28g) define a linear power flow model, commonly known as "LinDistFlow" [57]. Constraint (3.28h) limits the squared voltage magnitude. Constraints (3.28i) and (3.28j) define the net power injection from system operator owned battery systems. Constraints (3.28k) and (3.28l) define the net power injection from customer nodes with PV systems. Constraints (3.28m) and (3.28n) define the net power injection from nodes with price-responsive refrigerated warehouses. Constraints (3.28o) and (3.28p) define the net power injection from nodes with uncontrollable load. Constraint (3.28q) is structural and prevents simultaneous export and import rom nodes with PV systems. Constraints (4.10a) – (4.10f) define the operational limits of the system operator's battery systems. Finally, constraint (3.28w) says that the lower level decisions y must be optimal for the lower level problem (3.29).

$$\min_{\boldsymbol{P},\boldsymbol{Q},\boldsymbol{w},\boldsymbol{x},\boldsymbol{y},\boldsymbol{\lambda}} \text{ pwf} \sum_{t\in\mathcal{T}} \left(c_{\text{LMP},t} x_{0,t} + \sum_{n\in\mathcal{N}_{\text{PV}}} [\lambda_{n,t} y_{e,n,t}] \right) + \sum_{n\in\mathcal{N}_{\text{B}}} \left(c_{\text{BkW}} x_{\text{BkW},n} + c_{\text{BkWh}} x_{\text{BkWh},n} \right)$$
(3.28a)

$$\text{s.t. } x_{0,t} \geq 0, \ x_{e,t} \geq 0, \ x_{i,t} \geq 0, \quad \forall t \in \mathcal{T} \tag{3.28b}$$

$$P_{0,t} = P_{01,t}, \quad \forall t \in \mathcal{T} \tag{3.28c}$$

$$Q_{0,t} = Q_{01,t}, \quad \forall t \in \mathcal{T} \tag{3.28d}$$

$$P_{ij,t} + P_{j,t} - \sum_{k:j\to k} P_{jk} = 0, \quad \forall j \in \mathcal{N}_+, \ \forall t \in \mathcal{T} \tag{3.28e}$$

$$Q_{ij,t} + Q_{j,t} - \sum_{k:j\to k} Q_{jk} = 0, \quad \forall j \in \mathcal{N}_+, \ \forall t \in \mathcal{T} \tag{3.28f}$$

$$w_{j,t} = w_{i,t} - 2 \left(r_{ij} P_{ij,t} + x_{ij} Q_{ij,t} \right), \quad \forall j \in \mathcal{N}_+, \ \forall t \in \mathcal{T} \tag{3.28g}$$

$$(v_j^{\max})^2 \geq w_{j,t} \geq (v_j^{\min})^2, \quad \forall j \in \mathcal{N}, \ \forall t \in \mathcal{T} \tag{3.28h}$$

$$P_{j,t} = x_{\text{B}^-,j,t} - x_{\text{B}^+,j,t}, \quad \forall j \in \mathcal{N}_{\text{B}}, \ \forall t \in \mathcal{T} \tag{3.28i}$$

$$Q_{j,t} = f_{pf,j,t} \left(x_{\text{B}^-,j,t} - x_{\text{B}^+,j,t} \right), \quad \forall j \in \mathcal{N}_{\text{B}}, \ \forall t \in \mathcal{T} \tag{3.28j}$$

$$P_{j,t} = y_{e,j,t} - y_{i,j,t}, \quad \forall j \in \mathcal{N}_{\text{PV}}, \ \forall t \in \mathcal{T} \tag{3.28k}$$

$$Q_{j,t} = f_{pf,j,t} \left(y_{e,j,t} - y_{i,j,t} \right), \quad \forall j \in \mathcal{N}_{\text{PV}}, \ \forall t \in \mathcal{T} \tag{3.28l}$$

$$P_{j,t} = -y_{i,j,t}, \quad \forall j \in \mathcal{N}_W, \ \forall t \in \mathcal{T} \tag{3.28m}$$

$$Q_{j,t} = -f_{pf,j,t} y_{i,j,t}, \quad \forall j \in \mathcal{N}_W, \ \forall t \in \mathcal{T} \tag{3.28n}$$

$$P_{j,t} = -d_{j,t}, \quad \forall j \in \mathcal{N}_U, \ \forall t \in \mathcal{T} \tag{3.28o}$$

$$Q_{j,t} = -f_{pf,j,t} d_{j,t}, \quad \forall j \in \mathcal{N}_U, \ \forall t \in \mathcal{T} \tag{3.28p}$$

$$y_{e,j,t} \perp y_{i,j,t}, \quad \forall j \in \mathcal{N}_{\text{PV}}, \ \forall t \in \mathcal{T} \tag{3.28q}$$

$$x_{\text{SOC},j,t} = x_{\text{SOC},j,t-1} + f_{hr} \left(x_{\text{B}^+,j,t}\eta - x_{\text{B}^-,j,t}/\eta \right) \quad \forall j \in \mathcal{N}_{\text{B}}, \ \forall t \in \mathcal{T}$$
(3.28r)

$$x_{\text{BkW},j} \geq x_{\text{B}^+,j,t} + x_{\text{B}^-,j,t} \quad \forall j \in \mathcal{N}_{\text{B}}, \ \forall t \in \mathcal{T} \tag{3.28s}$$

$$x_{\text{BkWh},j} \geq x_{\text{SOC},j,t} \quad \forall j \in \mathcal{N}_{\text{B}}, \ \forall t \in \mathcal{T} \tag{3.28t}$$

$$x_{\text{SOC},j,0} = 0.5 x_{\text{BkWh},j} \quad \forall j \in \mathcal{N}_{\text{B}} \tag{3.28u}$$

$$x_{\text{SOC},j,N_t} = 0.5 x_{\text{BkWh},j} \quad \forall j \in \mathcal{N}_{\text{B}} \tag{3.28v}$$

$$\boldsymbol{y} = \boldsymbol{y}^\star(\boldsymbol{x}) \tag{3.28w}$$

$$\boldsymbol{y}^{\star}(\boldsymbol{x}) = \arg\min_{\boldsymbol{y}} \ \mathrm{pwf} \sum_{t \in \mathcal{T}} \sum_{n \in \mathcal{N}_W} \left(y_{i,n,t} \left[c_{i,n,t} + x_{i,n,t} \right] \right) + \mathrm{pwf} \sum_{t \in \mathcal{T}} \sum_{n \in \mathcal{N}_{\mathrm{PV}}} \left(c_{i,t} y_{i,n,t} - x_{e,n,t} y_{e,n,t} \right)$$

$$+ \sum_{n \in \mathcal{N}_{\mathrm{PV}}} c_{\mathrm{PV}} y_{\mathrm{PV},n} \tag{3.29a}$$

$$\text{s.t. } y_{i,n,t} + y_{\mathrm{pvprod},n,t} = d_{n,t} + y_{e,n,t}, \ (\lambda_{n,t}) \quad \forall n \in \mathcal{N}_{\mathrm{PV}}, \ \forall t \in \mathcal{T} \tag{3.29b}$$

$$y_{i,n,t} = d_{n,t} + y_{\mathrm{HVAC},n,t}/\mathrm{COP} \quad \forall n \in \mathcal{N}_W, \ \forall t \in \mathcal{T} \tag{3.29c}$$

$$y_{\mathrm{pvprod},n,t} \leq y_{\mathrm{PV},n} f_{\mathrm{PV},n,t} \quad \forall n \in \mathcal{N}_{\mathrm{PV}}, \ \forall t \in \mathcal{T} \tag{3.29d}$$

$$y_{\mathrm{T},n,t} = y_{\mathrm{T},n,t-1} + f_{hr} \left(\boldsymbol{A} y_{\mathrm{T},n,t-1} + \boldsymbol{B} \left[y_{\mathrm{HVAC},n,t}, \boldsymbol{u}_{n,t} \right]^T \right)$$
$$\forall n \in \mathcal{N}_{\mathrm{PV}}, \ \forall t \in \mathcal{T} \tag{3.29e}$$

$$y_{\mathrm{T},n,0} = \mathrm{T}_{n,t=0} \quad \forall n \in \mathcal{N}_{\mathrm{PV}} \tag{3.29f}$$

$$\mathrm{T}_{\mathrm{hi}} \geq y_{\mathrm{T},n,t} \geq \mathrm{T}_{\mathrm{lo}} \quad \forall n \in \mathcal{N}_{\mathrm{PV}}, \ \forall t \in \mathcal{T} \tag{3.29g}$$

$$y_{e,n,t} \geq 0, y_{i,n,t} \geq 0, \quad \forall n \in \mathcal{N}_{\mathrm{PV}}, \ \forall t \in \mathcal{T} \tag{3.29h}$$

Problem (3.29) shows the lower level problem, with the objective to minimize the total cost of energy for all customers in the distribution system. Tables 3.3, 3.4, and 3.5 summarize the variables, parameters and sets in (3.29). The first half of the lower level objective (3.29a) represents the cost of energy for price responsive refrigerated warehouses that have a known retail rate $c_{i,n,t}$ and a time-varying price signal from the upper level problem $x_{i,n,t}$. The second half of (3.29a) represents the cost of energy for customers that can install PV systems. These customers also pay the retail rate $c_{i,n,t}$ for imported power but can also receive compensation for exported, excess PV power from the upper level via $x_{e,n,t}$. Constraints (3.29b) and (3.29c) are the load balance constraints for the PV and warehouse customers respectively. Constraint (3.29d) limits the PV power used to meet load to the PV capacity times a known, normalized solar PV production factor from [58]. Constraints (3.29e) - (3.29g) define the refrigerated warehouse temperature dynamics, starting condition, and temperature limits.

We select Austin, Texas as the testbed to generate inputs for demonstrating

the method. Warehouses have freezing units that can at most reach zero °C but can be cooled to as low as -20 °C in order to lower their energy costs by coasting through high price periods. PV production factors and ambient temperatures from Austin are used as an input to the refrigerated warehouse models.

By inspection the lower level model (3.29) is separable between the set of PV nodes $\mathcal{N}_{\mathrm{PV}}$ and the warehouse nodes $\mathcal{N}_W$. Because we wish to linearize the bilinear product $\lambda_{n,t} y_{e,n,t}$ in (3.28a), which is only defined for the PV nodes, we only need to check the linearization conditions for the components of the lower level model (3.29) that are relevant to the PV nodes. A *Julia* module to programatically check the linearization conditons, including for separable problems like this example, is available in [59][4].

The upper level is allowed to install battery systems at up to three nodes (2, 7, and 24) in the network while the lower level can install PV systems on up to five nodes (9, 17, 22, 31, and 34). Using the baseline values the optimal solution is for the lower level customers to install small PV systems to reduce their utility bills and it is not economical for the upper level to install storage systems. To produce more interesting results we increase the bulk energy costs by integer values from the baseline 1× to 5×. Table 3.2 summarizes the results with increasing bulk energy costs. In table 3.2 we can see some expected trends: as the bulk energy costs increase less energy is purchased on the bulk market and more PV energy is purchased from customers, which encourages larger PV systems. However, there are not clear trends in the battery sizes nor energy throughput. The lack of trends in the battery results is not surprising: batteries can serve many purposes including energy arbitrage, peak shaving, and grid services. In fact, in the 5× bulk cost scenario so much PV energy

---

[4]The module in [59] will be merged into [30] for ease-of-use. When debug logging is enabled the module will report which conditions did not pass.

cost multi- plier	Bulk MWh Pur- chased	PV MWh Pur- chased	PV MW	Battery MW	Battery MWh	Battery MWh throughput
1×	129,895	2,396	[0.04, 0.00, 0.89, 0.12, 0.97]	[0.00, 0.00, 0.00]	[0.00, 0.00, 0.00]	0
2×	127,952	4,162	[0.06, 0.00, 1.42, 0.19, 1.66]	[0.27, 0.29, 0.31]	[0.58, 0.61, 0.66]	1,026
3×	121,799	9,890	[0.14, 0.42, 2.84, 0.40, 3.50]	[0.79, 0.18, 0.00]	[1.47, 0.34, 0.00]	1,020
4×	94,092	36,981	[0.35, 2.66, 8.24, 1.53, 12.8]	[0.30, 0.35, 0.00]	[0.62, 0.74, 0.00]	752
5×	72,352	61,378	[0.56, 5.00, 13.3, 2.13, 21.2]	[0.34, 0.46, 0.28]	[0.72, 0.96, 0.58]	1,313

Table 3.2: Results for the use-case example in Section 3.2.2. Energy purchased and throughput values are per year. The cost multiplier is applied to the bulk energy costs only. PV capacities are listed in order of nodes [9, 22, 31, 34, 17]. Battery capacities are listed in order of nodes [2, 7, 24].

is exported that it is necessary to use the storage systems to keep the voltage within limits.

For more information regarding model results readers are encouraged to see the code available online [60]. The examples in this section are meant is demonstrative use-cases and only represent a fraction of the types of questions that might be answered using the linearization technique for power system planning. Furthermore, the price signal from the upper level to the lower level can also be used in transactive control context by removing capacity decisions, shortening the time horizon, increasing the time resolution, and using forecasts for the uncontrolled demand and PV production.

Table 3.3: Decision variables for Problems (3.28) and (3.29). Scalar parameter values are shown in square brackets and some vector parameters include source references.

$P_{0,t}, Q_{0,t}$	real, reactive power imported at feeder head, node 0 in time step t
$P_{j,t}, Q_{j,t}$	real, reactive power injected at node j in time step t
$P_{ij,t}, Q_{ij,t}$	real, reactive power flow on line ij in time step t
$w_{j,t}$	voltage magnitude squared at node j in time step t
$x_{i,j,t}$	retail price adder to refrigerated warehouse at node j in time step t
$x_{\mathrm{B}^+,j,t}$	battery charge rate at node j in time step t
$x_{\mathrm{B}^-,j,t}$	battery discharge rate at node j in time step t
$x_{\mathrm{BkW},j}$	battery inverter power rating at node j
$x_{\mathrm{BkWh},j}$	battery storage capacity at node j
$x_{\mathrm{SOC},j,t}$	battery state of charge at node j in time step t
$y_{i,n,t}$	imported power at node n in time step t
$y_{e,n,t}$	exported power at node n in time step t
$y_{\mathrm{HVAC},n,t}$	HVAC thermal power at node n in time step t
$y_{\mathrm{T},n,t}$	interior temperature at node n in time step t
$y_{\mathrm{HVAC},n,t}$	thermal power of HVAC system at node n in time step t
$y_{\mathrm{PV},n}$	PV capacity at node n
$y_{\mathrm{pvprod},n,t}$	PV production used at node n in time step t

Table 3.4: Parameters for Problems (3.28) and (3.29). Scalar parameter values are shown in square brackets and some vector parameters include source references.

$c_{\text{LMP},t}$	Locational Marginal Price paid by upper level in time step t [ref. [55]]
$c_{i,n,t}$	retail price of energy [$0.25/kWh]
c_{BkW}	cost of battery inverter [$700/kW]
c_{BkWh}	cost of battery capacity [$350/kWh]
c_{PV}	cost of PV capacity [$1,400/kWh]
$f_{pf,j,t}$	power factor at node j in time step t [0.1]
r_{ij}, x_{ij}	resistance, reactance of line ij [ref. [7]]
$f_{\text{PV},n,t}$	PV production factor at node n in time step t [ref. [58]]
f_{hr}	fraction of hour in each time step (for example, $f_{hr} = 0.25$ for 15 minute time steps) [1.0]
$d_{n,t}$	uncontrolled demand at node n in time step t [ref. [56]]
COP	HVAC system coefficient of performance [4.55]
η	battery charge and discharge efficiency [0.95]
$\text{T}_{\text{hi}}, \text{T}_{\text{lo}}$	upper, lower temperature limit [0, -20]
$\text{T}_{n,t=0}$	initial interior temperature at node n in time step t [-1]
$\boldsymbol{A}$	HVAC system state matrix $[[\frac{-1}{RC}]$ where $R = 0.00025$ K/kW and $C = 10^5$ kJ/K]
$\boldsymbol{B}$	HVAC system input matrix $[[\frac{1}{RC} \quad \frac{1}{C}]]$
$\boldsymbol{u}_{n,t}$	HVAC system exogenous inputs at node n in time step t (outdoor temperature) [ref. [58]]
N_t	integer number of time steps [8,760]
pwf	present worth factor assuming an annual cash flow year over year for the analysis period of 20 years and a discount rate of 5% [12.46]
$v_j^{\max}, v_j^{\min}$	maximum, minimum voltage limit at node j

Table 3.5: Sets and indices for Problems (3.28) and (3.29).

$\mathcal{T}$	set of integer time steps, $1, \ldots, N_t$
$\mathcal{N}$	set of integer nodes in the network, $\{0, 1, \ldots, N\}$
$\mathcal{N}_+$	set of positive integer nodes, $\{1, \ldots, N\}$
$\mathcal{N}_{\mathrm{PV}} \subset \mathcal{N}$	set of integer nodes that can buy PV in lower level
$\mathcal{N}_U \subset \mathcal{N}$	set of integer uncontrolled nodes
$\mathcal{N}_W \subset \mathcal{N}$	set of integer refrigerated warehouse nodes
$\mathcal{N}_{\mathrm{B}}$	set of integer nodes that have battery decisions

3.2.3   Solution time impact

Using the example from Section (3.2.2) we compare solution times with and without the upper level bilinear terms $\lambda_t y_{e,t}$ replaced with the linearization. In both cases the model is reformulated as a single level problem. Both the mixed integer-linear and the mixed integer-bilinear problems were solved using Gurobi 9.1 on 16-core 3.4GHz Linux PC with 32GB of RAM using "big M" constraints for the complementary constraints. The mixed integer-bilinear problem is (3.28) combined with the KKT conditions for (3.29). The mixed integer-linear problem is not shown due to space constraints, but is available in the public repository [60].

Both the linearized and bilinear problems have 350,405 binary variables and 2,417,777 continuous variables. The bilinear problem also has 43,800 bilinear objective terms. After 25 seconds in the presolve the linearized problem has 103,588 binary variables and 519,031 continuous variables. The linear problem solves in 128 seconds with a gap of 0.01%. After 21 seconds in the presolve the bilinear problem has 83,143 binary variables, 540,209 continuous variables, and 21,180 bilinear constraints. The bilinear model takes 8,447 seconds to get to a 57% gap, which is not improved until the operating system kills the problem at 16,032 seconds due to running out of memory. In short, the linearization method makes the otherwise intractable bilinear bilevel

problem from Section (3.2.2) solve in a few minutes. Similar results are expected for other large planning problems like the example in Section (3.2.2).

3.3 Conclusions

This work presents a method for linearizing bilinear products of lower level primal and dual variables in the upper level of bilevel optimization problems, and the conditions required for the linearization to be exact. The linearization method is especially relevant for modeling large scale energy distribution systems with many stakeholders and is therefore applicable to a growing number of problems as energy markets expand and adapt to new regulations such as FERC Order 2222 [9] and the increasing adoption of distributed energy resources [61].

For future work we intend to leverage the method in an open source mathematical programming package [30, 62]. for studying compensation mechanisms of distributed energy resources serving as power system upgrade deferrals (c.f. [7]). Another future research direction involves using the optimal price signals from one level to the other as a transactive control mechanism. We will also explore more accurate and complex power flow approximations such as the second-order cone approximation for the Branch Flow Model.

Chapter 4

A method to assess the techno-economic potential of DER for distribution system upgrade deferrals

Building upon the methodology from RO1, this thesis develops a scalable modeling framework for valuing DER as non-wires alternatives (NWA) that accounts for the DER owners' objectives and the market operator's objective. The framework allows distribution system operators and DER aggregators to ascertain the cost optimal locations and capacities of DER to avoid traditional system upgrade costs while accounting for DER owner objectives.

DER owner benefits are accounted for in terms of the minimum life-cycle cost of energy. Transactions between the DER owners and the DSO occur in the form of payment from the DSO to customers for exported DER power and demand response. A bilevel optimization model is proposed to account for the competing objective functions, in which the DSO's cost is the customers' profit.

The optimal price signal from the DSO to DER owners should not be determined a priori (c.f. [7]) since customer behavior will change based on the price signal. A well known example of the consequences of pre-determined price signals is the rebound effect that can occur from time-of-use pricing applied to customers with

---

load-shifting capabilities [63]. By applying high prices during times of expected high demand customers will shift demand from the high-price periods to the lower price periods. As more customers gain the ability to shift their loads a new peak demand period occurs during the lowest price period, which creates a game of whack-a-mole for tariff designers.

In this work the non-linear products of the price-signals and dispatch decisions are linearized using the result of RO1. Since the method requires only inputs that are within a DSO's purview it can be used by distribution system planners to compare traditional wires upgrade cost to the cost of purchasing power and demand response from BTM DER.

4.1 Methodology

To account for the objectives and constraints of *both* the DSO and the potential DER investors we employ a bilevel optimization framework. Bilevel optimization problems, also known as Stackelberg Games, are generally intractable. However, by ensuring that the lower level problem is linear given upper level decisions the bilevel problem can be converted into an equivalent single level problem [64]. Furthermore, under certain conditions the bilinear products of dual variables, i.e. shadow prices, and primal variables can be linearized [12]. This last point is especially important since we seek to optimize the product of the price signal from the DSO and the power injection decisions of the DER investors.

Table 4.1: Decision Variables

$\boldsymbol{x} \in \mathcal{R}^M$	upper level primal decision variables
$\boldsymbol{y} \in \mathcal{R}^N$	lower level primal decision variables
$\boldsymbol{z} \in \{0,1\}^K$	upper level primal binary decision variables
$\boldsymbol{\lambda} \in \mathcal{R}^J$	lower level, dual variables for equality constraints
$\overline{\boldsymbol{\mu}} \in \mathcal{R}^N_+$	lower level dual variables for upper bounds
$\underline{\boldsymbol{\mu}} \in \mathcal{R}^N_+$	lower level dual variables for lower bounds
$x^{\text{BkW}}_{j,\phi}$	BESS inverter capacity [kW]
$x^{\text{BkWh}}_{j,\phi}$	BESS energy capacity [kWh]
$x^{\text{B}^+}_{j,\phi,t}$	BESS charge rate [kW]
$x^{\text{B}^-}_{j,\phi,t}$	BESS discharge rate [kW]
$x^{\text{SOC}}_{j,\phi,t}$	BESS state-of-charge [kWh]
$x^{\lambda}_{j,t}$	Price of DER exported energy [\$/kWh]
z^{TRF}_j	binary for transformer upgrade [0/1]
z^{LINE}_j	binary for transformer upgrade [0/1]
y^{kW}_j	capacity of DER at node j [kW]
$y^{\text{IMP}}_{j,t}$	energy imported [kWh]
$y^{\text{EXP}}_{j,t}$	energy exported [kWh]
$y^{\text{DER}}_{j,t}$	energy produced [kWh]

Table 4.2: Parameters

$\boldsymbol{V} \in \mathcal{R}^{J \times N}$	lower level equality constraint coefficients
$\boldsymbol{w} \in \mathcal{R}^{J}$	lower level equality constraints right-hand-side
$\overline{\boldsymbol{y}} \in \mathcal{R}^{N}$	upper bounds for lower level, primal decision variables
$\underline{\boldsymbol{y}} \in \mathcal{R}^{N}$	lower bounds for lower level, primal decision variables
a	upper level scaling coefficient for cost of DER energy
b	lower level scaling coefficient for income from selling energy to upper level
$\boldsymbol{c} \in \mathcal{R}^{N}$	lower level cost coefficients for lower level decisions $\boldsymbol{y}$
c^{BkW}	cost of BESS inverter [\$/kW]
c^{BkWh}	cost of BESS capacity [\$/kWh]
c_j^{TRF}	cost of a new transformer [\$]
c_j^{LINE}	cost of a new line [\$]
c_t^{LMP}	wholesale cost of energy [\$/kWh]
c_s^{DEM}	peak demand cost in period s [\$/kW]
η	BESS efficiency [fraction]
$\Delta R_j^{\mathrm{TRF}}$	increase in transformer rating [kW]
$\overline{R}_j^{\mathrm{TRF}}$	existing transformer rating [kW]
$\Delta R_j^{\mathrm{LINE}}$	increase in line rating [kW]
$\overline{R}_j^{\mathrm{LINE}}$	existing line rating [kW]
r_e	energy cost growth rate [year^{-1}]
r_e	energy consumption growth rate [year^{-1}]
r_{WACC}	weighted avg. cost of capital [year^{-1}]
c_j^{kW}	cost of DER at node j [\$/kW]
c^{OM}	annual cost of operations and maintenance [\$/(kW-year)]
$c_{j,t}^{\mathrm{IMP}}$	cost of energy imported [\$/kWh]
$d_{j,t}$	uncontrollable demand [kW]
$f_{j,t}^{\mathrm{prod}}$	production factor, 0–1
r_e	energy cost growth rate [year^{-1}]
r_e	energy consumption growth rate [year^{-1}]
ROR	required rate of return [year^{-1}]

Table 4.3: Sets and Indices

$\mathcal{E}$	set of edges in the network
$\mathcal{N}$	set of nodes in the network
$\mathcal{N}_{\text{DER}}$	set of nodes for potential DER investors
$\mathcal{N}_{\text{BESS}}$	set of nodes for potential BESS installations
$\mathcal{N}_{\text{TRFX}}$	set of nodes for potential transformer upgrades
$\mathcal{N}_{\text{LINE}}$	set of nodes for potential line upgrades
$\mathcal{S}$	set of demand charge periods
$\mathcal{T}$	set of time steps
Φ_j	set of phases connected to node j

The general bilevel optimization framework is shown in Problem 4.1 (with nomenclature in Table 4.1).

$$\min_{\boldsymbol{x},\boldsymbol{y}} f(\boldsymbol{x},\boldsymbol{y}) + \frac{a}{b} \sum_{j\in\mathcal{N}_{\text{DER}}} \sum_{t\in\mathcal{T}} \lambda_{j,t}\ y_{j,t}^{\text{EXP}} \tag{4.1a}$$

$$\text{s.t. } g(\boldsymbol{x},\boldsymbol{y}) \leq \boldsymbol{0} \tag{4.1b}$$

$$\boldsymbol{y} \in \arg\min_{\boldsymbol{y}\in\mathcal{R}^N}\ \boldsymbol{c}^{\mathsf{T}}\boldsymbol{y} - b \sum_{j\in\mathcal{N}_{\text{DER}}} \sum_{t\in\mathcal{T}} x_{j,t}^{\lambda}\ y_{j,t}^{\text{EXP}} \tag{4.1c}$$

$$\text{s.t. } \underline{\boldsymbol{y}} \leq \boldsymbol{y} \leq \overline{\boldsymbol{y}} \quad (\underline{\boldsymbol{\mu}}, \overline{\boldsymbol{\mu}}) \tag{4.1d}$$

$$\boldsymbol{V}\boldsymbol{y} = \boldsymbol{w} \quad (\boldsymbol{\lambda}). \tag{4.1e}$$

The components of the framework in (4.1) are:

- the upper level cost (4.1a), which includes a generic function $f(\boldsymbol{x},\boldsymbol{y})$ and a second term that represents the payment to DER owners via the product of the lower level shadow price $\lambda_{j,t}$ and export decisions $y_{j,t}^{\text{EXP}}$;

- the upper level generic constraint set $g(\boldsymbol{x},\boldsymbol{y}) \leq \boldsymbol{0}$;

- the upper level is constrained by the lower level decisions $\boldsymbol{y}$ being in the optimal space of the lower level problem;

- the lower level problem has a linear cost function given $\boldsymbol{x}$ (4.1c), which includes:

  - a generic cost $\boldsymbol{c}^\intercal \boldsymbol{y}$ and

  - the income from the upper level via price signal $x^\lambda_{j,t}$ times the exported DER energy $y^{\text{EXP}}_{j,t}$;

- and the linear lower level constraints with the associated dual variables in parentheses (4.1d)-(4.1e).

The key feature of the framework is the exchange of money between the DSO in the upper level and the DER investors in the lower level via the products of the upper level price signal decisions and the lower level export decisions in the objective functions (4.1a) and (4.1c). Since bilevel programs are by default optimistic, i.e. the lower level acts in the upper level's best interests [64], the framework guarantees the the total system cost is minimized, i.e. the social welfare is maximized. However, to realistically account for DER investor decisions we scale the monetary exchange such that DER investors get a required rate of return on their investments (if any).

One way to explain the framework is to first think of a DER investor in isolation, without the price signal from the DSO. Including the investor required rate of return can be done in the same fashion as done in the bilevel framework, specifically by scaling costs and benefits appropriately using present worth factors [65]. In brief, the DER investor will purchase a system if and only if the benefits are greater than or equal to the costs – and the benefits must provide at least the required rate of return. The same is true in the bilevel framework. But in the bilevel framework the benefits can include an income from selling energy to the DSO (or aggregator or
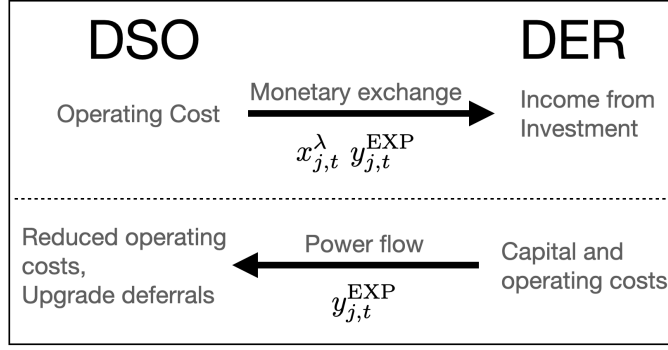
Figure 4.1: Summary of the interactions between the DSO and DER. The DSO pays DER for energy exported, which can only be accomplished if DER invest in a system. If it is optimal for DER investors to purchase a system then they can benefit from the monetary exchange from the DSO as well as by reducing their cost of energy to meet demand. The DSO will only send a price signal if it reduces the system operating costs, including deferring capital investments.

whatever entity is represented in the upper level). Furthermore, since the framework is optimistic the DER investor will get *no more* than the required rate of return.

As we show in the following, the DSO in the upper level can effectively set the marginal price of DER investors when the DSO wishes; and the sum of the total compensation paid to DER investors must meet the investors' required rate of return.

As shown in [12][1]:

$$\lambda_{j,t} = b \ x_{j,t}^{\lambda} \tag{4.2}$$

which means that the upper level payment to DER can be written:

$$\frac{a}{b} \sum_{j \in \mathcal{N}_{\mathrm{DER}}} \sum_{t \in \mathcal{T}} \lambda_{j,t} \ y_{j,t}^{\mathrm{EXP}} = a \sum_{j \in \mathcal{N}_{\mathrm{DER}}} \sum_{t \in \mathcal{T}} x_{j,t}^{\lambda} \ y_{j,t}^{\mathrm{EXP}}. \tag{4.3}$$

In other words, we have formed a zero-sum game in which the upper level, or DSO's, cost of DER energy is equal to the DER owners' income (with the exception of the scaling coefficients a and b that we will use to account for each party's cost of capital).

---

[1]See Equation (9) in [12] when the index k is equal to the index for a given $y_{j,t}^{\mathrm{EXP}}$, the variable has zero coefficients in the cost vector $\boldsymbol{c}$, and no bounds are binding (i.e. $\underline{\boldsymbol{\mu}} = 0$ and $\overline{\boldsymbol{\mu}} = 0$).

Furthermore, the product of the dual variable $\lambda_{j,t}$ and the DER dispatch variable $y_{j,t}^{\text{EXP}}$ can be shown to equal a linear sum [12]:

$$\sum_{j \in \mathcal{N}_{\text{DER}}} \sum_{t \in \mathcal{T}} \lambda_{j,t} y_{j,t}^{\text{EXP}} = \frac{1}{V_{y^{\text{EXP}}}} \left(\boldsymbol{w}^{\mathsf{T}} \boldsymbol{\lambda} - \boldsymbol{c}^{\mathsf{T}} \boldsymbol{y} - \overline{\boldsymbol{\mu}}^{\mathsf{T}} \overline{\boldsymbol{y}} + \underline{\boldsymbol{\mu}}^{\mathsf{T}} \underline{\boldsymbol{y}} \right) \tag{4.4}$$

where $V_{y^{\text{EXP}}}$ is the coefficient of the lower level export variable in the lower level load balance equations.

To convert the bilevel problem (4.1) into a single level problem it is important to note that the the lower level problem described by (4.1c) – (4.1e) is linear given $\boldsymbol{x}$. The conversion to a single level is achieved by replacing the lower level problem with its Karush-Kuhn-Tucker (KKT) conditions [66]. The KKT conditions make the lower problem a mixed-integer linear problem. Problem (4.5) shows the single level equivalent of (4.1):

$$\min_{\boldsymbol{x}, \boldsymbol{y}, \boldsymbol{z}, \boldsymbol{\lambda}, \overline{\boldsymbol{\mu}}, \underline{\boldsymbol{\mu}}} f(\boldsymbol{x}, \boldsymbol{y}, \boldsymbol{z}) + \frac{a}{b} \sum_{j \in \mathcal{N}_{\text{DER}}} \sum_{t \in \mathcal{T}} \lambda_{j,t} \ y_{j,t}^{\text{EXP}} \tag{4.5a}$$

$$\text{s.t. } g(\boldsymbol{x}, \boldsymbol{y}) \leq 0 \tag{4.5b}$$

$$\boldsymbol{c} + \boldsymbol{b}^{T} \boldsymbol{x} + \boldsymbol{V}^{\mathsf{T}} \boldsymbol{\lambda} + \overline{\boldsymbol{\mu}} - \underline{\boldsymbol{\mu}} = \boldsymbol{0} \tag{4.5c}$$

$$\underline{\boldsymbol{y}} \leq \boldsymbol{y} \leq \overline{\boldsymbol{y}} \tag{4.5d}$$

$$\boldsymbol{V}\boldsymbol{y} = \boldsymbol{w} \tag{4.5e}$$

$$\overline{\boldsymbol{\mu}} \perp (\boldsymbol{y} - \overline{\boldsymbol{y}}) \tag{4.5f}$$

$$\underline{\boldsymbol{\mu}} \perp (\underline{\boldsymbol{y}} - \boldsymbol{y}) \tag{4.5g}$$

Note that the complementary constraints (4.5f) and (4.5g) can be handled with integer variables or special order sets [67]. Also, the entries of the vector $\boldsymbol{b}$ in (4.5c) are zero except for the entries that correspond with the price signal $x_{j,t}^{\lambda}$. The non-zero values of $\boldsymbol{b}$ are set to pwf_{LL}, the present worth factor for the lower level, in the examples.

The present worth factor accounts for the DER investors' required rate of return by scaling their costs according the number of years they expect to operate a system, as well as any expected cost growth rates and their discount rate.

Problem 4.5 is a mixed integer *non-linear problem*. Using the result from [12] the product of $\boldsymbol{\lambda}$ and $\boldsymbol{y}$ in (4.5a) can be linearized as shown in (4.4). Also, if the upper level cost function $f(\boldsymbol{x}, \boldsymbol{y})$ and constraints $g(\boldsymbol{x}, \boldsymbol{y})$ are linear then the single level problem is mixed-integer linear. However, there are no requirements on the form of the upper level problem within the framework. For example, the constraints in the upper level can represent any power flow equations and integer decisions.

4.1.1 Accounting for Uncertainty

The framework allows for using optimization methods under uncertainty, such as stochastic and robust optimization. For example, when there is uncertainty surrounding input parameters such as the price of battery energy storage systems (BESS) one could leverage a minimax formulation to account for the range of possible BESS prices. However, often these methods are insufficient for accounting for the level of uncertainty inherent in power system planning problems (also argued in [68]). Methods such as stochastic and robust optimization, which assume full knowledge of the probability distribution or uncertainty set respectively [69], account for what is known as "shallow" uncertainty in the field of Decision Science (c.f. [70]). For example, past works account for shallow uncertainty by minimizing the expected cost over load scenarios with known probabilities [36]. Deep uncertainty, in contrast to shallow uncertainty, exists when probabilities are unknown, or when experts do not agree on what the future looks like. For example, what will the DER developers require for their rate of return in the future? And what will wholesale electricity costs look like as DER are integrated into wholesale markets under FERC Order 2222?

61

Methods such as stochastic optimization follow a paradigm of predict-then-act; whereas methods that account for deep uncertainty stress test feasible actions under possible scenarios, as well as integrate the decision makers into the process directly. The realm of Decision Making Under Deep Uncertainty is a rich and vibrant field and readers are referred to the book [71] for an excellent introduction. The method proposed in this work can be leveraged in Decision Making Under Deep Uncertainty methods, such as Robust Decision Making [72] or Adaptive Pathways [73]. For example, by leveraging the market price model developed in Research Objective 3 the framework for valuing DER presented in this chapter could be solved for many different possible future market price scenarios. By stress-testing the model over many price scenarios decision makers can make more informed decisions based on the range of optimal solutions.

4.2 Use-case Examples

To demonstrate the value of the proposed framework we start with a system that has expected transformer and line overloads. The system planner or DSO, as the first player in the upper level, seeks to find the lowest cost solution to the expected overloads by choosing from:

- line and transformer upgrades,

- battery energy storage systems (BESS),

- and/or purchasing DER energy at a time and space varying price of its choosing.

The DSO makes these choices with knowledge of how the lower level, i.e. potential DER investors, will react to the price signal. The DER investors, as the second players in the lower level, choose from:

- purchasing energy at a known fixed price to meet demand,

- and/or investing in DER to meet load as well as (possibly) receive compensation for exported energy.

We emphasize that this example is only one of infinite ways that the framework for valuing DER as non-wires alternatives can be leveraged. Other examples include:

- voltage support: by using voltage regulator investment decision in the upper level and including a price signal for reactive power from the lower level

- electric vehicle charging infrastructure: the upper level pays for vehicle-to-grid services while the charging station owners select locations that provide the most profit

- demand response: compensating dispatchable loads to avoid system upgrades, where the lower level chooses how to dispatch given the price signal

We presume that the DER investors' required rate of return (RoR) is known. The model is formulated such that DER will only be purchased if the RoR can be reached. The DSO decisions are also subject to power flow constraints, such as line flow and transformer loading limits.

For reference we compare three scenarios in each use-case:

1. The base case with component overloads and the traditional upgrade costs.

2. The minimum cost solution considering only utility owned BESS (no DER value).

3. The minimum cost solution considering BESS and valuing DER as a non-wires alternative.

The input data and the results are summarized in Figure 4.2. Note that we assume that the DER are PV systems by using a time-varying production factor from [58]. We presume to have expected hourly load profiles over a year (8760 time steps) for each load bus in the network[2]. An annual load growth rate is included to account for expected electrification over the analysis period. In the base case the utility must pay for new lines and transformers due to expected overloads. The examples are built upon the IEEE 13 bus distribution test system. Transformer upgrade costs are estimated using values from [74] and line costs were obtained from a large municipal distribution utility.

Inputs

- Network model
- Wholesale energy cost for one year
- Loads for one year
- Transformer and line limits
- Upgrade costs and capacities
- DER capital and O&M costs

Outputs

- Location and capacity of:
  - utility BESS
  - third party DER
- Transformer and line upgrades
- Utility operating costs of:
  - DER services
  - bulk energy
  - upgrades
  - BESS
  - demand charges
- DER investor costs and income

$$\min_{\boldsymbol{x},\boldsymbol{y}} \; f(\boldsymbol{x},\boldsymbol{y}) + \frac{a}{b} \sum_{j\in\mathcal{N}_{\mathrm{DER}}} \sum_{t\in\mathcal{T}} \lambda_{j,t} \; y_{j,t}^{\mathrm{EXP}}$$

$$\text{s.t. } g(\boldsymbol{x},\boldsymbol{y}) \leq \boldsymbol{0}$$

$$\boldsymbol{y} \in \arg\min_{\boldsymbol{y}\in\mathcal{R}^N} \; \boldsymbol{c}^{\mathsf{T}}\boldsymbol{y} - b \sum_{j\in\mathcal{N}_{\mathrm{DER}}} \sum_{t\in\mathcal{T}} x_{j,t}^{\lambda} \; y_{j,t}^{\mathrm{EXP}}$$

$$\text{s.t. } \underline{\boldsymbol{y}} \leq \boldsymbol{y} \leq \overline{\boldsymbol{y}} \quad (\underline{\boldsymbol{\mu}}, \overline{\boldsymbol{\mu}})$$

$$\boldsymbol{V}\boldsymbol{y} = \boldsymbol{w} \quad (\boldsymbol{\lambda}).$$
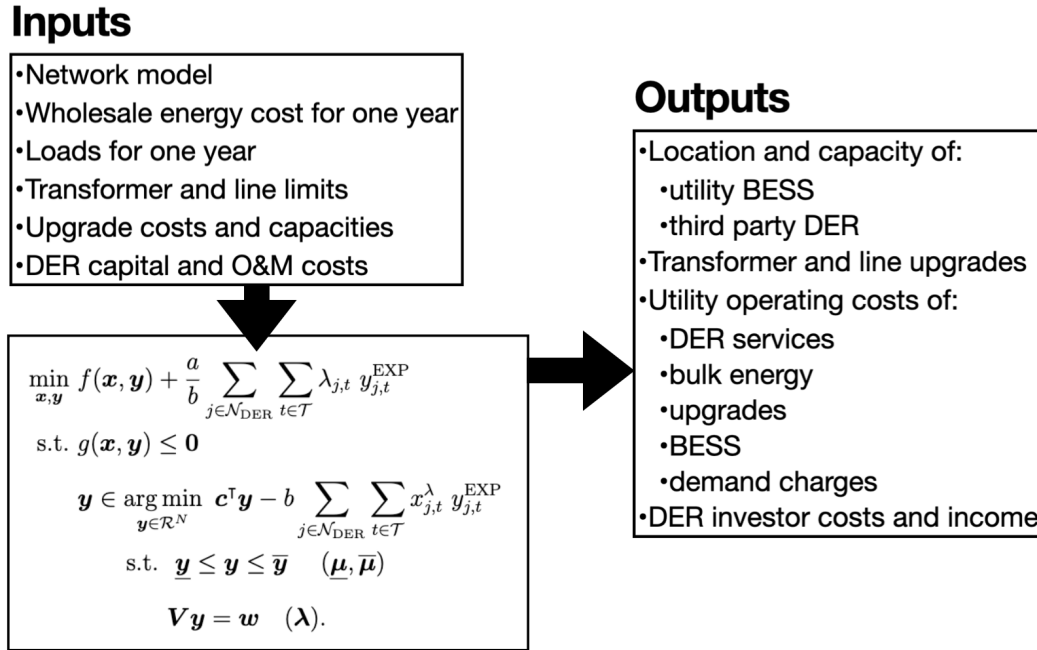
Figure 4.2: Summary of the use-case example inputs and outputs used to demonstrate the method for valuing DER for non-wires alternatives.

Figure 4.3 gives an overview of the overloaded network components, where the DSO is considering installing BESS, and where it is possible for the DER investors

[2]Random combinations of profiles from [56] were scaled to match the test system.

to install PV systems.
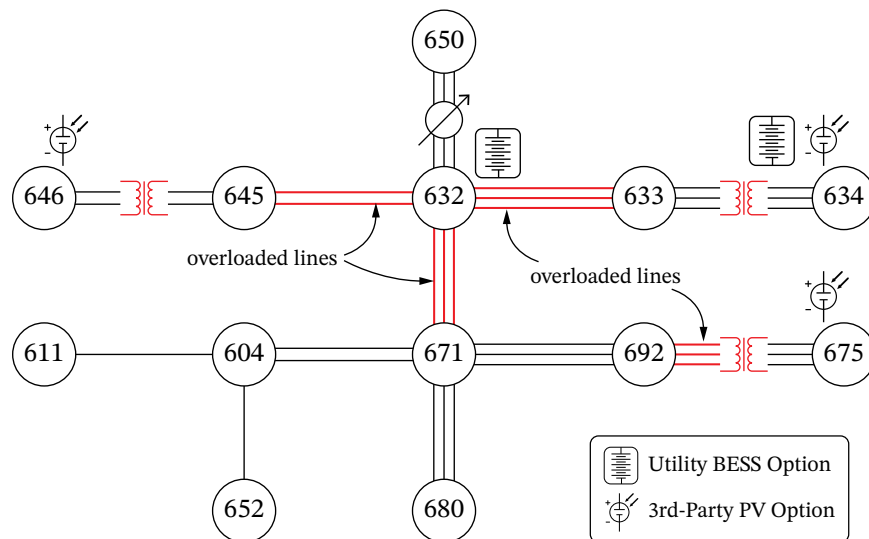
Figure 4.3: Overview of the IEEE 13 Bus Test System showing the DER and BESS options as well as the overloaded lines and transformers. Secondary transformers at buses 634, 646, and 675 have peak loads of 143%, 111%, and 167% as percent of ratings respectively. Overloaded lines are all assumed to have 110% overloads compared to their capacity ratings. Graphic by Jeffrey M. Phillips.

4.2.1 System Planner Problem

The upper level problem in the bilevel framework represents the system planner's perspective. The upper level cost function $f(\boldsymbol{x}, \boldsymbol{y})$ is the sum of battery capital costs, the cost of transformer and line upgrades, the cost of bulk energy purchased, and the peak demand charges:

$$
\begin{aligned}
f(\boldsymbol{x}, \boldsymbol{y}) = & \sum_{j \in \mathcal{N}^{\mathrm{BESS}}, \forall \phi \in \Phi_j} \left(c^{\mathrm{BkW}} x_{j,\phi}^{\mathrm{BkW}} + c^{\mathrm{BkWh}} x_{j,\phi}^{\mathrm{BkWh}} \right) \\
& + \sum_{j \in \mathcal{N}^{\mathrm{TRF}}} c_j^{\mathrm{TRF}} z_j^{\mathrm{TRF}} + \sum_{j \in \mathcal{N}^{\mathrm{LINE}}} c_j^{\mathrm{LINE}} z_j^{\mathrm{LINE}} \\
& + \mathrm{pwf}_{\mathrm{UL}} \sum_{t \in \mathcal{T}} \left(c_t^{\mathrm{LMP}} \sum_{\phi \in \Phi_0} P_{0,\phi,t}^+ \right) \\
& + \mathrm{pwf}_{\mathrm{UL}} \sum_{s \in (1,\dots,|\mathcal{S}|)} c_s^{\mathrm{DEM}} P_s^{\mathrm{MAX}}
\end{aligned}
\tag{4.6}
$$

The cost coefficients in (4.6) are defined in Table 4.4 and the variables in (4.6) are defined in Table 4.1. Note that the net power at the feeder head $P_{0,\phi,t}$ decisions implicitly include lower level decisions via the power flow constraints shown below. Also, we assume that the DSO is not compensated for exported power by including only the non-negative power $P_{0,\phi,t}^+$ (defined in (4.7)) at the feeder head in the objective function.

$$P_{0,\phi,t}^+ \geq 0 \tag{4.7a}$$

$$P_{0,\phi,t}^+ \geq P_{0,\phi,t}, \forall \phi \in \Phi, \forall t \in \mathcal{T} \tag{4.7b}$$

DSO are not typically compensated for exported power and can even be restricted to not export at all by contractual agreements or regulations.

The upper level present worth factor pwf_{UL} accounts for annual recurring costs, and is defined as:

$$a = \text{pwf}_{\text{UL}} = \sum_{y \in 1..N_{\text{years}}} \left(\frac{(1 + r_e)(1 + r_c)}{1 + r_{\text{WACC}}} \right)^y \tag{4.8}$$

where r_e is the annual cost of electricity growth rate, r_c is the annual energy consumption growth rate, and r_{WACC} is the planner's weighted average cost of capital rate. Present worth factors are commonly used to account for long time-horizon financial analyses. The present worth factor effectively makes any costs that it multiplies an annuity that grows each year at the rates in the numerator, and is discounted into present value by the rate in the denominator. The DSO's present worth factor accounts for the annual growth of bulk energy costs and energy consumption. The cost of capital rate accounts for the DSO guaranteed rate of return on investment (if the DSO is investor owned) or the cost of borrowing money to upgrade the system (if the DSO is publicly owned such as a cooperative).

The system planner also has the option to purchase energy from DER (as described in the Section 5.1). For these use-case examples we set the coefficient a in (4.3) equal to the system planner's present worth factor pwf_{UL}. The additional cost component for the planner is thus:

$$\text{pwf}_{\text{UL}} \sum_{j \in \mathcal{N}_{\text{DER}}} \sum_{t \in \mathcal{T}} x_{j,t}^{\lambda} \, y_{j,t}^{\text{EXP}}. \tag{4.9}$$

Together equations (4.6) and (4.9) make up the upper level objective function.

Table 4.4: Parameter values for the distribution system planner in the use-case example.

name	description	value
c^{BkW}	cost of BESS inverter [\$/kW]	300
c^{BkWh}	cost of BESS capacity [\$/kWh]	250
c_j^{TRF}	cost of a new transformer [\$]	150,000
c_j^{LINE}	cost of a new line [\$]	length×200+15,000
c_t^{LMP}	wholesale cost of energy [\$/kWh]	varies
c_s^{DEM}	peak demand cost in period s [\$/kW]	50
η	BESS efficiency [fraction]	0.96
ΔR_j^{TRF}	increase in transformer rating [kW]	varies
$\overline{R}_j^{\text{TRF}}$	existing transformer rating [kW]	varies
ΔR_j^{LINE}	increase in line rating [kW]	varies
$\overline{R}_j^{\text{LINE}}$	existing line rating [kW]	varies
r_e	energy cost growth rate [year^{-1}]	0.03
r_e	energy consumption growth rate [year^{-1}]	0.03
r_{WACC}	weighted avg. cost of capital [year^{-1}]	0.10

Battery Energy Storage Systems

The system planner considers purchasing BESS systems, which can preclude or reduce the size of system upgrades, lower the cost of bulk energy purchases via energy arbitrage, as well as reduce peak demand charges. The BESS operational constraints are shown in (4.10).

$$x_{j,\phi,t}^{\text{SOC}} = x_{j,\phi,t-1}^{\text{SOC}} + x_{j,\phi,t}^{\text{B}^+}\eta - x_{j,\phi,t}^{\text{B}^-}/\eta$$

$$\forall j \in \mathcal{N}_{\text{BESS}}, \forall \phi \in \Phi_j, \forall t \in \mathcal{T} \tag{4.10a}$$

$$x_{j,\phi}^{\text{BkW}} \geq x_{j,\phi,t}^{\text{B}^+} + x_{j,\phi,t}^{\text{B}^-}, \ \ \forall j \in \mathcal{N}_{\text{BESS}}, \forall \phi \in \Phi_j, \forall t \in \mathcal{T} \tag{4.10b}$$

$$x_{j,\phi}^{\text{BkWh}} \geq x_{j,\phi,t}^{\text{SOC}}, \ \ \forall j \in \mathcal{N}_{\text{BESS}}, \forall \phi \in \Phi_j, \forall t \in \mathcal{T} \tag{4.10c}$$

$$x_{j,\phi,0}^{\text{SOC}} = 0.5 x_{j,\phi}^{\text{BkWh}}, \ \ \forall j \in \mathcal{N}_{\text{BESS}}, \forall \phi \in \Phi_j \tag{4.10d}$$

$$x_{j,\phi,T}^{\text{SOC}} = 0.5 x_{j,\phi}^{\text{BkWh}}, \ \ \forall j \in \mathcal{N}_{\text{BESS}}, \forall \phi \in \Phi_j \tag{4.10e}$$

$$x_{j,\phi,t}^{\text{SOC}} \geq 0, x_{j,\phi}^{\text{BkWh}} \geq 0, \ \ \forall j \in \mathcal{N}_{\text{BESS}}, \forall \phi \in \Phi_j, \forall t \in \mathcal{T} \tag{4.10f}$$

In words, the BESS constraints are:

- (4.10a) defines the time evolution of the battery state of charge;

- (4.10b) says that the sum of the battery power decisions can be at most the inverter rating;

- (4.10c) says that the battery state of charge is at most the battery energy rating;

- (4.10d) says that the initial state of charge is half of the energy rating;

- (4.10e) says that the final state of charge is half of the energy rating; and

- (4.10f) says that the state of charge and energy rating decisions are non-negative.

Note that though it is common to use binary variables to restrict a BESS from charging and discharging in a single time step of a mathematical program, the additional binary variables are generally unnecessary (unless some specific control context requires the restriction). In most cases an optimal solution will not include simultaneous charging and discharging of a battery due to the round trip losses. However, when the benefit of one action exceeds the cost of the other (including losses) then an optimal solution can include simultaneous charging and discharging. For planning problems such as this, with generally long time steps (one hour in the examples), the simultaneous dispatch is a non-issue because we include the constraint (4.10b), i.e. the total energy through the battery still obeys the physics. For example, say that a BESS with 10% roundtrip losses can charge at a cost of 0.1\$/kWh, discharge for income of 1.1\$/kWh, has a zero state-of-charge, and a 1 kW inverter rating. The optimal solution for the BESS is to charge for approximately 0.91 of the hour and discharge for 0.09 of the hour to profit \$0.009. In other words, one can think of the battery doing two independent actions for parts of the hour in order to profit.

In practice, system planners should account for the degradation of BESS over their operational life. However, degradation mechanisms are non-linear and therefore difficult to model in large mathematical programs for system planning (c.f. [75]). Recent work has identified two primary explanatory variables for modeling degradation (besides temperature): equivalent full cycles (EFC) and depth of discharge (DoD) [76]. In collaboration with the first author of [76] the first author of this work determined a method to model non-linear battery degradation using the EFC and DoD variables in a mixed integer linear program [77]. The model is publicly available in the National Renewable Energy Laboratory's flag-ship techno-economic optimization model for DER sizing and dispatch: REopt [78]. For simplicity of exposition we do not include the degradation model in the use-case example. The impact of including

a degradation model is to effectively raise the upfront cost of the BESS. However, the cost of degradation is small when compared to bulk energy arbitrage and peak cost reduction opportunities that BESS enable and therefore the inclusion of degradation costs in the use-case examlpes would not significantly change the results.

Transformer and Line Upgrades

The system planner has binary decisions for transformer and line upgrades (see Table 4.1). If a component is upgraded then its operational limits are expanded by the difference in capacity between the original component and the new component. This fact is reflected in Equation (4.11) for transformers and Equation (4.12) for lines.

$$-\overline{R}_j^{\text{TRF}} - z_j^{\text{TRF}} \Delta R_j^{\text{TRF}} \leq P_{j,\phi,t} \leq \overline{R}_j^{\text{TRF}} + z_j^{\text{TRF}} \Delta R_j^{\text{TRF}},$$
$$\forall j \in \mathcal{J}^{\text{TRF}}, \forall \phi \in \Phi_j, \forall t \in \mathcal{T} \tag{4.11}$$

$$-\overline{R}_j^{\text{LINE}} - z_j^{\text{LINE}} \Delta R_j^{\text{LINE}} \leq P_{ij,\phi,t} \leq \overline{R}_j^{\text{LINE}} + z_j^{\text{LINE}} \Delta R_j^{\text{LINE}},$$
$$\forall j \in \mathcal{J}^{\text{LINE}}, \forall \phi \in \Phi_j, \forall t \in \mathcal{T} \tag{4.12}$$

Power Flow

The planner's constraint set also includes a three phase, unbalanced LinDist-Flow model [79].[3] The power flow constraints are shown in (4.13).

$$P_{ij,\phi,t} + P_{j,\phi,t} - \sum_{k:j\to k} P_{jk,\phi,t} = 0,$$
$$\forall j \in \mathcal{N}, \forall \phi \in \Phi_j, \forall t \in \mathcal{T} \tag{4.13a}$$

$$Q_{ij,\phi,t} + Q_{j,\phi,t} - \sum_{k:j\to k} Q_{jk,\phi,t} = 0,$$
$$\forall j \in \mathcal{N}, \forall \phi \in \Phi_j, \forall t \in \mathcal{T} \tag{4.13b}$$

---

[3]As part of this work an open-source *Julia* implementation of LinDistFlow was created [80].

$$\boldsymbol{v}_{j,t} = \boldsymbol{v}_{i,t} + \boldsymbol{M}_{ij}^{P}\boldsymbol{P}_{ij,t} + \boldsymbol{M}_{ij}^{Q}\boldsymbol{Q}_{ij,t},$$

$$\forall (i,j) \in \mathcal{E}, \ \forall t \in \mathcal{T} \tag{4.13c}$$

$$P_{0,\phi,t} = P_{01,\phi,t} \ \forall \phi \in \Phi_0, \forall t \in \mathcal{T} \tag{4.13d}$$

$$Q_{0,\phi,t} = Q_{01,\phi,t}, \ \forall \phi \in \Phi_0, \forall t \in \mathcal{T} \tag{4.13e}$$

$$\underline{P}_{j,\phi} \le P_{j,\phi,t} \le \overline{P}_{j,\phi} \ \forall j \in \mathcal{N}, \forall \phi \in \Phi_j, \forall t \in \mathcal{T} \tag{4.13f}$$

$$\underline{Q}_{j,\phi} \le Q_{j,\phi,t} \le \overline{Q}_{j,\phi} \ \forall j \in \mathcal{N}, \forall \phi \in \Phi_j, \forall t \in \mathcal{T} \tag{4.13g}$$

$$\underline{P}_{ij,\phi} \le P_{ij,\phi,t} \le \overline{P}_{ij,\phi} \ \forall (i,j) \in \mathcal{E}, \forall \phi \in \Phi_j, \forall t \in \mathcal{T} \tag{4.13h}$$

$$\underline{Q}_{ij,\phi} \le Q_{ij,\phi,t} \le \overline{Q}_{ij,\phi} \ \forall (i,j) \in \mathcal{E}, \forall \phi \in \Phi_j, \forall t \in \mathcal{T} \tag{4.13i}$$

$$\underline{v} \le v_{j,\phi,t} \le \overline{v}, \ \forall j \in \mathcal{N}, \ \forall \phi \in \Phi_j, \ \forall t \in \mathcal{T} \tag{4.13j}$$

The real and reactive power balances are shown in (4.13a) and (4.13b) respectively. Equation (4.13c) defines the vector of voltage magnitudes squared for each phase, where $\boldsymbol{M}_{ij}^{P}$ and $\boldsymbol{M}_{ij}^{Q}$ are 3×3 matrices of line resistances and reactances (see equations (20) and (21) in [79]), the vector $\boldsymbol{v}_{j,t} = [v_{j,1,t}, v_{j,2,t}, v_{j,3,t}]^{\mathsf{T}}$ collects the phase voltages (squared), and similarly the vectors $\boldsymbol{P}_{ij,t} = [P_{ij,1,t}, P_{ij,2,t}, P_{ij,3,t}]^{\mathsf{T}}$ and $\boldsymbol{Q}_{ij,t} = [Q_{ij,1,t}, Q_{ij,2,t}, Q_{ij,3,t}]^{\mathsf{T}}$ collect the phase line flows. Equations (4.13d) and (4.13e) state that the net power at the feeder head is equal to power transferred along the lines from node zero to one. And the remaining constraints (4.13f) – (4.13j) define upper and lower bounds.

Note that the power injection variables at busses without potential DER are not decision variables. However for busses with candidate DER the power injections are as defined in 4.14.

$$P_{j,\phi,t} = -d_{j,\phi,t} - x_{j,\phi,t}^{\mathrm{B}^+} + x_{j,\phi,t}^{\mathrm{B}^-} + y_{j,\phi,t}^{\mathrm{DER}}$$

$$\forall j \in \mathcal{N}_{\mathrm{DER}} \cap \mathcal{N}_{\mathrm{BESS}}, \forall \phi \in \Phi_j, \forall t \in \mathcal{T} \tag{4.14a}$$

$$P_{j,\phi,t} = -x^{\mathrm{B}^+}_{j,\phi,t} + x^{\mathrm{B}^-}_{j,\phi,t}$$

$$\forall j \in \mathcal{N}_{\mathrm{BESS}} \cap \mathcal{N}_{\mathrm{DER}}, \forall \phi \in \Phi_j, \forall t \in \mathcal{T}$$

(4.14b)

$$P_{j,\phi,t} = -d_{j,\phi,t} + y^{\mathrm{DER}}_{j,\phi,t}$$

$$\forall j \in \mathcal{N}_{\mathrm{DER}} \setminus \mathcal{N}_{\mathrm{BESS}}, \forall \phi \in \Phi_j, \forall t \in \mathcal{T}$$

(4.14c)

The peak demand in each demand period P^{MAX}_s is defined as the highest demand at the substation in a demand period:

$$P^{\mathrm{MAX}}_s \geq \sum_{\phi \in \Phi_0} P_{0,\phi,t} \quad \forall t \in s, \forall s \in \mathcal{S}$$

(4.15)

Lastly, the upper level includes a structural constraint that prevents simultaneous import and export of energy (which we model with special order sets of type 1):

$$y^{\mathrm{IMP}}_{j,\phi,t} \perp y^{\mathrm{EXP}}_{j,\phi,t}, \quad \forall j \in \mathcal{N}_{\mathrm{DER}}, \forall \phi \in \Phi_j, \forall t \in \mathcal{T}$$

(4.16)

4.2.2 DER Investor Problem

The potential DER investors have known demands and a time varying cost of energy. Note that if DER costs are low enough (or energy costs high enough) it is possible that DER capacity is installed even in the absence of the price signal.

The lower level costs are:

$$\sum_{j \in \mathcal{N}_{\mathrm{DER}}} \left(c^{\mathrm{kW}}_j y^{\mathrm{kW}}_j + \mathrm{pwf}_{\mathrm{LL}} \left[c^{\mathrm{OM}} y^{\mathrm{kW}}_j + \sum_{t \in \mathcal{T}} c^{\mathrm{IMP}}_{j,t} y^{\mathrm{IMP}}_{j,t} \right] \right),$$

(4.17)

which in words is the sum over all potential DER investor nodes $\mathcal{N}_{\mathrm{DER}}$ of:

- the capital cost of DER $c^{\mathrm{kW}}_j y^{\mathrm{kW}}_j$,

- the operations and maintenance cost of DER $c^{\mathrm{OM}} y^{\mathrm{kW}}_j$,

- and the cost of energy $c^{\mathrm{IMP}}_{j,t} y^{\mathrm{IMP}}_{j,t}$.

The DER investor parameters and variables are summarized in Tables (4.5) and (4.1) respectively.

The lower level benefits (negative costs) are the sum of the price signal $x_{j,t}^{\lambda}$ from the upper level and the exported energy $y_{j,t}^{\text{EXP}}$ over time and space:

$$-\text{pwf}_{\text{LL}} \sum_{j \in \mathcal{N}_{\text{DER}}} \sum_{t \in \mathcal{T}} x_{j,t}^{\lambda} \, y_{j,t}^{\text{EXP}}. \tag{4.18}$$

Note that the bilinear product of upper and lower level decisions in (4.18) are linearized when the lower level problem is replaced with its KKT conditions (see (4.5)).

The lower level present worth factor pwf_{LL}, defined in (4.19), accounts for the:

- years of the analysis period N_{years},

- the RoR,

- the annual cost of energy growth rate r_e,

- and the annual energy consumption growth rate r_c.

$$b = \text{pwf}_{\text{LL}} = \sum_{\text{year} \in 1..N_{\text{years}}} \left(\frac{(1 + r_e)(1 + r_c)}{1 + \text{RoR}} \right)^{\text{year}} \tag{4.19}$$

The DER investor load balance defines the net power injection for each node and time step:

$$d_{j,t} - y_{j,t}^{\text{DER}} = y_{j,t}^{\text{IMP}} - y_{j,t}^{\text{EXP}} \; (\lambda_{j,t}), \; \forall j \in \mathcal{N}_{\text{DER}}, \forall t \in \mathcal{T} \tag{4.20}$$

Lastly, the real power production of any DER is limited by the purchased capacity and a time-varying production factor (between zero and one):

$$y_{j,t}^{\text{DER}} \leq y_{j}^{\text{kW}} f_{j,t}^{\text{prod}}, \; \forall j \in \mathcal{N}_{\text{DER}}, \forall t \in \mathcal{T} \tag{4.21}$$

Table 4.5: DER investor baseline parameter values for the use-case example.

name	description	value
c_j^{kW}	cost of DER at node j [\$/kW]	1,600
c^{OM}	annual cost of operations and maintenance [\$/(kW-year)]	17
$c_{j,t}^{\text{IMP}}$	cost of energy imported [\$/kWh]	0.15
$d_{j,t}$	uncontrollable demand [kW]	[56]
$f_{j,t}^{\text{prod}}$	production factor, 0–1	[58]
r_e	energy cost growth rate [year^{-1}]	0.03
r_e	energy consumption growth rate [year^{-1}]	0.03
ROR	required rate of return [year^{-1}]	0.15

4.3 Results

Figure 4.4 provides a high level summary of the results. In the baseline case the system planner must upgrade the overloaded components and cannot invest in BESS nor purchase DER energy. The total lifecycle cost (LCC) for the planner is \$8.41M over 20 years of operations, including the capital costs of upgrades. A break down of the planner's baseline costs are summarized in Table 4.6.
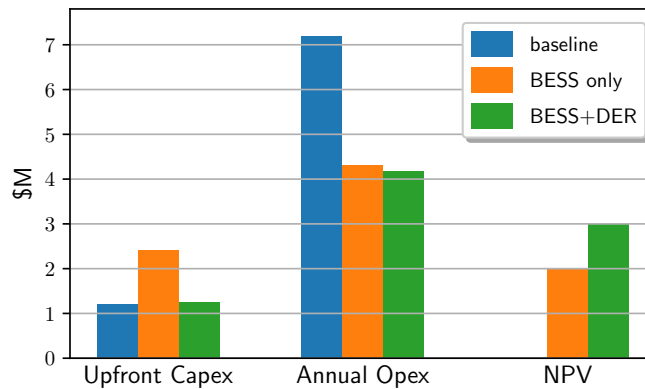

Figure 4.4: Case study summary results. See Table 4.6 for a break down of the upfront capital costs (capex) and the annual operating costs (opex). The net present value (NPV) is by definition zero in the baseline case.

74

Figure 4.5 shows the annual costs in the base scenario. Note that the first bar represents the upfront capital costs, which in the base case include the traditional upgrade costs for the lines and transformers with expected overloads. The annual operating costs include the cost of bulk energy as well as the coincident peak demand charges.

Table 4.6: A summary of the use-case example results for the baseline, BESS only, and BESS with DER valued as non-wires alternatives. All dollar values are in millions. (Abbreviations: "LCC" = lifecycle cost, "Trfx" = transformer, "capex" = capital cost.). The DSO capital costs include the transformer upgrades, line upgrades, and BESS "capex". The DSO operating costs include the cost of bulk energy, demand charges, and DER energy.

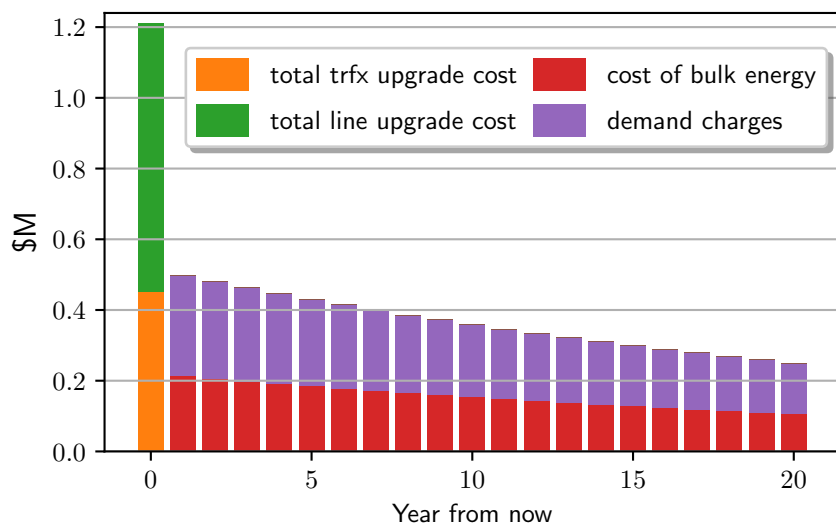|	Baseline	BESS only	BESS & DER
Total LCC	$8.41	$6.43	$5.42
Net present value	–	$1.98	$2.99
Trfx upgrades	$0.45	$0.30	$0.15
Line upgrades	$0.76	$0.65	$0.12
Bulk energy	$3.09	$1.70	$1.17
Demand charges	$4.11	$2.61	$2.25
BESS capex	–	$1.47	$0.96
DER energy	–	–	$0.75
Lines upgraded	4/4	3/4	1/4
Trfxs upgraded	3/3	2/3	1/3

Figure 4.5: Upfront capital costs (in year zero) and annual, discounted operating costs for the DSO in the base case with traditional upgrades.

Next, we present the results for the system planner when considering only BESS investments (without purchasing DER energy). The DSO can install BESS at nodes 632 and/or 634 (see Figure 4.3). In this scenario it is cost optimal for the DSO to install a 4.4 hour, 21.8 kW BESS at bus 634 and a 4.8 hour, 961 kW BESS at bus 632. With these BESS the total life cycle cost is $6.43M, yielding $1.98M in savings over the base scenario. The addition of the BESS also prevent the need to upgrade one of the lines (632-633) as well as the transformer at bus 634.
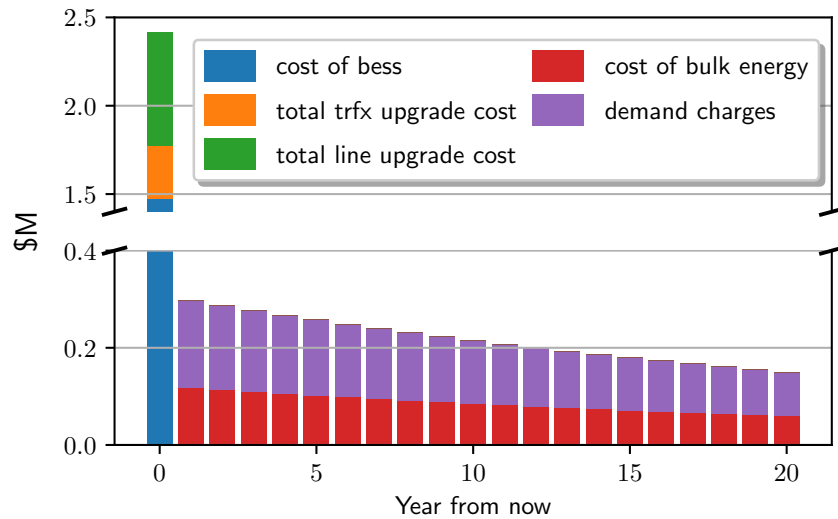
Figure 4.6: Upfront capital costs (in year zero) and annual, discounted operating costs for the DSO considering only BESS (no DER). Note the much higher upfront costs when compared to the base line upfront costs in Figure 4.5 come with the benefit of lower annual operating costs as compared to the base scenario.

Comparing the cash flows with and without BESS in Figures 4.5 and 4.6 respectively, yields two key observations: i) the planner's upfront capital costs are approximately doubled with the BESS investment, even though the line and transformer upgrade costs are reduced relative to the base case; and ii) the first year operating costs are reduced by approximately $0.2M with the optimal BESS.

In the third and final scenario we include the value of DER for non-wires alternatives. Now, with the option to purchase DER energy the DSO total lifecycle cost is $5.42M, yielding an additional cost reduction of $1.01M over the BESS only scenario for a total net present value of $2.99M. The DSO reduces its cost of energy by purchasing DER exported energy at the DER investor's marginal cost, in this case 15 cents/kWh[4]. Additionally, with the DER contributions the DSO only needs to

---

[4]We do not use time-varying retail rates to keep the use-case examples relatively easy to understand. However, there is no limit on the form of the retail rates.

upgrade one of the three overloaded transformers (at bus 675) and one set of the four overloaded lines (692-675). Table 4.6 summarizes the costs when valuing DER.

Figure 4.7 shows the annual cash flows for the third scenario with DER valued. Note that the upfront costs are comparable to the base scenario but the annual operating costs are significantly reduced when compared to the base scenario cash flows in Figure 4.5.
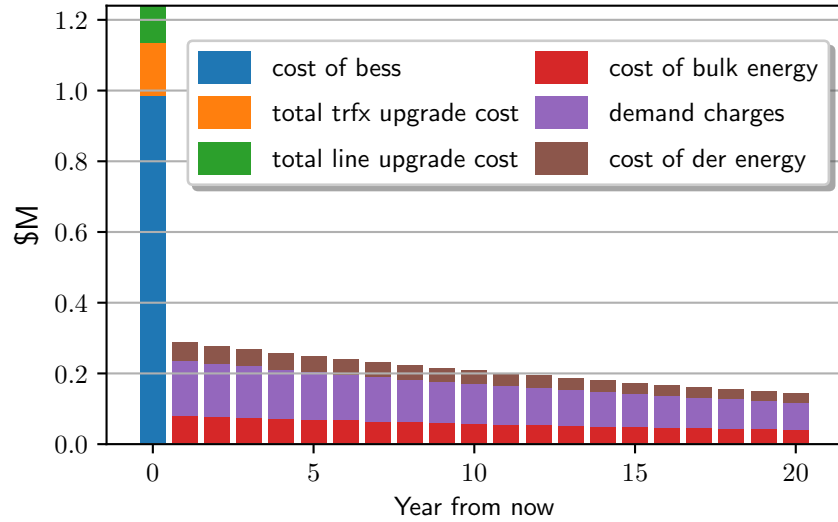
Figure 4.7: Upfront capital costs (in year zero) and annual, discounted operating costs for the DSO considering BESS and DER for non-wires alternatives. The upfront capital costs are comparable to the traditional upgrade costs and much lower than the upfront costs in the BESS only scenario shown in Figure 4.6. Also, the annual operating costs are much lower than the baseline scenario shown in Figure 4.5 and lower than the BESS only scenario, even with the additional cost of purchasing DER energy.

For reference we also provide the DER investor results with and without the DSO price signal in Table 4.7. Note that the net present cost values are the same with and without the price signal. In both cases the DER investors obtain their required rate of returns. However, in the case with the price signal the additional costs of the larger DER systems are offset with the income from selling energy as well as the

additional energy cost savings.

Table 4.7: Use-case example results summary for DER investors with and without the price signal from the DSO. All dollar values are in millions, total present value. (Abbreviations: "capex" = capital cost, "opex" = operating cost.)

	no signal	with signal
Net present cost	$2.79	$2.79
DER capex	$0.43	$1.59
DER opex	$0.04	$0.16
Income	–	$0.51
Energy cost savings	$0.53	$1.30
Bus 634 capacity	67 kW	138 kW
Bus 646 capacity	124 kW	305 kW
Bus 675 capacity	79 kW	550 kW
Internal Rate of Return	16.6%	15.2%

4.4 Discussion

Using the proposed framework for valuing DER as non-wires alternatives, the use-case examples demonstrate the potential for reducing system operating costs in ways that benefit the DSO as well as DER investors. Ultimately, it is reasonable to expect that lower system costs will lead to lower costs for all customers.

The use-case examples assumed that DER investors consider PV systems since they are cost-competitive in many areas and are not subject to emission regulations like back-up gas generators. However, back-up gas generators could provide a significant value proposition for both the DSO and DER investors by providing power during evening peak loads (unlike PV systems) as well as serve customer critical loads during outages. The proposed framework for valuing DER can account for gas generators by removing the time varying limit on the DER production and adjusting the

cost parameters.

All scenarios were solved on a 2017 Macbook Pro with two each 2.8 GHz Quad-Core Intel i7 chips, 16 GB of RAM, and Gurobi version 9. The bilevel problem solve time was limited to one hour, in which it reached an optimality gap of less than two percent. While the long solve time may indicate that the bilevel method may not scale well to large problems, no efforts were made to make the bilevel problem easier to solve. Future work could include appropriately scaling the problem coefficients as well as decomposing the problem into sub-problems and leveraging advanced solution techniques.

A major advantage of the proposed framework is its flexibility. For example, it is straightforward to account for different DER types in the lower level problem, as long as they can be modeled in a linear fashion. The upper level problem is not limited to linear equations, as demonstrated in the use-case example with the inclusion of integer decisions for the transformer and line upgrades. Another example of leveraging the flexibility of the framework would be to replace the non-negative bulk power purchases $P_{0,\phi,t}^{+}$ with the net power $P_{0,\phi,t}$ in the upper level objective (4.6). Valuing power exported to the bulk system would increase the value of DER for non-wires alternatives by adding another value stream for the DSO. For example, it is possible that DSO could sell excesss energy in a bulk market.

4.5 Conclusion

Valuing DER for non-wires alternatives appropriately is a difficult task. The framework proposed in this work accounts for both the system planner's perspective and the DER investor perspectives. The bilevel optimization framework guarantees that solutions minimize the planner's costs over the chosen horizon as well that the

DER investors achieve their required rate of returns. In light of FERC Order 2222 [9] and expected growth in load and DER adoption [81] it is becoming more and more important for system planners to work with DER investors to plan efficient distribution power systems.

Using a use-case example we showed how the framework can be leveraged to value DER for non-wires alternatives. Comparing life cycle costs over 20 years for the system planner, the results show that by valuing DER for non-wires alternatives the DSO can avoid upgrading most of the overloaded components as well as achieve a net present value of nearly $3M relative to the cost of the traditional upgrades. We also compared the solution with DER valued to a scenario with utility owned batteries and no third-party DER value. The results show that the DSO can achieve an additional $1M in net present value when valuing DER relative to the scenario with utility owned batteries.

In future work we intend to leverage the bilevel framework in a transactive control context. Transactive control methods that account for the DSO perspective and the DER owner objectives are necessary to appropriately motivate DER to provide services that benefit the entire system.

Chapter 5

A method to generate realistic synthetic electricity market price scenarios

Advances in regulatory policies that expand market access to renewable energy (RE) generation and energy storage technologies are bringing a broader and more diverse set of market participants to wholesale electricity markets in the United States. Regulatory directives such as Federal Energy Regulatory Commission (FERC) Order 841 focus on creating avenues for the participation of energy storage resources in wholesale markets [82]. Similarly, FERC Order 2222 is opening up market participation to aggregations of distributed energy resources (DER), ensuring market access to a diverse set of new market actors [9]. The expanded market access that these regulatory directives afford is happening in conjunction with rapid cost declines for RE and storage technologies [83]. These factors — as well as other considerations such as decarbonization and energy resilience — are combining to drive more installations of RE and storage assets, bringing more resources online at a rapid pace [84].

The increase in number and diversity of energy resources in wholesale electricity markets is happening in tandem with an increase in the uncertainty in wholesale electricity prices. Increased price volatility is driven in large part by growing pene-

---

Sections of this chapter were adapted from the technical report: [14]. The majority of this paper's research, analysis, and writing were completed by the author of this dissertation. The co-authors contributed to the literature review, editing, writing, and technical development.

trations of variable renewable energy generation (primarily wind and solar) [85], but also by extreme weather events and overall net demand variability [86] [87].

Participants need effective bidding models to enable profitable participation in these increasingly diverse and volatile markets. While many approaches to strategic bidding exist — including optimization, equilibrium, and simulation approaches — there is a significant amount of ongoing research in establishing the most effective methods. One attribute that is common to most of the bidding approaches is that they rely on the ability to form an accurate expectation of market prices [88]. Thus, to assess the performance of the various approaches being proposed, methods to model expected market prices and associated uncertainty are needed. This will enable researchers to understand (and improve) the performance of different bidding approaches. Accurate characterization of price forecast uncertainty can help market participants evaluate the efficacy of potential bidding strategies under many different possible pricing regimes and futures.

A key challenge in modeling day-ahead and real-time electricity prices is that the underlying probability distribution often has heavy or fat tails [89]. Fat-tailed distributions are highly skewed and have an undefined variance, which makes them difficult to model. Occurrences of extreme price events are typically characterized as a stochastic process, but stochastic processes that arise from fat-tailed distributions are not mathematically well-behaved; using a probability function with a defined variance will under-represent the probability of extreme observations [90]. In electricity markets, extreme observations can be disruptive and/or result in high profit or loss, which strongly impacts the profitability of a given bidding strategy.

This work presents an approach for generating statistically representative time series that exhibit high-periodicity and heavy tails, and capture the uncertainty ob-

served in electricity markets. To achieve an accurate characterization of electricity prices, the price generation process is divided into two components: a deterministic component and a stochastic component. The two components are synthesized into time series. The methodology to stochastically generate synthetic prices is presented in the following. A discussion of the goodness of fit and moments as compared to realized prices is also presented. To evaluate the performance of the methods, synthetic, price scenarios are generated for the Electricity Reliability Council of Texas's (ERCOT) Houston Hub for the years 2018 and 2019 [91]. The price scenarios are used to demonstrate the method, but the techniques are applicable to any hourly or sub-hourly electricity pricing data from deregulated wholesale markets across the United States and throughout the world.

The synthetic price generation methodology builds on considerable research in two distinct areas: stochastic differential equations (SDE) for forecasting electricity prices (specifically mean-reversion and jump-diffusion modeling) and auto-regressive integrated moving average (ARIMA) modeling for price forecasting. Previous work in applying SDEs to electricity prices has generally focused on daily average prices [40]. To extend these methods to hourly or sub-hourly pricing, the mean-reversion component of the SDE is replaced with an ARIMA process that is better able (than standard linear regression approaches) to characterize the daily and weekly patterns. The jump process is extended to account for conditional probabilities of price spikes occurring in consecutive hours. Next, to capture the conditional probabilities, the traditional Poisson process for modeling jumps is replaced with a generalized point process model, including a conditional intensity function. Finally, traditional methods of estimating spike intensity (e.g. sampling into estimated distribution parameters) are replaced with a Markov chain where the transition matrices are derived from observed price spike transitions.

In addition to presenting the results on the quality of the synthetic price time series, a use-case of the synthetic price generation method for testing market bidding approaches in a stochastic optimization model is presented. For each bidding period 1,000 price scenarios are generated along with probabilities using the synthetic pricing methodology. Then, k-means clustering is applied on the 1,000 scenarios to generate 10 scenarios that are used as input to the stochastic optimization model. Finally, profit performance of this stochastic model is compared against a persistence forecast model.

In summary, a synthetic price generation methodology is developed that brings together jump diffusion modeling and ARIMA modeling to generate hourly electricity prices that capture both the seasonal (including weekly/hourly and annual seasonality) mean-reverting trend and the stochastic nature of price spikes (including inter-hour spike dependencies). To the author's knowledge this is the first application of jump-diffusion modeling to electricity markets, specifically enabled by the integration of ARIMA models and generalized point processes for jump arrivals. Specific contributions include:

- The integration of ARIMA models as the deterministic component of an SDE

- Replacement of the standard Poisson process in jump modeling by a generalized point process allowing for non-homogeneous and history-dependent spike modeling

- Integration of Markov chain transition matrices to model spike intensities and enable improved estimation of price transitions during multi-hour spike events

5.1 Method

The methodology is laid out as follows: first, an overview of the SDE used in the price generation approach is presented (contrasting it to previous work in the field); second, each of the three terms in the SDE are discussed and the derivation of relevant parameters is outlined.

5.1.1 Summary of the Stochastic Differential Equation

The approach builds from a general SDE that captures the mean-reversion and jump-diffusion characteristics of the electricity spot price S_t at time t. The baseline approach for the mean-reverting, jump-diffusion model is as follows. The log-price process is defined as:

$$\ln S_t = g(t) + Y_t \tag{5.1}$$

where $g(t)$ is a deterministic function and Y_t is a stochastic process. The stochastic process, Y_t, is defined as:

$$dY_t = -\alpha Y_t dt + \sigma(t) dZ_t + \ln J dq_t \tag{5.2}$$

The first term, $-\alpha Y_t dt$, is the mean-reversion term. The speed of mean-regression α is typically derived by linear regression and often combined with $g(t)$ to capture the deterministic component of the log-price process. The second term, $\sigma(t) dZ_t$, is the diffusion term, which combines the volatility observed in the de-spiked prices $(\sigma(t))$ and the increment of a standard Brownian motion (dZ_t). The last term, $\ln J dq_t$, is the jump process that combines a random variable (J), which characterizes the jump size, with a Poisson process (dq_t), which determines the arrival rate of the jump. The arrival rate is based on some intensity λ, which is often empirically derived from the data.

Actual prices are modeled (rather than log-prices) for two reasons. First, the log-transform can affect the skewness of the data that the jump component is aiming to capture, and level prices have been empirically shown to have better performance in capturing spikes [48] [92]. Second, hourly electricity pricing in many markets can take on negative values, which are inherently undefined in log-pricing.

The deterministic component (the combination of $g(t)$ and the mean reversion term) is replaced with an ARIMA process, X_t, that is able to capture the inter-day seasonality of hourly day-ahead and real-time pricing. The modeling of price-levels rather than log-prices and the use of an ARIMA model to capture the deterministic component of the SDE allows us to rewrite equation (5.1) and combine with an integrated equation (5.2) to derive the price process:

$$S_t = X_t + \int_0^t \sigma(\tau)dZ_\tau + \int_0^t Jdq_\tau \tag{5.3}$$

In the following sections, the individual terms in Equation 5.3 are described as well as the methods for deriving the associated parameters.

5.1.2 Mean Reversion Term – ARIMA Modeling

Data Preparation: an ARIMA model is used to capture the mean-reversion component of the realized price time series. Prior to fitting the ARIMA model, the interquartile method is used to remove prices that are considered extreme (i.e. spikes). Equations (5.4) and (5) describe the process for spike identification.

$$IQR \triangleq Q_3 - Q_1 \tag{5.4}$$

$$K_t \notin [(Q_1 - c \times IQR), (Q_3 + c \times IQR)] \tag{5.5}$$

IQR is the inter-quartile range, Q_1 is the 25th empirical quartile, Q_3 is the 75th empirical quartile, c is a multiplier on the IQR, and K_t is a spike at time t. [1]

It is important to note that prior to fitting the ARIMA model he de-spiked time series is tested for a unit root using the Augmented Dickey-Fuller (ADF) test [90]. The ERCOT day-ahead pricing data used in this study do not have a unit root at the 0.01-level, which provides further rationale for using actual prices instead of log-pricing.

In addition to the actual prices, hourly temperature data is used as a co-variate in the ARIMA models. The ADF test was used to verify that these hourly temperature data also do not have a unit root. Based on this, first-order differencing is performed on the hourly temperatures and used as the hourly temperature differences in the ARIMA models. Figure 5.1 shows the data preparation process described here for a representative period in 2019.

ARIMA Fitting: To better capture short-term seasonality (diurnal and weekly), rolling window approach is used to fit an ARIMA model for each consecutive one-week (168 hours) subset of the time series (5.3). The Python package pmdarima was used to fit a unique ARIMA model to each 168-hour window [93]. These models were used to generate the price forecasts discussed below.

$$\text{ARIMA}(\phi, \theta) : X_t = \phi y_{t-1} + e_t - \theta e_{t-1} + \beta(T_t - \phi T_{t-1}) \tag{5.6}$$

In equation (5.6), the auto-regressive portion is the product of ϕ and the time-lagged price; the moving average component is a white noise coefficient at time t (e_t) less the product of θ and the time-lagged white noise, and the covariate component is the

---

[1]In the results and use-case example wa c-value of 3 is used to capture a broader non-spike band than the commonly used 1.5 multiplier.

product of β and the hourly temperature difference at time t (T_t) less the product of ϕ and the time-lagged temperature difference.

5.1.3 Diffusion Term

The diffusion term in the proposed model aligns closely with traditional diffusion modeling where volatility $(\sigma(t))$ is the standard deviation of the residuals from the ARIMA process and the stochastic portion (dZ_t) is standard Brownian motion, using the normal distribution with a zero mean. The volatility is defined on an hourly basis or as a static value. In the time-varying case the volatility is defined based on a rolling window with the number of look-back days, or samples, acting as a hyperparameter in the model.

5.1.4 Jump Term

The jump component of the model extends and modifies the standard approaches used in jump diffusion modeling in two significant ways: (1) a generalized point process is utilized that allows for history dependent arrival rates (as opposed to a standard Poisson process), and (2) a Markov chain with transition matrices is used to characterize jump intensities instead of modeling them as independent and identically distributed random variables.

First, the Poisson process commonly used in jump diffusion models is replaced with a more generalized point process that includes a conditional intensity function, allowing us to characterize arrival rates that are non-homogeneous and history dependent. This extension was based on work in neural spike trains where the firing of different neurons in the brain are dependent both on the timing of the events and on preceding spike events [94] [95]. This switch was driven primarily by the transition to hourly price generation instead of the daily average price estimation seen in the liter-

ature. In hourly pricing, price spikes are more likely to occur during certain times of the day (e.g. more likely in the mid-afternoon than the middle of the night). It is also common to observe spikes that are longer than 1-hour in duration. The generalized point process is leveraged to model both conditions.

To model time-dependent, multi-hour spike events, two sets of expected probabilities are utilized: (1) a set of initial arrival probabilities indexed on hour of the day ($\lambda_o(h)$) and (2) a conditional intensity function ($\lambda_c(p)$) that is dependent on the number of prior consecutive hours in which spikes occurred. These two sets of probabilities combine into the general point process (dq_t), which uses the initial intensity and conditional intensity functions to determine whether or not a spike occurs at time t:

$$dq_t = \begin{cases} 1 & \text{with prob. } \lambda_0(h) \text{ if no spike in prior hour or prob. } \lambda_c(p) \text{ if } p \text{ spikes have occurred in succession.} \\ 0 & \text{with prob. } 1 - \lambda_0(h) \text{ if no spike in prior hour or prob. } 1 - \lambda_c(p) \text{ if } p \text{ spikes have occurred in succession.} \end{cases}$$
$$(5.7)$$

In equation (5.7) $\lambda_0(h)$ is the probability of a spike occurring in hour h of the day if no spike occurred in hour $h-1$; and $\lambda_c(p)$ is the probability of a spike occurring given that a spike has occurred in p consecutive hours prior. Both sets of probabilities are determined empirically based on spikes observed over the chosen look-back window (e.g. 30 days prior).

An example of calculated probabilities for two randomly selected days from two seasons in 2019 (August 30th and November 2nd) is shown in Figure 5.2. Note that the summer day (left column) shows much higher initial arrival rate probabilities, with the noon hour having a probability over 40%. The summer day also has a higher likelihood of additional spikes after the initial spike, and those probabilities stay high longer than the on late fall day shown in the right column.

The preceding discussion on jumps has centered around the arrival of the

jumps (dq_t), but the spike intensity (J) should be considered as well. Traditionally, J has been defined as a normal, log-normal, or exponential random variable, but this approach presents challenges due to the heavy tails of the underlying distribution [40]. Using a random variable to characterize the spike intensity especially presents problems in the context of multi-hour spike events. Most multi-hour spike events follow a pattern (e.g. spike in the first hour is lower than the second, and then the intensity fades in the final hours), but using a random variable to calculate intensity leads to spikes in adjacent hours that are uncorrelated. To address these issues the proposed method implements a Markov process to determine the spike intensity.

The Markov process for spike intensity is built from conditional transition probabilities from one price-bin to another price bin. Once the Poisson process indicates that an initial spike is occurring, the Markov process begins for determining the spike intensity, or the market price. The zeroth bin is defined from the lowest observed price up to the highest de-spiked price. Subsequent bins can be determined in many ways. It is important to capture relevant price ranges to reflect realistic spike chains. Thus, determining the price bins should be done based on familiarity with the market data. Transition probabilities are determined empirically from the data. The length of any chain of price spikes is determined by the Bernoulli sampling that determines dq_t.

Figure 5.3 shows a Hinton diagram of the transition probabilities, where the increasing size and darkness of the squares signify a higher likelihood of transitioning from the state on the vertical axis to the state on the horizontal axis. For example, upon the first spike in a chain one samples from the zeroth row in Figure 5.3. The most likely outcome is that the first spike intensity lands in the first price bin so let us assume that occurs. Say that the first price bin extends from \$100/MWh to

$300/MWh. Then, the spike intensity is determined by uniformly sampling within the bin, resulting in a spike intensity between $100/MWh to $300/MWh. Now, when a second consecutive spike occurs, one would sample from the distribution in the first row. Let us say that the second most likely outcome happens, which is a transition to the second bin or row of the transition matrix shown in Figure 5.3. Now, the second price intensity is determined by uniformly sampling from the second bin, which might extend from $300/MWh to $600/MWh for example. The process continues for as many time steps as indicated by the arrival process described above.

In summary, the combination of the non-homogeneous, history-dependent point process for spike arrival and the Markov chain transition matrix for spike intensity allows the approach to more fully capture the characteristics of hourly electricity pricing. First, the approach can model clusters of spikes of different durations and their varying likelihoods throughout the year. Next, the approach developed here can handle spike intensity relationships both within a multi-hour spike event and conditioned on time of the year.

5.1.5 Parameter Weighting

The primary hyperparameter to the model in both the diffusion term (Section 2.3) and the jump term (Section 2.4) is the number of look-back days, or number of samples used to derive the empirical values. The model considers this hyperparameter when building the parameters that define the diffusion and jump terms from the historical realized pricing. Sometimes it is better to use a larger window (e.g. 3-6 months of data) to obtain large sample sizes for estimating the arrival probabilities or transition matrix elements and one might not want to treat all of those days equally. This is especially true when estimating parameters for periods with higher spikes (in both arrival and intensity), which may persist for a few weeks to a month or two.

To address this issue, weighting hyper-parameters are added to the model that allows one to select among a few features for ordering the importance of days in the look-back window. For example, "days prior", "average pricing", and "weekend/weekday" are used as features of the data along with linear, quadratic, or exponential weighting of sample days based on those features. Using weighting hyper-parameters allows the model to preferentially weight recent days, days with similar average (de-spiked) pricing, or weekends/weekdays (relative to the day being modeled). Additionally, it allows for three methods for calculating those weights, with linear, quadratic, and exponential giving increasingly more weight to more 'similar' days (e.g. similar average price or very recent days), and exponential putting the highest weight on "similar" days. In the following results section, the impacts of switching between these weighting approaches for two different look-back lengths is shown.

5.2 Results

The efficacy of the approach is evaluated by analyzing the synthetic price data for the year of 2019, with look-back windows stretching back into 2018. Two different look-back window lengths are used (30- and 180-day windows) along with two different weighting approaches ('prior days' and 'average price' weighting). A linear function is used when applying each weighting. For example, in a 30-day look-back, the 15th day prior receives 0.5 weighting, while the day immediately preceding the modeled day receives a weighting of 1.0.

One-thousand synthetic prices traces are generated for each day of 2019 and each window/weighting combination. Each of the traces contains the same deterministic signal generated with the forecast from the ARIMA model, combined with an

instance of the jump-diffusion components from the SDE. Figures 5.4, 5.5, and 5.6 display synthetic pricing traces for three distinct days using the 30-day look-back window and linear weighting on prior days. Figures 5.4 and 5.5 show two different days in the summer period, with the August day exhibiting significant price spikes (over $2,000/MWh for two consecutive hours) and the July day exhibiting more moderate price spikes ($150/MWh for three consecutive hours). The realized price from the settled day-ahead market is shown in blue. The realized price is not exposed to the model during generation of synthetic pricing.

A range of spike intensities and durations are captured on these days, and they generally cover the range of prices that are realized in the day-ahead market. While many spikes are included in the generated pricing, many of the simulated traces have no spike, or a much lower spike (demonstrated by the dark gray clustering under the realized price spike).

Figure 5.6 shows a winter day in December that has no realized price spikes. The synthetic pricing for this day primarily shows the impacts of the ARIMA and diffusion portions of the model. The ARIMA portion sets the deterministic signal and the diffusion term simulates the expected variability around that mean signal. Since the diffusion term is a function of the hour of the day, more volatility is seen in the generated prices during the morning and afternoon, which ends up aligning with the two small peaks in the realized pricing for the day. One trace out of the thousand simulated pricing sets includes a price spike. This result indicates that the initial arrival rates for this day had a non-zero value at 6am (the value is in fact 0.02652, suggesting that one would expect more predicted morning spikes if one generated another 1,000 traces).

To characterize the performance of the model, the moments of the data are

calculated for each of the window/weighting combinations and compared these results to the moments of the realized pricing. Comparing model-based moments to empirical moments is a common approach to evaluate the performance of the model [45]. Figure 5.7 and Figure 5.8 show the mean and standard deviation of the generated prices for each look-back length/weighting approach combination compared with the moments of the realized pricing. The figures show the moments by season of the year, as the mean price shape varies significantly throughout the year. The shorter, 30-day look-back window performs better overall than the 180-day look-back in terms of matching the realized price moments. In contrast, the weighting approach does not appear to have a significant impact on the accuracy of the moments. The model captures the mean signal of the empirical data well, but it sometimes fails to capture the full magnitude of price spikes observed in the data (for example in summer and fall months).

Due to the infrequency of price spikes it is not possible to validate the price spike model using traditional statistical methods. However, through discussions at a multinational oil and gas company and a large US municipal electric utility it was determined that the price spike model does generate realistic price scenarios. In fact, the price spike model is being leveraged to evaluate bidding strategies in European markets by the major oil and gas company.

5.3   Use-case Example

To demonstrate the value of the stochastic price generation method a use-case example for bidding a battery energy storage system (BESS) in an energy market is presented. The energy market is modeled after the Electric Reliability Council of Texas (ERCOT) system, with day-ahead and real-time energy markets. Optimal

price-quantity bids are determined using a stochastic optimization program modeled after the work in [96], which is extended by considering the Conditional Value at Risk (CVaR) as well as adding a two-stage program for the real-time bidding model to address the issue of infeasible BESS dispatch strategies that might result from the bid clearing process.

The goal of the BESS bidding model is to maximize the expected profit from executing energy arbitrage. Price scenarios are used to represent a discrete distribution of market prices in the stochastic programs to form a sample average approximation of the expected profit [97]. The probabilities of price scenarios are determined by first generating 1,000 price scenarios with a rolling look-back window of 30 days. Second, the 1,000 price scenarios are clustered using the k-means algorithm to create 10 clusters and 10 price scenarios from the centroids of the clusters [98]. The probability of each of the 10 scenarios is calculated as the ratio of the number of members in each cluster to the total number of scenarios.

Once the ten price scenarios and their probabilities are determined, the first step in the stochastic bidding model is to form price-quantity bids in the day-ahead market. Equation C.3 in Appendix C shows the day ahead bidding model. The day-ahead market model uses price scenarios to determine the optimal price-quantity pairs to bid in each hour for tomorrow.

Next, the real-time market model C.4 maximizes the weighted sum of the real-time market profit and the CVaR given the cleared day-ahead market energy quantities. The real-time market model is a two-stage stochastic program, with here-and-now decisions for the real-time price-quantity bids in the next clearing period and wait-and-see decisions for the price-quantity decisions in all subsequent time-steps. For this use-case the real-time market model is executed in a rolling fashion, starting

with optimizing the price-quantity bid in the first hour of the operating day. As the simulation time advances the real-time market model horizon shrinks because the cleared day-ahead market quantities are unknown until the 14th hour in the operating day. In each operating day the day-ahead price-quantity bids for the next day are optimized in the 9th hour to reflect the 10 AM deadline in ERCOT. The day-ahead market is assumed to clear by the 14th hour, at which point the real-time model horizon is extended to 24 hours again. Figure 5.9 shows a graphical representation of the simulation horizons in the day-ahead and real-time models. Table 5.1 lists the BESS technical inputs.

Table 5.1: Technical inputs

Battery assumptions	Value
Storage Capacity	2 MWh
Inverter Capacity	1 MW
Total Round Trip Efficiency	90.25%
Inverter Efficiency	95%
Rectifier Efficiency	95%
Initial State of Charge	0%

Table 5.2 shows the total profits from the simulation of 168 days in 2019 using ERCOT day-ahead and average hourly real-time market prices. For comparison results from using a persistence forecast for the expected energy market prices are included. CVaR weightings of zero and 50% are used. The scenarios with a 50% CVaR weighting show the highest profit, with a 47% improvement over the persistence forecast profit. Considering no CVaR results in a 24% improvement over the persistence forecast profit. The benefit of considering the CVaR is likely due to the fact that being conservative in the day-ahead market allows for more opportunities in the real-time market. Indeed, as shown in Table 5.2, the stochastic model with a 50% CVaR weight resulted in lower day-ahead market profits than the stochastic

model with no CVaR considered; yet when considering CVaR the stochastic model is able to get more net profits by performing better in the real-time market than the model with zero CVaR weight.

Figures 5.10 and 5.11 show a side-by-side comparison of the realized price, persistence foreacast, and stochastic price scenarios for a certain day in the day-ahead and real-time markets respectively. It interesting to note that the poorer performance in terms of profits in the real-time market is likely due to the more volatile nature of the real-time market. From Figure 5.11 one can see that the stochastic scenarios also suffer from some persistence assumptions: most of the price scenarios show a price peak much later than actually occurs - similar to the persistence forecast.

Table 5.2: Total profits from stochastic optimization models and persistence forecast simulations. The total profits are from simulating 168 days from 2019 with ERCOT day-ahead and average hourly real-time market prices.

Battery assumptions	CVaR weight	Total profit	Day-ahead	Real-time
Persistence forecast	n/a	$35,040	$48,147	-$13,107
Stochastic model	0	$43,318	$57,134	-$13,815
Stochastic model	0.5	$51,514	$53,729	-$2,215

5.4   Conclusions

This work extends the state-of-the-art for modeling daily average electricity market prices with stochastic differential equations to sub-daily time intervals. The goal is not to provide better price forecasts, though the methods may be applied to price forecasting; rather, the method is intended to generate realistic price time series for evaluating different market bidding strategies. Like any model built upon statistics of past data, the method cannot predict new features of price time series (such as a consecutive spike series twice as long as any series observed in the past). However, the proposed method can generate an unlimited amount of price series that

are statistically and qualitatively similar to historical prices. With this capability researchers can compare different market bidding strategies over long time periods that may be otherwise unachievable due to data availability or recent changes in market rules that make all but the most recent prices irrelevant.

Despite the limitations of generating price scenarios from past prices, the model parameters can be modified by practitioners to represent market behavior that has not been witnessed but might be anticipated. For example, adjustments to the conditional intensity function, the initial arrival rates, the variance of the diffusion term or the state switching probabilities of the Markov chain all can be used to simulate hitherto unseen market conditions. Futhermore, quantifying the range of these market price attributes in different wholesale electricity markets is an area of future work and would enable more informed research into how market evolution will impact stochasticity and volatility. This research could be valuable in assessing the costs (and risk) associated with procuring 24/7 renewable power or in providing firm renewable generation from hybrid renewable plus energy storage plants. The application of the synthetic pricing model to stochastic bidding models demonstrates that these data can be utilized to programmatically test bidding models and provide a mechanism to quantify the value in acknowledging and incorporating the increasing uncertainty that the day-ahead and real-time electricity markets are experiencing.
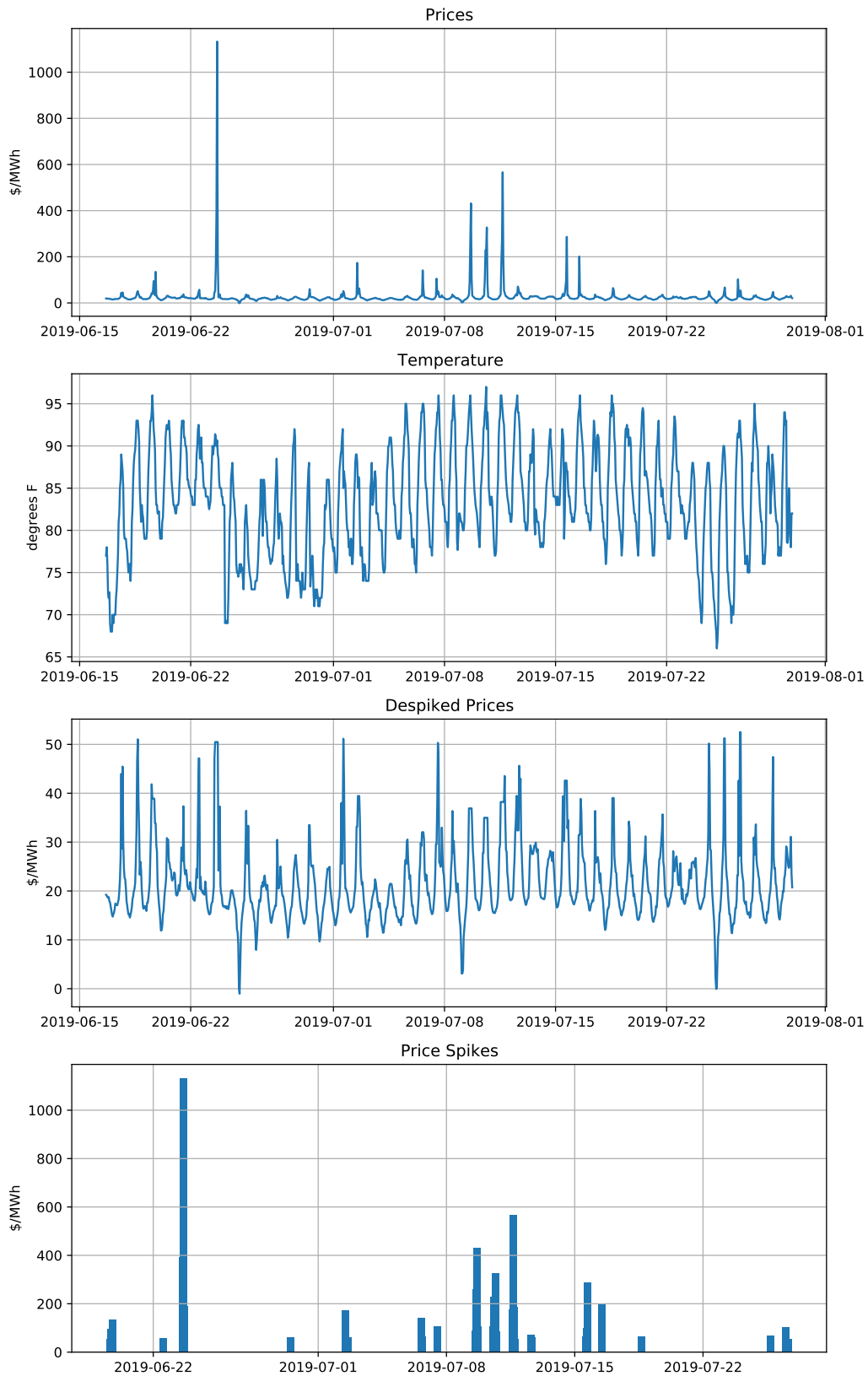
Figure 5.1: Representative sample of the time series data used to demonstrate the price generation method. Prices are from ERCOT Day Ahead Market [91]. Temperature values from [58].
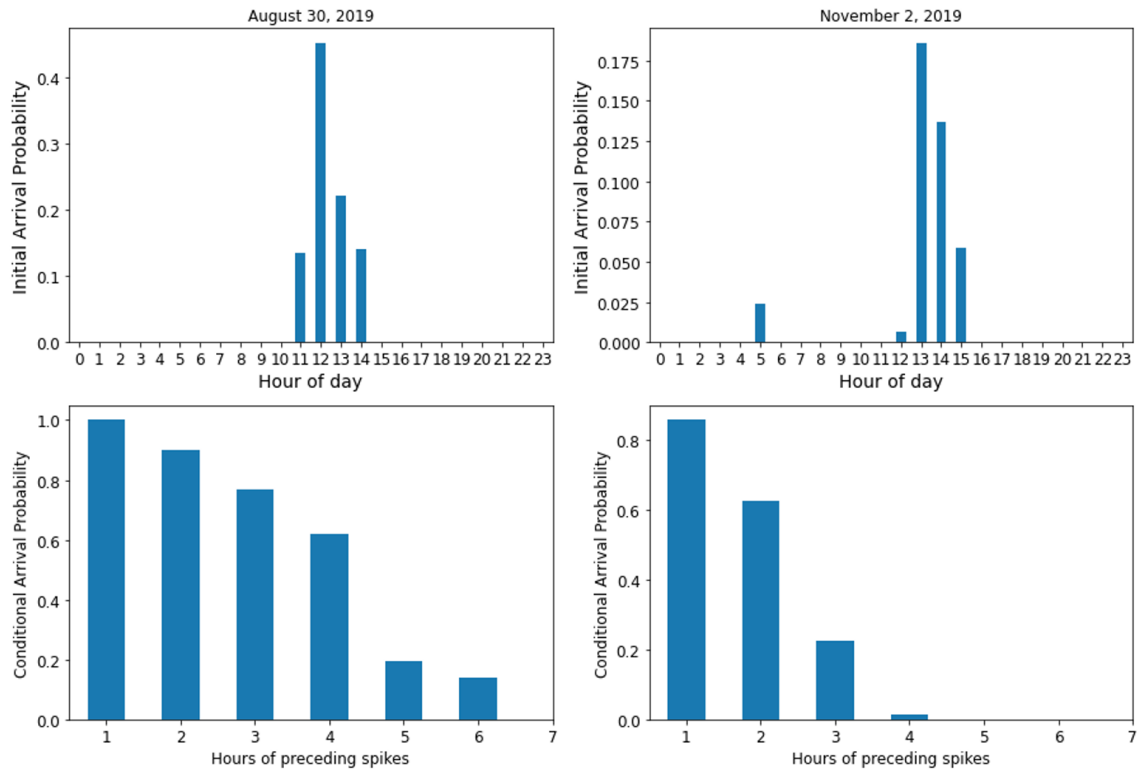
Figure 5.2: Initial arrival rate probabilities (top row) and conditional intensity functions (bottom row), shown for two days in 2019 (August 30th in left column and November 2nd in right column). Probabilities are derived empirically from the previous 30 days of price samples.
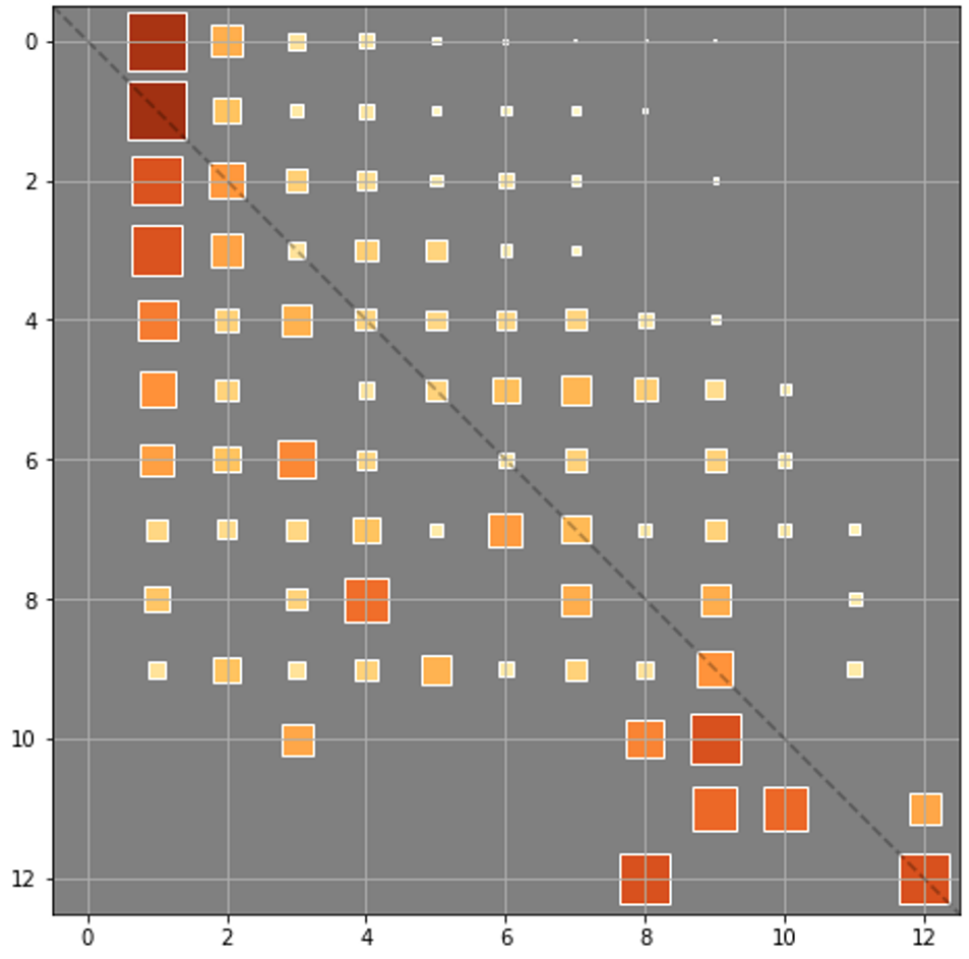
Figure 5.3: Hinton diagram of an example Markov chain transition matrix for spike intensity. The axes are integer price bins. Individual square sizes and darkness represent the probability of transition from one price bin to another. Rows of probabilities sum to one and are sampled uniformly. The zeroth row is sampled first for every set of price spikes to determine the bin for the first price spike.
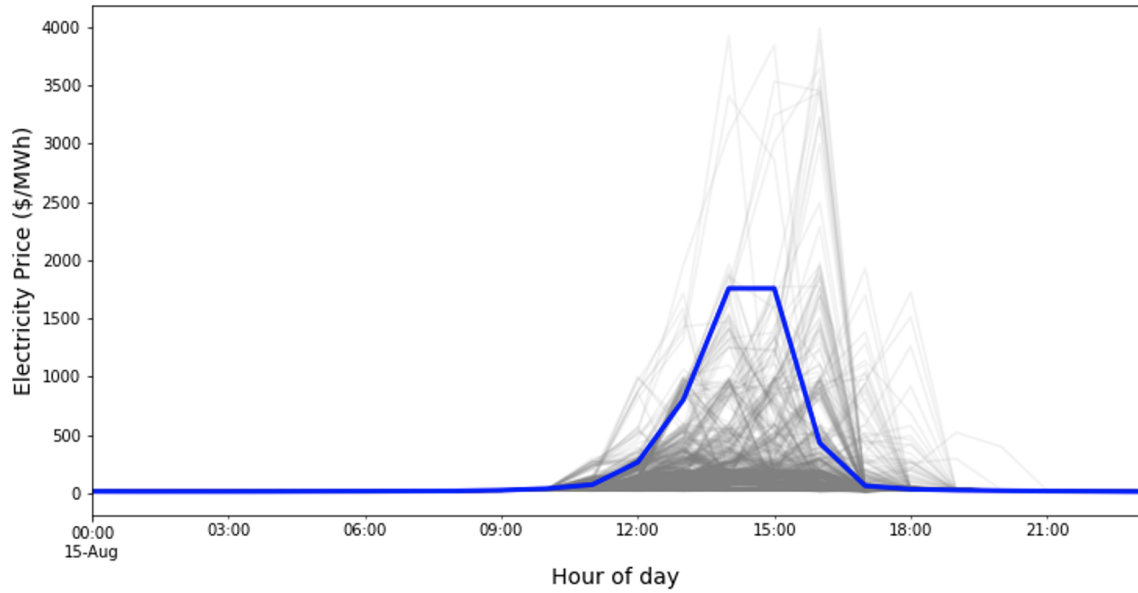
Figure 5.4: Synthetic pricing traces (thin grey lines) and realized price (thick blue line) for August 15th of 2019.
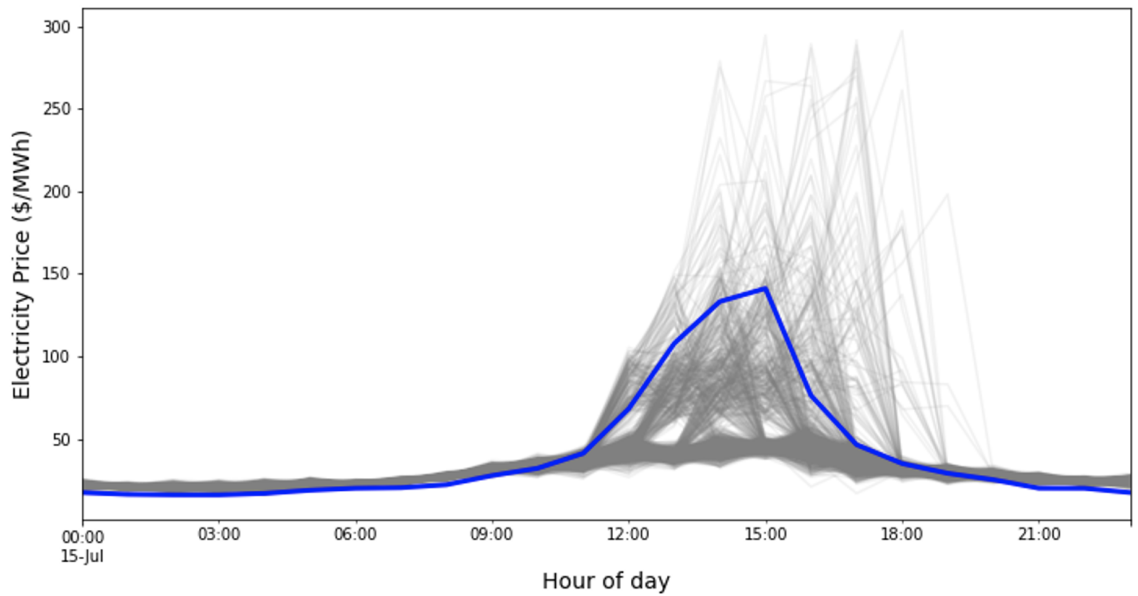

Figure 5.5: Synthetic pricing traces (thin grey lines) and realized pricing (thick blue line) for July 15th of 2019.
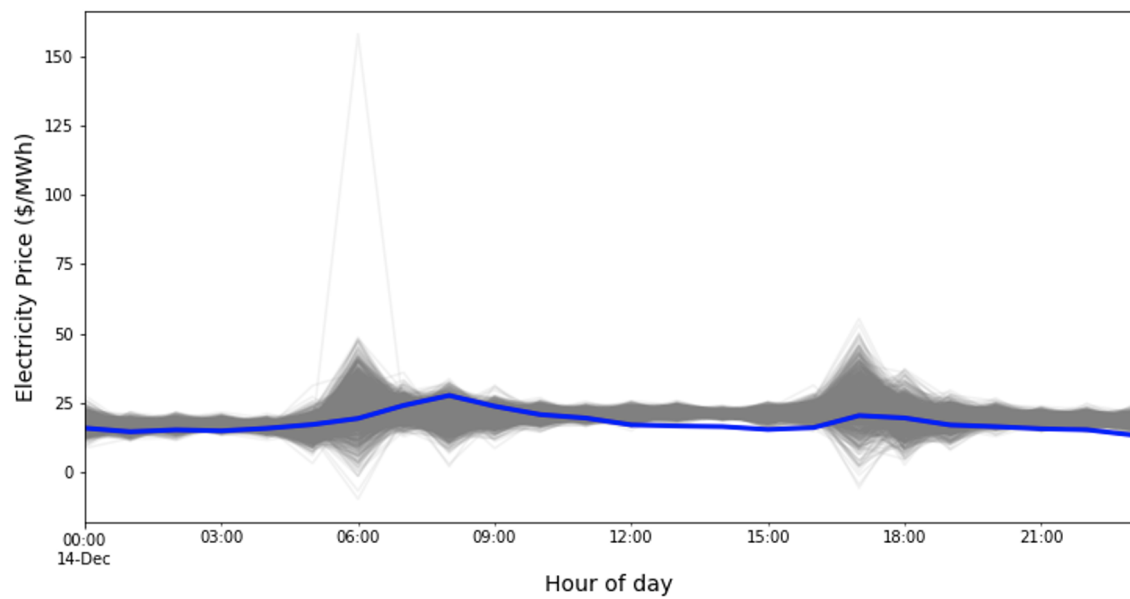
Figure 5.6: Synthetic pricing traces (thin grey lines) and realized pricing (thick blue line) for December 14th of 2019.
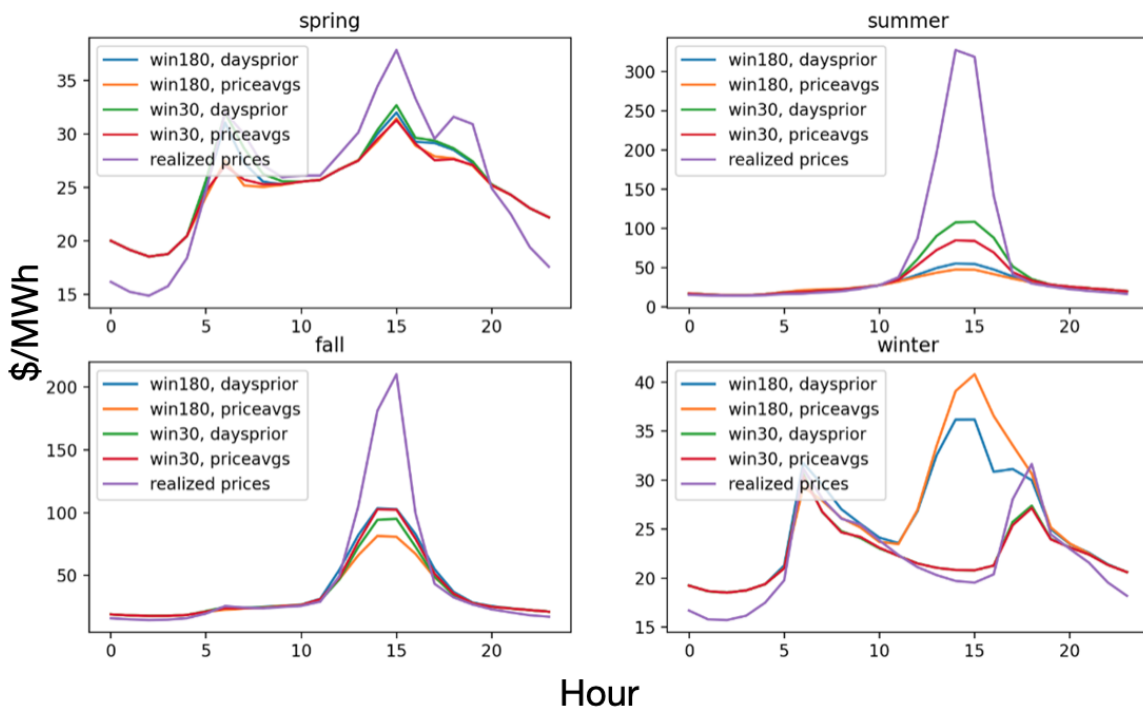
Figure 5.7: First moment (mean) of the synthetic pricing compared to realized prices. The synthetic pricing mean is shown for four cases: two look-back windows (30 and 180 day, or "win30" and "win180" in the legend) and two weighting functions (prior days and average price, or "daysprior" and "priceavgs" in the legend).
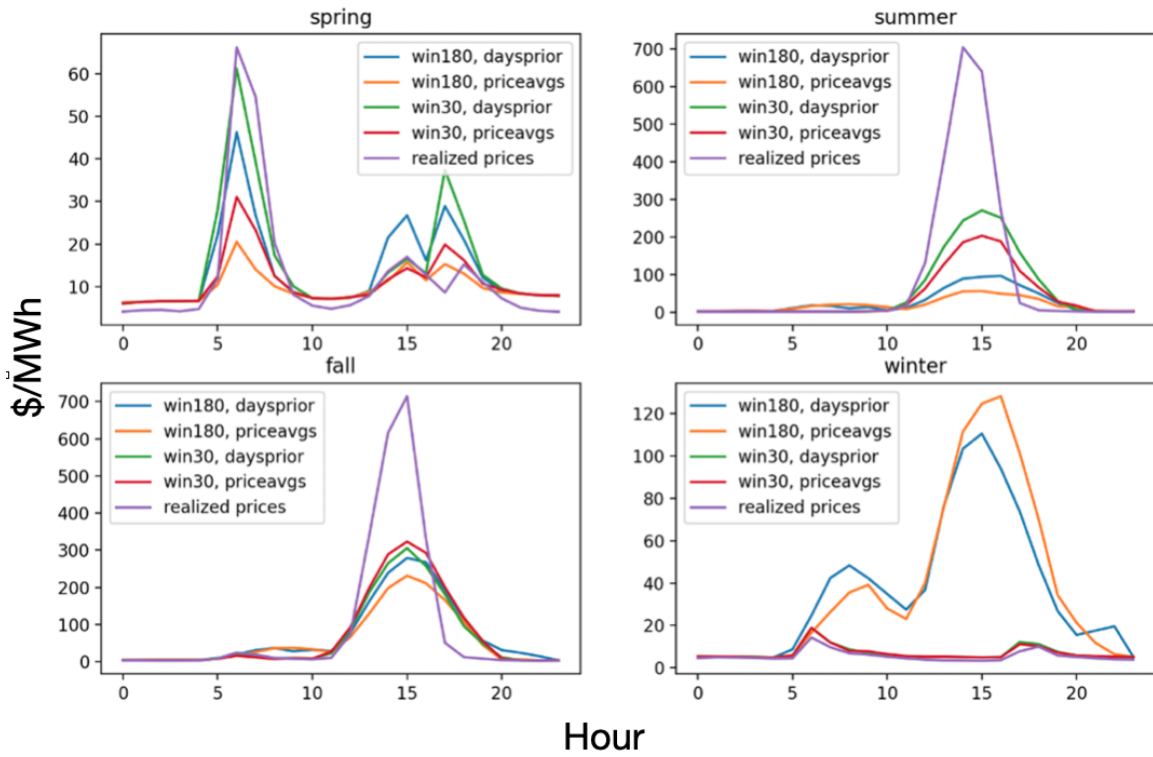
Figure 5.8: Second moment (standard deviation) of synthetic pricing compared to realized prices. The synthetic pricing mean is shown for four cases: two look-back windows (30 and 180 day, or "win30" and "win180" in the legend) and two weighting functions (prior days and average price, or "daysprior" and "priceavgs" in the legend).
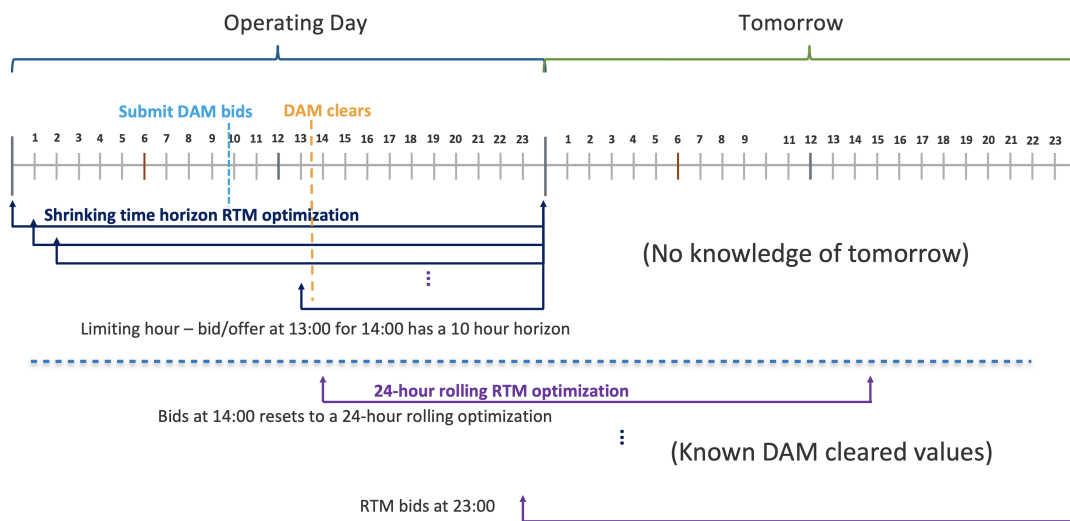
Figure 5.9: Simulation horizon for the real-time market model simulation, which is designed to reflect the ERCOT market. Day-ahead bids are due by 10 AM in the operating day and are cleared by the 14th hour. The real-time market model horizon shrinks and grows to reflect the knowledge of cleared day-ahead market quantities.
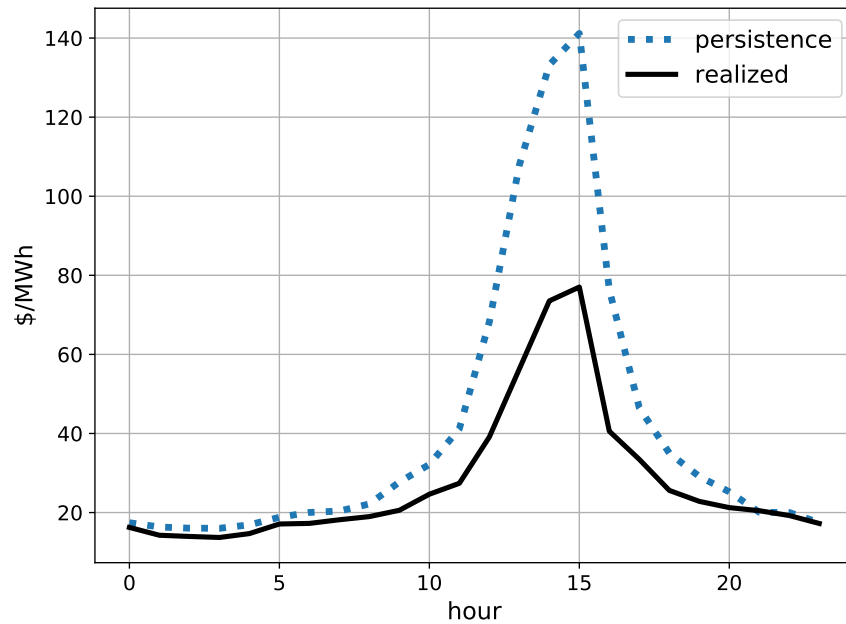
(a) Realized price and persistence forecast in day-ahead market on July 7th, 2019.
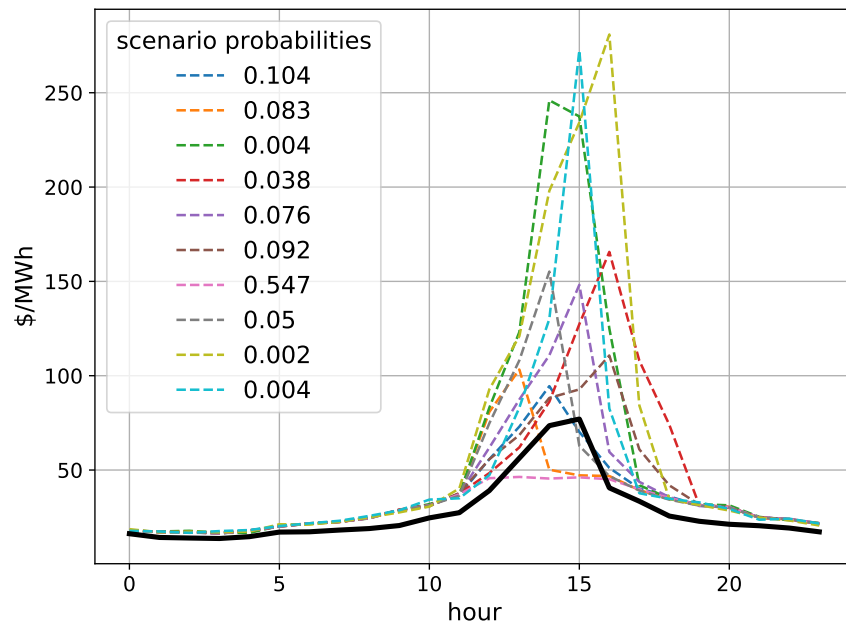
(b) Realized price and stochastic price scenarios in day-ahead market on July 7th, 2019. The legend shows the probability of each scenario, which is determined via the k-means clustering of 1,000 synthetic price scenarios. The thicker black line is the realized price.

Figure 5.10: Comparison of realized price, persistence forecast, and stochastic price scenarios in the day-ahead market on July 7th, 2019.
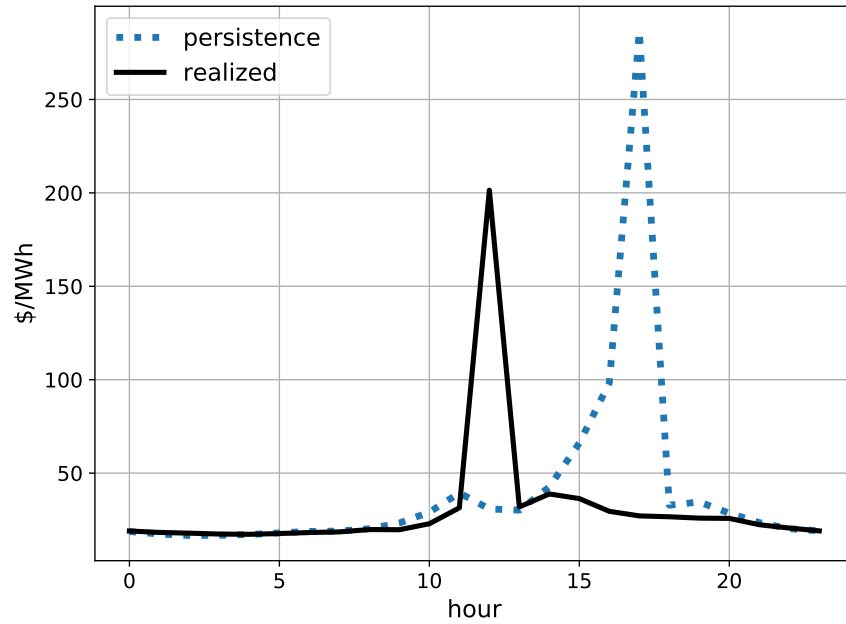
(a) Realized price and persistence forecast in real-time market on July 7th, 2019.
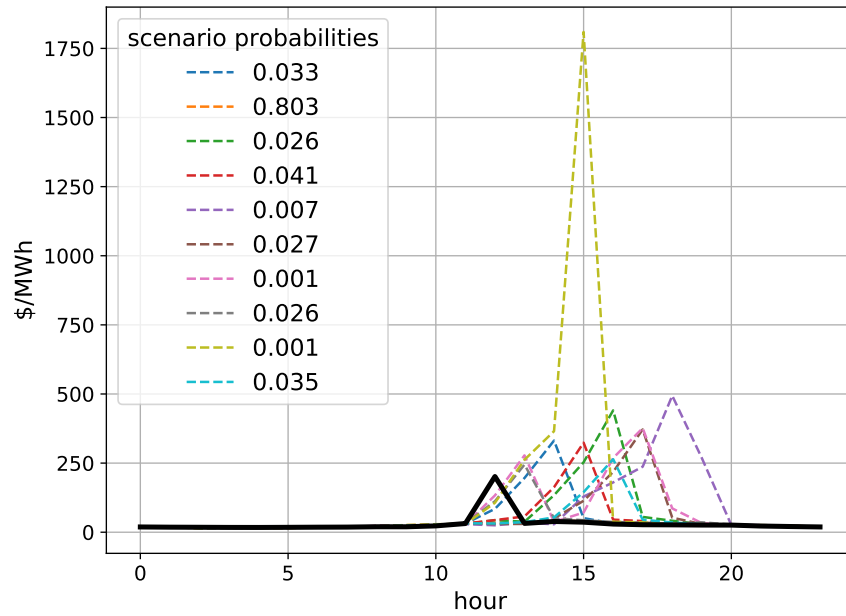
(b) Realized price and stochastic price scenarios in real-time market on July 7th, 2019. The legend shows the probability of each scenario, which is determined via the k-means clustering of 1,000 synthetic price scenarios. The thicker black line is the realized price.

Figure 5.11: Comparison of realized price, persistence forecast, and stochastic price scenarios in the real-time market on July 7th, 2019.

Chapter 6

Conclusions and Future Work

The goal of this dissertation was to develop new methods for valuing distributed energy resources in electricity transmission and distribution systems, with a particular focus on accounting for multiple perspectives. This goal was achieved by developing a new linearization technique for bilevel optimization problems that allows modeling energy system optimization problems at scales that matter. The linearization technique was leveraged to develop a new framework for valuing distributed energy resources in transmission and distribution systems. The proposed framework allows for competing perspectives to be modeled. Furthermore, a new method for creating synthetic electricity price scenarios was developed and its value demonstrated in a stochastic optimization framework. The major findings of the three research objectives, detailed in Chapters 3, 4, and 5, are summarized below.

6.1 Summary of results

Research Objective 1: The focus of this objective (detailed in Chapter 3) was developing a general method for linearizing bilinear products of price and dispatch variables to facilitate the solution of large scale bilevel optimization problems. The

---

Some sections of this chapter were adapted from the journal article: TODO?. The majority of this paper's research, analysis, and writing were completed by the author of this dissertation. The co-authors contributed to defining the direction of this project and editing the manuscript.

linearization methodology was determined for the most general case as well as the conditions required to linearize for particular model formats with applications to power systems planning and operations. The methodology was also implemented in an open source *Julia* package to facilitate its use within the research community. The major findings from this portion of the work are as follows:

- Only light conditions are required to linearize the products of dispatch variables and shadow prices when the upper level model variables within the lower level objective are integer (or no upper level variables are in the lower level objective)

- More restrictive conditions are necessary to linearize when the upper level model variables within the lower level objective are continuous; however, many interesting energy system optimization problems meet the conditions.

- Problems at scales that matter that were intractable without linearization can now be solved within reasonable time frames.

Research Objective 2: The focus of this objective (detailed in Chapter 4) was to develop a method to assess the techno-economic potential of DER for distribution system upgrade deferrals. The linearization technique from RO1 was leveraged to develop a new optimization framework to value DER as non-wires alternatives. A use-case was presented, in which both the distribution system operator and third-party DER investor perspectives were optimized. The results show how both the system operator and investors can mutually benefit, thereby reducing electricity costs for all consumers. The major findings from this portion of the work are as follows:

- Co-optimal solutions for DER investors and system operators can be determined using the proposed framework.

- The proposed framework can be leveraged in transactive control contexts, providing price signals that benefit the system first and investors second.

Research Objective 3: The focus of this objective (detailed in Chapter 5) was to develop a method to generate realistic synthetic electricity market price scenarios. The value of the developed model was demonstrated in a stochastic optimization framework for bidding a battery energy storage system into day-ahead and real-time markets simultaneously. The state-of-the art in electricity price modeling was advanced by

- The integration of ARIMA models as the deterministic component of the stochastic differential equation.

- Replacement of the standard Poisson process in the jump component with a generalized point process, which allows for non-homogeneous and history-dependent spike modeling.

- Integration of Markov chain transition matrices to model spike intensities, which enables improved estimation of price transitions during multi-period spike events.

Several cross-cutting observations emerge from the findings of the three research objectives of this dissertation. First, by leveraging the linearization method developed in this thesis, bilevel optimization models for power system planning and operations can model the bilinear monetary exchanges between operators and distributed energy resource owners at scales that matter. Second, distributed energy resources can delay and replace traditional power system upgrades when valued appropriately. Finally, as distributed energy resources integrate into wholesale electricity markets more advanced price modeling techniques are required to evaluate and plan optimal distributed energy resource dispatch strategies.

6.2   Future work

There are several direction of future work that could build upon this work. One major thrust of future work could focus on leveraging the linearization method in a transactive control context. When using a power flow model in the lower level of the bilevel model, the price signal decisions are effectively distribution locational marginal prices (DLMP). However, the bilevel framework might affect the traditional DLMP values because the framework requires that solutions are in the optimization space for the lower level (in addition to minimizing the upper level cost function). Future research might find that prices from the bilevel framework or more fair than traditional DLMP values, in the sense that the prices from the framework account for more than the system operator's perspective.

Another area of interesting research could include more adversarial models, or a more pessimistic view point in the bilevel framework. The framework developed in this work is "optimistic" in that the parties represented by the lower level always act in the best interest of the upper level (given the constraints). Pessimistic bilevel problems, that typically use a minimax to represent the worst-case reaction from the lower level (to the upper level decisions), are generally intractable. Future research might find tractable modeling frameworks to capture more pessimistic optimization of power systems; thereby producing more robust solutions.

Lastly, as power systems become more complex and more DER are connected to grids, larger and larger models will be necessary. Future work could research decomposition techniques to make otherwise unwieldy problems solvable on modern cloud-based, distributed computing systems.

Appendices

Appendix A

Publications

Journal Articles

1. **Laws**, **Nicholas D**, Chen, Dongmei, and Webber, Michael J. "Valuing Distributed Energy Resources for Non-Wires Alternatives". In: *Submitted* (2023)

2. **Laws**, **Nicholas D** and Hanasusanto, Grani A. "Linearizing bilinear products of shadow prices and dispatch variables in bilevel problems for optimal power system planning and operations". In: *IEEE Transactions on Power Systems* 38.1 (2022), pages 668–680

3. Mishra, Sakshi, Pohl, Josiah, **Laws**, **Nicholas D**, Cutler, Dylan, Kwasnik, Ted, Becker, William, Zolan, Alex, Anderson, Kate, Olis, Dan, and Elgqvist, Emma. "Computational framework for behind-the-meter DER techno-economic modeling and optimization: REopt Lite". In: *Energy Systems* (2021), pages 1–29. URL: https://arxiv.org/pdf/2008.05873

4. McLaren, Joyce, **Laws**, **Nicholas D**, Anderson, Kate, DiOrio, Nicholas, and Miller, Hannah. "Solar-plus-storage economics: What works where, and why?" In: *The Electricity Journal* 32.1 (2019), pages 28–46. URL: https://www.sciencedirect.com/science/article/am/pii/S1040619018302744

5. **Laws**, **Nicholas D**, Anderson, Kate, DiOrio, Nicholas A, Li, Xiangkun, and McLaren, Joyce. "Impacts of valuing resilience on cost-optimal PV and storage systems for commercial buildings". In: *Renewable energy* 127 (2018),

pages 896–909. URL: `https://www.sciencedirect.com/science/article/am/pii/S0960148118305305`

6. Anderson, Kate, **Laws**, **Nicholas D**, Marr, Spencer, Lisell, Lars, Jimenez, Tony, Case, Tria, Li, Xiangkun, Lohmann, Dag, and Cutler, Dylan. "Quantifying and monetizing renewable energy resiliency". In: *Sustainability* 10.4 (2018), page 933. URL: `https://www.mdpi.com/2071-1050/10/4/933/pdf`

Technical Reports and Conference Papers

1. **Laws**, **Nicholas D**, Cutler, Dylan S, Dunham, Hallie, Johnson, Sam, Inman, Daniel, Granger, Nikita, Jones, Wayne, and Chalenski, David. *Stochastic Price Generation for Evaluating Wholesale Electricity Market Bidding Strategies.* Technical report. National Renewable Energy Laboratory (NREL), 2023. URL: `https://www.nrel.gov/docs/fy23osti/82005.pdf`

2. Gasper, Paul, **Laws**, **Nicholas D**, Rathod, Bhavesh, Olis, Dan, Smith, Kandler, and Thakkar, Foram. "Optimization of Energy Storage System Economics and Controls by Incorporating Battery Degradation Costs in REopt". In: *243rd Electrochemical Society Meeting.* Boston, MA, 2023

3. Murphy, Caitlin, Hotchkiss, Elizabeth L, Anderson, Katherine H, Barrows, Clayton P, Cohen, Stuart M, Dalvi, Sourabh, **Laws**, **Nicholas D**, Maguire, Jeffrey B, Stephen, Gordon W, and Wilson, Eric J. *Adapting Existing Energy Planning, Simulation, and Operational Models for Resilience Analysis.* Technical report. National Renewable Energy Lab.(NREL), Golden, CO (United States), 2020. URL: `https://www.osti.gov/servlets/purl/1602705`

4. Torres, Juan and **Laws**, **Nicholas D**. *Energy Resilience Through Grid Modernization and Renewables Integration.* Technical report. Presented at the

Critical Infrastructure Resilience Workshop, Washington, D.C. National Renewable Energy Lab.(NREL), Golden, CO (United States), Dec. 2018. URL: https://www.nrel.gov/docs/fy19osti/72884.pdf

Appendix B

Examples to demonstrate the Algorithms

Example 1. The simplest case for linearizing a certain $\lambda_j y_n$ term occurs when the y_n in the upper level objective bilinear term is in only one lower level constraint. In this case, step 1 of Algorithm 1 returns and (3.10) provides the linearization of $\lambda_j y_n$. Note that (3.10) is a particular instance of (3.9). In this example we present the *next* simplest case, which is when y_n is in more than one constraint but the other $\boldsymbol{y}$ variables in constraint j are in no other lower level constraints.

In Step 2 of Algorithm 1 the indices of (D_k) in the set $\{k \in \mathcal{N} \setminus \{n\} : V_{jk} \neq 0\}$ are added to the set of column indices to check using the recursive Algorithm 2. And the set $\mathcal{J}_j$ is initialized with $\{j\}$. Algorithm 2 then checks for non-zero values of $\boldsymbol{V}$ above and below each V_{jk} entry for each of the column indices. If no non-zero values are found then Algorithm 2 returns the same sets that were passed to it, meaning that no more equation indices are needed to linearize the $\lambda_j y_n$ term.

Take one particular k' in $\mathcal{N} \setminus \{n\}$ for example. The special case that $V_{ik'} = 0 \ \forall i \in \mathcal{J} \setminus \{j\}$ is illustrated as follows:

$$
\boldsymbol{V} = \begin{matrix} \\ j\text{-th row} \end{matrix} \overset{\displaystyle k'\text{-th col.}}{\begin{bmatrix} & & 0 & \\ & & \vdots & \\ & & 0 & \\ \dots V_{jn} \dots & & V_{jk'} & \dots \\ & & 0 & \\ & & \vdots & \\ & & 0 & \end{bmatrix}}.
\tag{B.1}
$$

When $y_{k'}$ is only in constraint j then $(D_{k'})$ is:

$$\lambda_j V_{jk'} y_{k'} = c_{k'} y_{k'} + \overline{\mu}_{k'} \overline{y}_{k'} - \underline{\mu}_{k'} \underline{y}_{k'} + y_{k'} \sum_{m \in \mathcal{M}} B_{mk'} x_m. \tag{B.2}$$

Equation (B.2) can then be substituted into (P_j), shown in (3.11), to eliminate the bilinear term of λ_j and $y_{k'}$ in the sum over $k \in \mathcal{N} \setminus \{n\}$. A similar result follows for eliminating all of the $\lambda_j y_k$ terms on the right hand side of (3.11). ∎

Example 2. Continuing from our previous example, now let us assume that the k'-th column of $\mathbf{V}$ has one other non-zero entry. Now, additional combinations of the (P_i) and (D_k) equations are necessary to eliminate the $\lambda_j y_{k'}$ term in (3.11). This is where step three of Algorithm 1, which relies on Algorithm 2, comes in.

For this example let $V_{i'k'} \neq 0$ for a particular i' in $\mathcal{J} \setminus \{j\}$, and let $V_{ik'} = 0 \ \forall i \in \mathcal{J} \setminus \{j, i'\}$. Also, let the i'-th row of $\mathbf{V}$ contain one other non-zero value $V_{i'\ell}$, and let $V_{i\ell} = 0 \ \forall i \in \mathcal{J} \setminus \{i'\}$. This case is illustrated in (B.3).

$$V = \begin{matrix} & & & \ell\text{-th col.} \ k'\text{-th col.} & \\ & & & \\ & & \begin{bmatrix} & 0 & 0 & \\ & \vdots & \vdots & \\ & \vdots & 0 & \\ j\text{-th row} & \dots V_{jn} \quad 0 & V_{jk'} \quad \dots & \\ i'\text{-th row} & 0 \dots \ 0 \quad V_{i'\ell} & V_{i'k'} \quad 0 \ \dots 0 & \\ & 0 & 0 & \\ & \vdots & \vdots & \\ & 0 & 0 & \end{bmatrix} \end{matrix} \tag{B.3}$$

Algorithm 2 is passed row j and column k' from step 3 of Algorithm 1. Algorithm 2 first finds all the row indices of non-zero values of $\mathbf{V}$ in column k' (except $V_{jk'}$) and checks that those rows have not already been added to the set of rows. (Recall that redundant rows or columns found by the Algorithms indicate an underdetermined system of equations). The set of rows in Algorithm 2 now contains i' since $V_{i'k'} \neq 0$. Finally, Algorithm 2 loops over each row found to check for non-zero values

of $\boldsymbol{V}$. If any values are found they are added to the columns set to search in another call to Algorithm 2 (hence the name "recursive_array_search"). In this case column ℓ is appended to the empty set of columns and so Algorithm 2 calls itself once with $r = i'$, $c = \ell$, $rows = \{i'\}$, $cols = \{\ell\}$, which finds no more non-zero entries in $\boldsymbol{V}$. Thus Algorithm 2 returns $rows = \{i'\}$, $cols = \{\ell\}$ to Algorithm 1, which appends the returned sets to $\mathcal{J}_j$ and $\mathcal{N}_n$, making the final sets $\mathcal{J}_j = \{j, i'\}$ and $\mathcal{N}_n = \{k', \ell\}$,

Now $(D_{k'})$ gives:

$$
\begin{aligned}
\lambda_j V_{jk'} y_{k'} + \lambda_{i'} V_{i'k'} y_{k'} = {} & c_{k'} y_{k'} + \overline{\mu}_{k'} \overline{y}_{k'} - \underline{\mu}_{k'} \underline{y}_{k'} \\
& + y_{k'} \sum_{m \in \mathcal{M}} B_{mk'} x_m.
\end{aligned}
\tag{B.4}
$$

Since the i'-th row of $\boldsymbol{V}$ contains only one other non-zero value $V_{i'\ell}$, and the other values in column ℓ of $\boldsymbol{V}$ are zero as illustrated in (B.3), then adding equations $(P_{i'})$ and (D_ℓ) allows one to linearize the $\lambda_{i'} V_{i'k'} y_{k'}$ term in (B.4) in a similar fashion to the previous example. ∎

Appendix C

Energy Market Stochastic Optimization Model

The stochastic optimization models used to demonstrate a use-case for the stochastic price generation method are described in the following. The models are based on the work in [96]. The day-ahead stochastic optimization model first determines the optimal price-quantity pairs to bid (to buy) or offer (to sell) in the day-ahead market. The real-time stochastic optimization model then takes the cleared day-ahead market energy obligations as inputs to determine the optimal price-quantity pair to bid or offer in the next real-time clearing period. For simplicity both models assume hourly time-steps.

C.1 Day-ahead market price-quantity stochastic optimization model

The day-ahead model maximizes the weighted sum of the expected profit and the conditional value at risk. Table C.1 presents the sets, parameters, and variables of the day-ahead model, which is shown in C.3.

Constraints C.1a through C.1h are operational constraints for the BESS. The constraints C.2a through C.2j require that one price-quantity strategy be chosen over

---

Sections of this appendix were adapted from the technical report: [14]. The majority of this paper's research, analysis, and writing were completed by the author of this dissertation. The co-authors contributed to the literature review, editing, writing, and technical development.

the horizon of T time-steps from all scenarios. Constraints C.2k and C.2l define the CVaR value [97]. And constraints C.2m through C.3g define non-negative variables.

$$x_{s,t,\text{charge}} \leq B_{\text{MW}} \ \forall s \in \mathcal{S}, \forall t \in \mathcal{T} \tag{C.1a}$$

$$x_{s,t,\text{discharge}} \leq B_{\text{MW}} \ \forall s \in \mathcal{S}, \forall t \in \mathcal{T} \tag{C.1b}$$

$$x_{s,t,\text{MWh}} \leq B_{\text{MWh}} \ \forall s \in \mathcal{S}, \forall t \in \mathcal{T} \tag{C.1c}$$

$$x_{s,t,\text{MWh}} \leq B_{\text{MWh}} \ \forall s \in \mathcal{S}, \forall t \in \mathcal{T} \tag{C.1d}$$

$$x_{s,t,\text{charge}} = x_{s,t,\text{Ebuy}} \eta_{\text{charge}} \ \forall s \in \mathcal{S}, \forall t \in \mathcal{T} \tag{C.1e}$$

$$x_{s,t,\text{discharge}} = x_{s,t,\text{Esell}}/\eta_{\text{discharge}} \ \forall s \in \mathcal{S}, \forall t \in \mathcal{T} \tag{C.1f}$$

$$x_{s,1,\text{MWh}} = f_{t=1} B_{\text{MWh}} - x_{s,1,\text{discharge}} + x_{s,1,\text{charge}} \ \forall s \in \mathcal{S} \tag{C.1g}$$

$$x_{s,t,\text{MWh}} = x_{s,t-1,\text{MWh}} - x_{s,t,\text{discharge}} + x_{s,t,\text{charge}} \ \forall s \in \mathcal{S}, \forall t \in \{2, \ldots, T\} \tag{C.1h}$$

$$x_{s,t,\text{Ebuy}} \leq z_{s,t,\text{Ebuy}} B_{\text{MW}} \ \forall s \in \mathcal{S}, \forall t \in \mathcal{T} \tag{C.2a}$$

$$x_{s,t,\text{Esell}} \leq z_{s,t,\text{Esell}} B_{\text{MW}} \ \forall s \in \mathcal{S}, \forall t \in \mathcal{T} \tag{C.2b}$$

$$x_{t,\text{Ebuy}} - x_{s,t,\text{Ebuy}} \leq (1 - z_{s,t,\text{Ebuy}}) B_{\text{MW}} \ \forall s \in \mathcal{S}, \forall t \in \mathcal{T} \tag{C.2c}$$

$$x_{t,\text{Esell}} - x_{s,t,\text{Esell}} \leq (1 - z_{s,t,\text{Esell}}) B_{\text{MW}} \ \forall s \in \mathcal{S}, \forall t \in \mathcal{T} \tag{C.2d}$$

$$x_{t,\text{Ebuy}} - x_{s,t,\text{Ebuy}} \geq 0 \ \forall s \in \mathcal{S}, \forall t \in \mathcal{T} \tag{C.2e}$$

$$x_{t,\text{Esell}} - x_{s,t,\text{Esell}} \geq 0 \ \forall s \in \mathcal{S}, \forall t \in \mathcal{T} \tag{C.2f}$$

$$x_{t,\$\text{buy}} \leq \pi_{s,t} + M z_{s,t,\text{Ebuy}} \ \forall s \in \mathcal{S}, \forall t \in \mathcal{T} \tag{C.2g}$$

$$x_{t,\$\text{buy}} \geq \pi_{s,t} - M(1 - z_{s,t,\text{Ebuy}}) \ \forall s \in \mathcal{S}, \forall t \in \mathcal{T} \tag{C.2h}$$

$$x_{t,\$\text{sell}} \geq \pi_{s,t} - M z_{s,t,\text{Esell}} \ \forall s \in \mathcal{S}, \forall t \in \mathcal{T} \tag{C.2i}$$

$$x_{t,\$\text{sell}} \leq \pi_{s,t} + M(1 - z_{s,t,\text{Esell}}) \ \forall s \in \mathcal{S}, \forall t \in \mathcal{T} \tag{C.2j}$$

$$x_{\text{CVaR}} = x_{\text{VaR}} + \frac{1}{\alpha} \sum_{s \in \mathcal{S}} p_s x_{s,M} \tag{C.2k}$$

$$x_{s,M} \geq - \sum_{t \in \mathcal{T}} \pi_{s,t}(x_{s,t,\text{Esell}} - x_{s,t,\text{Ebuy}}) - x_{\text{VaR}} \ \forall s \in \mathcal{S} \tag{C.2l}$$

$$x_{t,\$\text{sell}} \geq 0, \ x_{t,\$\text{buy}} \geq 0, \ x_{t,\text{Ebuy}} \geq 0, \ x_{t,\text{Esell}} \geq 0 \ \forall t \in \mathcal{T} \tag{C.2m}$$

$$\max_{\boldsymbol{x}\in\mathcal{R},\boldsymbol{z}\in\mathcal{Z}} \beta \sum_{s\in\mathcal{S}} p_s \sum_{t\in\mathcal{T}} \pi_{s,t}(x_{s,t,\text{Esell}} - x_{s,t,\text{Ebuy}}) - (1-\beta)x_{\text{CVaR}} \quad \text{(C.3a)}$$

$$\text{s.t. } x_{s,t,\text{charge}} \geq 0 \; \forall s \in \mathcal{S}, \forall t \in \mathcal{T} \quad \text{(C.3b)}$$

$$x_{s,t,\text{discharge}} \geq 0 \; \forall s \in \mathcal{S} \; \forall t \in \mathcal{T} \quad \text{(C.3c)}$$

$$x_{s,t,\text{MWh}} \geq 0 \; \forall s \in \mathcal{S}, \forall t \in \mathcal{T} \quad \text{(C.3d)}$$

$$x_{s,t,\text{Ebuy}} \geq 0 \; \forall s \in \mathcal{S}, \forall t \in \mathcal{T} \quad \text{(C.3e)}$$

$$x_{s,t,\text{Esell}} \geq 0 \; \forall s \in \mathcal{S}, \forall t \in \mathcal{T} \quad \text{(C.3f)}$$

$$x_{s,M} \geq 0 \; \forall s \in \mathcal{S} \quad \text{(C.3g)}$$

$$C.1a - C.2m \quad \text{(C.3h)}$$

C.2 Real-time market price-quantity stochastic optimization model

The two-stage real-time market price-quantity stochastic optimization model maximizes the weighted sum of the expected profit and the conditional value at risk (CVaR). The real-time model takes the cleared day-ahead energy obligations as inputs to determine the real-time market profit using the method from the ERCOT market [106]. The primary difference from the day-ahead model is that only the price-quantity bid in the first time-step is constrained across the price scenarios. In other words, the price-quantity bids for all time steps beyond the first are "wait-and-see" decisions that vary over the price scenarios, whereas the "here-and-now" decision for the first time step is the same in all price scenarios.

Table C.2 presents the sets, parameters, and variables of the real-time model, which is shown in C.4.The here-and-now decisions are reflected in constraints C.4c through C.4h. Constraints C.4i through C.4m define whether or not the price bids

and offers clear the market (in a similar fashion to [96]). Constraint C.4n is used to define the CVaR value. And constraints C.4o and C.4p define non-negative variables.

$$\max_{\boldsymbol{x}\in\mathcal{R},\boldsymbol{z}\in\mathcal{Z}} \beta \sum_{s\in\mathcal{S}} p_s \sum_{t\in\mathcal{T}} \pi_{s,t} \left[(x_{s,t,\text{Esell}} - E_{t,\text{DAsell}}) - (x_{s,t,\text{Ebuy}} - E_{t,\text{DAbuy}}) \right] - (1-\beta)x_{\text{CVaR}}$$

$$\text{(C.4a)}$$

$$\text{s.t. } C.1a \ldots C.2b, C.2k \tag{C.4b}$$

$$x_{s,1,\text{charge}} = x_{\text{charge}} \ \forall s \in \mathcal{S} \tag{C.4c}$$

$$x_{s,1,\text{discharge}} = x_{\text{discharge}} \ \forall s \in \mathcal{S} \tag{C.4d}$$

$$x_{s,1,\$\text{buy}} = x_{\$\text{buy}} \ \forall s \in \mathcal{S} \tag{C.4e}$$

$$x_{s,1,\$\text{sell}} = x_{\$\text{sell}} \ \forall s \in \mathcal{S} \tag{C.4f}$$

$$x_{s,1,\text{Ebuy}} = x_{\text{Ebuy}} \ \forall s \in \mathcal{S} \tag{C.4g}$$

$$x_{s,1,\text{Esell}} = x_{\text{Esell}} \ \forall s \in \mathcal{S} \tag{C.4h}$$

$$x_{s,t,\$\text{buy}} \leq \pi_{s,t} + M z_{s,t,\text{Ebuy}} \ \forall s \in \mathcal{S}, \forall t \in \mathcal{T} \tag{C.4i}$$

$$x_{s,t,\$\text{buy}} \geq \pi_{s,t} - M(1 - z_{s,t,\text{Ebuy}}) \ \forall s \in \mathcal{S}, \forall t \in \mathcal{T} \tag{C.4j}$$

$$x_{s,t,\$\text{sell}} \geq \pi_{s,t} - M z_{s,t,\text{Esell}} \ \forall s \in \mathcal{S}, \forall t \in \mathcal{T} \tag{C.4k}$$

$$x_{s,t,\$\text{sell}} \leq \pi_{s,t} + M(1 - z_{s,t,\text{Esell}}) \ \forall s \in \mathcal{S}, \forall t \in \mathcal{T} \tag{C.4l}$$

$$x_{s,t,\$\text{sell}} \geq 0, \ x_{s,t,\$\text{buy}} \geq 0 \ \forall s \in \mathcal{S}, \forall t \in \mathcal{T} \tag{C.4m}$$

$$x_{s,M} \geq -\sum_{t\in\mathcal{T}} \pi_{s,t} \left[(x_{s,t,\text{Esell}} - E_{t,\text{DAsell}}) - (x_{s,t,\text{Ebuy}} - E_{t,\text{DAbuy}}) \right] - x_{\text{VaR}} \ \forall s \in \mathcal{S}$$

$$\text{(C.4n)}$$

$$x_{s,t,\text{charge}} \geq 0, \ x_{s,t,\text{discharge}} \geq 0, \ x_{s,t,\text{MWh}} \geq 0, \ x_{s,t,\text{Ebuy}} \geq 0, \ x_{s,t,\text{Esell}} \geq 0$$

$$\forall s \in \mathcal{S}, \forall t \in \mathcal{T}$$

$$\text{(C.4o)}$$

$$x_{s,M} \geq 0 \ \forall s \in \mathcal{S} \tag{C.4p}$$

Sets and Indices

$s \in \mathcal{S}$	integer scenarios for market prices and bidding strategies, $\mathcal{S} \triangleq \{1, \ldots, S\}$
$t \in \mathcal{T}$	integer time-steps, $\mathcal{T} \triangleq \{1, \ldots, T\}$

Parameters		**Units**
B_{MW}	battery inverter capacity	MW
B_{MWh}	battery energy capacity	MWh
$f_{t=1}$	fraction of battery energy capacity stored in first time-step	unitless
$\pi_{s,t}$	market price in scenario s, time-step t	\$/MWh
$p_{s,t}$	probability of market price scenario s,	unitless
β	weighting factor for profit vs. CVaR in objective function	unitless
α	quantile for CVaR (for example $\alpha = 0.05$ considers the 5% tail of the loss)	unitless

Decision Variables		**Units**
$x_{s,t,\mathrm{charge}}$	power sent to the battery in scenario s, time-step t	MW
$x_{s,t,\mathrm{discharge}}$	power discharged from the battery in scenario s, time-step t	MW
$x_{s,t,\mathrm{MWh}}$	battery state of charge in scenario s, time-step t	MWh
$x_{s,t,\mathrm{Ebuy}}$	energy purchased in scenario s, time-step t	MWh
$x_{s,t,\mathrm{Esell}}$	energy sold in scenario s, time-step t	MWh
$z_{s,t,\mathrm{Ebuy}}$	binary decision to purchase energy in scenario s, time-step t	MWh
$z_{s,t,\mathrm{Esell}}$	binary decision to sell energy in scenario s, time-step t	MWh
$x_{t,\mathrm{Ebuy}}$	energy purchased in time-step t, used for day-ahead market bids	MWh
$x_{t,\mathrm{Esell}}$	energy sold in time-step t, used for day-ahead market offers	MWh
$x_{t,\$\mathrm{buy}}$	market bid in time-step t	\$/MWh
$x_{t,\$\mathrm{sell}}$	market offer in time-step t	\$/MWh
x_{CVaR}	conditional value at risk	\$
x_{VaR}	value at risk	\$
$x_{s,M}$	maximum of loss minus the value at risk and zero, where loss is the profit multiplied with negative one; used to define the conditional value at risk	\$

Table C.1: Sets, indices, parameters, and decision variables for Equations C.1, C.2 and C.3.

Sets and Indices

$s \in \mathcal{S}$	integer scenarios for market prices and bidding strategies, $\mathcal{S} \triangleq \{1, \ldots, S\}$
$t \in \mathcal{T}$	integer time-steps, $\mathcal{T} \triangleq \{1, \ldots, T\}$

Parameters		**Units**
B_{MW}	battery inverter capacity	MW
B_{MWh}	battery energy capacity	MWh
$f_{t=1}$	fraction of battery energy capacity stored in first time-step	unitless
$\pi_{s,t}$	market price in scenario s, time-step t	\$/MWh
$p_{s,t}$	probability of market price scenario s,	unitless
β	weighting factor for profit vs. CVaR in objective function	unitless
α	quantile for CVaR (for example $\alpha = 0.05$ considers the 5% tail of the loss)	unitless
$E_{t,\mathrm{DAsell}}$	cleared energy sold obligations in day-ahead market	MWh
$E_{t,\mathrm{DAbuy}}$	cleared energy purchased obligations in day-ahead market	MWh

Decision Variables		**Units**
$x_{s,t,\mathrm{charge}}$	power sent to the battery in scenario s, time-step t	MW
$x_{s,t,\mathrm{discharge}}$	power discharged from the battery in scenario s, time-step t	MW
$x_{s,t,\mathrm{MWh}}$	battery state of charge in scenario s, time-step t	MWh
$x_{s,t,\mathrm{Ebuy}}$	energy purchased in scenario s, time-step t	MWh
$x_{s,t,\mathrm{Esell}}$	energy sold in scenario s, time-step t	MWh
$z_{s,t,\mathrm{Ebuy}}$	binary decision to purchase energy in scenario s, time-step t	MWh
$z_{s,t,\mathrm{Esell}}$	binary decision to sell energy in scenario s, time-step t	MWh
x_{charge}	power sent to the battery in first time-step	MW
$x_{\mathrm{discharge}}$	power discharged from the battery in first time-step	MW
x_{Ebuy}	energy purchased in first time-step, used for real-time market bid	MWh
x_{Esell}	energy sold in first time-step, used for real-time market offer	MWh
$x_{\$\mathrm{buy}}$	market bid in first time-step	\$/MWh
$x_{\$\mathrm{sell}}$	market offer in first time-step	\$/MWh
x_{CVaR}	conditional value at risk	\$
x_{VaR}	value at risk	\$
$x_{s,M}$	maximum of loss minus the value at risk and zero, where loss is the profit multiplied with negative one; used to define the conditional value at risk	\$

Table C.2: Sets, indices, parameters, and decision variables for Equation C.4.

Bibliography

[1]   Raineri, Ricardo. "Chile: Where it all started". In: *Electricity market reform: an international perspective* (2006), pages 77–108.

[2]   *US Distributed Energy Resources Outlook 2020*. Technical report. Wood Mackenzie, 2020.

[3]   Zummo, Paul. *America's Electricity Generation Capacity 2020 Update*. Technical report. American Public Power Association, 2020.

[4]   Commission, Federal Energy Regulatory. *Transmission Planning and Cost Allocation by Transmission Owning and Operating Public Utilities [18 CFR Part 35, [Docket No. RM10-23-000; Order No. 1000]*. July 2011.

[5]   Tabors, Richard, Andrianesis, P, Caramanis, M, and Masiello, R. "The value of distributed energy resources to the grid: Introduction to the concepts of marginal cost of capacity and locational marginal value". In: *Proc. 52nd HICSS*. 2019, pages 3465–3472.

[6]   Kinaci, Andrew, Engel, Clay, and Aweh, Amanda. "Demand-Side Management Evolution: New Roles and Models for Market Participation and Incentive Alignment". In: *Climate and Energy* 37.6 (), pages 1–12.

[7]   Andrianesis, Panagiotis, Caramanis, Michael, Masiello, Ralph D, Tabors, Richard D, and Bahramirad, Shay. "Locational marginal value of distributed energy resources as non-wires alternatives". In: *IEEE Transactions on Smart Grid* 11.1 (2019), pages 270–280.

[8]   Laws, Nicholas D, Anderson, Kate, DiOrio, Nicholas A, Li, Xiangkun, and McLaren, Joyce. "Impacts of valuing resilience on cost-optimal PV and storage systems for commercial buildings". In: *Renewable energy* 127 (2018), pages 896–909.

[9]   Federal Energy Regulatory Commission. "Participation of Distributed Energy Resource Aggregations in Markets Operated by Regional Transmission Organizations and Independent System Operators". In: *Federal Register* 85.204 (Oct. 2020). URL: https://www.federalregister.gov/d/2020-20973.

[10] Von Stackelberg, Heinrich. *Marktform und Gleichgewicht. (Market Structure and Equilibrium)*. J. Springer, Vienna, 1934.

[11] Dyson, ark, Prince, Jason, Shwisberg, Lauren, and Waller, Jeff. *The Non-Wires Solutions Implementation Playbook*. Technical report. Rocky Mountain Institute, 2018.

[15] Caramanis, Michael C, Bohn, Roger E, and Schweppe, Fred C. "Optimal spot pricing: Practice and theory". In: *IEEE Transactions on Power Apparatus and Systems* 9 (1982), pages 3234–3245.

[16] Schweppe, FC, Tabors, RD, Caraminis, MC, and Bohn, RE. "Spot pricing of electricity". In: (1988).

[17] Vickrey, William. "Responsive pricing of public utility services". In: *The Bell Journal of Economics and Management Science* (1971), pages 337–346.

[18] Sioshansi, Fereidoon and Pfaffenberger, Wolfgang. *Electricity market reform: an international perspective*. Elsevier, 2006.

[19] Bai, Linquan, Wang, Jianhui, Wang, Chengshan, Chen, Chen, and Li, Fangxing. "Distribution locational marginal pricing (DLMP) for congestion management and voltage support". In: *IEEE Transactions on Power Systems* 33.4 (2017), pages 4061–4073.

[20] Caramanis, Michael, Ntakou, Elli, Hogan, William W, Chakrabortty, Aranya, and Schoene, Jens. "Co-optimization of power and reserves in dynamic T&D power markets with nondispatchable renewable generation and distributed energy resources". In: *Proceedings of the IEEE* 104.4 (2016), pages 807–836.

[21] Li, Ruoyang, Wu, Qiuwei, and Oren, Shmuel S. "Distribution locational marginal pricing for optimal electric vehicle charging management". In: *IEEE Transactions on Power Systems* 29.1 (2013), pages 203–211.

[22] Bard, Jonathan F. *Practical bilevel optimization: algorithms and applications*. Volume 30. Springer Science & Business Media, 2013.

[23] Ruiz, Carlos and Conejo, Antonio J. "Pool strategy of a producer with endogenous formation of locational marginal prices". In: *IEEE Transactions on Power Systems* 24.4 (2009), pages 1855–1866.

[24] Fernández-Blanco, Ricardo, Arroyo, José M, and Alguacil, Natalia. "On the solution of revenue-and network-constrained day-ahead market clearing under marginal pricing—Part I: An exact bilevel programming approach". In: *IEEE Transactions on Power Systems* 32.1 (2016), pages 208–219.

[25] Cornélusse, Bertrand, Savelli, Iacopo, Paoletti, Simone, Giannitrapani, Antonio, and Vicino, Antonio. "A community microgrid architecture with an internal local market". In: *Applied Energy* 242 (2019), pages 547–560.

[26] Wogrin, Sonja, Pineda, Salvador, and Tejada-Arango, Diego A. "Applications of Bilevel Optimization in Energy and Electricity Markets". In: *Bilevel Optimization*. Springer, 2020, pages 139–168.

[27] Naebi, Amir, SeyedShenava, SeyedJalal, Contreras, Javier, Ruiz, Carlos, and Akbarimajd, Adel. "EPEC approach for finding optimal day-ahead bidding strategy equilibria of multi-microgrids in active distribution networks". In: *International Journal of Electrical Power & Energy Systems* 117 (2020), page 105702.

[28] Xu, Xu, Li, Jiayong, Xu, Yan, Xu, Zhao, and Lai, Chun Sing. "A two-stage game-theoretic method for residential PV panels planning considering energy sharing mechanism". In: *IEEE Transactions on Power Systems* 35.5 (2020), pages 3562–3573.

[29] Bertsimas, Dimitris and Tsitsiklis, John N. *Introduction to linear optimization.* Volume 6. Athena Scientific Belmont, MA, 1997.

[30] *BilevelJuMP: A bilevel optimization extension of the JuMP package.* URL: https://github.com/joaquimg/BilevelJuMP.jl.

[31] Dunning, Iain, Huchette, Joey, and Lubin, Miles. "JuMP: A modeling language for mathematical optimization". In: *SIAM review* 59.2 (2017), pages 295–320.

[32] Piccolo, Antonio and Siano, Pierluigi. "Evaluating the impact of network investment deferral on distributed generation expansion". In: *IEEE Transactions on Power Systems* 24.3 (2009), pages 1559–1567.

[33] Contreras-Ocana, Jesus E, Chen, Yize, Siddiqi, Uzma, and Zhang, Baosen. "Non-wire alternatives: An additional value stream for distributed energy resources". In: *IEEE Transactions on Sustainable Energy* 11.3 (2019), pages 1287–1299.

[34] García-Santacruz, Carlos, Marano-Marcolini, Alejandro, and Martínez-Ramos, José Luis. "Optimal Location of Distributed Energy Resources Considering Investment Costs, Use of Resources and Network Constraints". In: *IEEE Access* 9 (2021), pages 163379–163390.

[35] Farivar, Masoud and Low, Steven H. "Branch flow model: Relaxations and convexification—Part I". In: *IEEE Transactions on Power Systems* 28.3 (2013), pages 2554–2564.

[36] Moradijoz, Mahnaz, Moghaddam, Mohsen Parsa, and Haghifam, Mahmoud-Reza. "A flexible distribution system expansion planning model: a dynamic bilevel approach". In: *IEEE Transactions on Smart Grid* 9.6 (2017), pages 5867–5877.

[37] Mozaffari, Mohammad, Abyaneh, Hossein Askarian, Jooshaki, Mohammad, and Moeini-Aghtaie, Moein. "Joint expansion planning studies of EV parking lots placement and distribution network". In: *IEEE Transactions on Industrial Informatics* 16.10 (2020), pages 6455–6465.

[38] Munoz-Delgado, Gregorio, Contreras, Javier, and Arroyo, José M. "Distribution system expansion planning considering non-utility-owned DG and an independent distribution system operator". In: *IEEE Transactions on Power Systems* 34.4 (2019), pages 2588–2597.

[39] Kabirifar, Milad, Fotuhi-Firuzabad, Mahmud, Moeini-Aghtaie, Moein, Pourghaderi, Niloofar, and Dehghanian, Payman. "A bi-level framework for expansion planning in active power distribution networks". In: *IEEE Transactions on Power Systems* 37.4 (2021), pages 2639–2654.

[40] Weron, Rafał. "Electricity price forecasting: A review of the state-of-the-art with a look into the future". In: *International journal of forecasting* 30.4 (2014), pages 1030–1081.

[41] Cartea, Alvaro and Figueroa, Marcelo G. "Pricing in electricity markets: a mean reverting jump diffusion model with seasonality". In: *Applied Mathematical Finance* 12.4 (2005), pages 313–335.

[42] Weron, Rafał, Bierbrauer, Michael, and Trück, Stefan. "Modeling electricity prices: jump diffusion and regime switching". In: *Physica A: Statistical Mechanics and its Applications* 336.1-2 (2004), pages 39–48.

[43] Geman, Hélyette and Roncoroni, Andrea. "Understanding the fine structure of electricity prices". In: *The Journal of Business* 79.3 (2006), pages 1225–1261.

[44] Benth, Fred Espen, Kiesel, Rüdiger, and Nazarova, Anna. "A critical empirical study of three electricity spot price models". In: *Energy Economics* 34.5 (2012), pages 1589–1616.

[45] Hayfavi, Azize and Talasli, Irem. "Stochastic multifactor modeling of spot electricity prices". In: *Journal of Computational and Applied Mathematics* 259 (2014), pages 434–442.

[46] Weron, Rafał. "Market price of risk implied by Asian-style electricity options and futures". In: *Energy Economics* 30.3 (2008), pages 1098–1115.

[47] Borovkova, Svetlana and Schmeck, Maren Diane. "Electricity price modeling with stochastic time change". In: *Energy Economics* 63 (2017), pages 51–65.

[48] Villaplana, Pablo. "Pricing power derivatives: A two-factor jump-diffusion approach". In: *Available at SSRN 493943* (2003).

[49] Kang, Yanfei, Hyndman, Rob J, and Li, Feng. "GRATIS: GeneRAting TIme Series with diverse and controllable characteristics". In: *Statistical Analysis and Data Mining: The ASA Data Science Journal* 13.4 (2020), pages 354–376.

[50] Smith-Miles, Kate and Bowly, Simon. "Generating new test instances by evolving in instance space". In: *Computers & Operations Research* 63 (2015), pages 102–113.

[51] Glover, Fred. "Improved linear integer programming formulations of nonlinear integer problems". In: *Management Science* 22.4 (1975), pages 455–460.

[52] Kleinert, Thomas, Labbé, Martine, Plein, Frank, and Schmidt, Martin. "There's no free lunch: on the hardness of choosing a correct big-M in bilevel optimization". In: *Operations research* 68.6 (2020), pages 1716–1721.

[53] Fortuny-Amat, José and McCarl, Bruce. "A representation and economic interpretation of a two-level programming problem". In: *Journal of the operational Research Society* 32.9 (1981), pages 783–792.

[54] Pineda, Salvador and Morales, Juan Miguel. "Solving linear bilevel problems using big-Ms: not all that glitters is gold". In: *IEEE Transactions on Power Systems* 34.3 (2019), pages 2469–2471.

[55] *ERCOT Real-Time Market Information.* URL: https://www.ercot.com/mktinfo/rtm.

[56] Deru et al. *U.S. Department of Energy Commercial Reference Building Models of the National Building Stock*. Technical report TP-5500-46861. National Renewable Energy Laboratory, 2011.

[57] Baran, Mesut and Wu, Felix F. "Optimal sizing of capacitors placed on a radial distribution system". In: *IEEE Transactions on power Delivery* 4.1 (1989), pages 735–743.

[58] National Renewable Energy Laboratory. *PVWatts Calculator*. 2020. URL: `https://developer.nrel.gov/docs/solar/pvwatts/`.

[59] *Github repository that extends BilevelJuMP.jl to automatically linearize the bilinear products in this paper*. URL: `https://github.com/NLaws/BilevelJuMP.jl/tree/bilinear`.

[60] *Github repository with code for the examples shown in the paper*. URL: `github.com/nlaws/coder_examples`.

[61] Brinkman, Gregory, Bain, Dominique, Buster, Grant, Draxl, Caroline, Das, Paritosh, Ho, Jonathan, Ibanez, Eduardo, Jones, Ryan, Koebrich, Sam, Murphy, Sinnott, et al. *The North American Renewable Integration Study (NARIS): A Canadian Perspective*. Technical report. National Renewable Energy Lab.(NREL), Golden, CO (United States), 2021.

[62] Dunning, Iain, Huchette, Joey, and Lubin, Miles. "JuMP: A modeling language for mathematical optimization". In: *SIAM review* 59.2 (2017), pages 295–320.

[63] Pimm, Andrew J, Cockerill, Tim T, and Taylor, Peter G. "Time-of-use and time-of-export tariffs for home batteries: Effects on low voltage distribution networks". In: *Journal of Energy Storage* 18 (2018), pages 447–458.

[64] Dempe, Stephan and Zemkoho, Alain. "Bilevel optimization". In: *Springer optimization and its applications. Vol. 161*. Springer, 2020.

[65] Jeynes, Paul H. "Present worth, or the time cost of money, as a factor in the economic comparison of alternative facilities". In: *Transactions of the American Institute of Electrical Engineers* 70.2 (1951), pages 1956–1962.

[66] Dempe, Stephan. *Foundations of bilevel programming*. Springer Science & Business Media, 2002.

[67] Beale, EML and Forrest, John JH. "Global optimization using special ordered sets". In: *Mathematical Programming* 10 (1976), pages 52–69.

[68] Decker, Christopher. "Utility and regulatory decision-making under conditions of uncertainty: Balancing resilience and affordability". In: *Utilities Policy* 51 (2018), pages 51–60.

[69] Sahinidis, Nikolaos V. "Optimization under uncertainty: state-of-the-art and opportunities". In: *Computers & chemical engineering* 28.6-7 (2004), pages 971–983.

[70] Stein, Seth and Stein, Jerome L. "Shallow versus deep uncertainties in natural hazard assessments". In: *Eos, Transactions American Geophysical Union* 94.14 (2013), pages 133–134.

[71] Marchau, Vincent AWJ, Walker, Warren E, Bloemen, Pieter JTM, and Popper, Steven W. *Decision making under deep uncertainty: from theory to practice.* Springer Nature, 2019.

[72] Kalra, Nidhi, Hallegatte, Stephane, Lempert, Robert, Brown, Casey, Fozzard, Adrian, Gill, Stuart, and Shah, Ankur. "Agreeing on robust decisions: new processes for decision making under deep uncertainty". In: *World Bank Policy Research Working Paper* 6906 (2014).

[73] Haasnoot, Marjolijn, Kwakkel, Jan H, Walker, Warren E, and Ter Maat, Judith. "Dynamic adaptive policy pathways: A method for crafting robust decisions for a deeply uncertain world". In: *Global environmental change* 23.2 (2013), pages 485–498.

[74] Horowitz, Kelsey. *2019 Distribution System Upgrade Unit Cost Database Current Version.* Technical report. National Renewable Energy Laboratory-Data (NREL-DATA), Golden, CO (United . . ., 2019.

[75] Schimpe, Michael, Kuepach, Markus Edler von, Naumann, Maik, Hesse, Holger C, Smith, Kandler, and Jossen, Andreas. "Comprehensive modeling of temperature-dependent degradation mechanisms in lithium iron phosphate batteries". In: *Journal of The Electrochemical Society* 165.2 (2018), A181.

[76] Gasper, Paul, Collath, Nils, Hesse, Holger C, Jossen, Andreas, and Smith, Kandler. "Machine-Learning Assisted Identification of Accurate Battery Lifetime Models with Uncertainty". In: *Journal of The Electrochemical Society* 169.8 (2022), page 080518.

[77] Gasper, Paul, Laws, Nick, Rathod, Bhavesh, Olis, Dan, Smith, Kandler, and Thakkar, Foram. "Optimization of energy storage system economics and controls by incorporating battery degradation costs in REopt". In: volume Boston May 18th – June 2nd. Electrochemical Society Conference. 2023. URL: https://ecs.confex.com/ecs/243/meetingapp.cgi/Paper/170697.

[78] National Renewable Energy Laboratory. *Renewable Energy Integration and Optimization.* The details of the degradation model are documented in the REopt Julia package at nrel.github.io/REopt.jl/dev/reopt/inputs/#REopt.Degradation. URL: reopt.nrel.gov.

[79] Arnold, Daniel B, Sankur, Michael, Dobbe, Roel, Brady, Kyle, Callaway, Duncan S, and Von Meier, Alexandra. "Optimal dispatch of reactive power for voltage regulation and balancing in unbalanced distribution systems". In: *2016 IEEE Power and Energy Society General Meeting (PESGM).* IEEE. 2016, pages 1–5.

[80] Laws, Nicholas D. *LinDistFlow, Julia Package.* URL: https://www.github.com/nlaws/LinDistflow.

[81] Nalley, Stephen and LaRose, Angelina. "Annual energy outlook 2022 (AEO2022)". In: *Energy Information Agency* (2022), page 23.

[82] Federal Energy Regulatory Commission. "Electric Storage Participation in Markets Operated by Regional Transmission Organizations and Independent System Operators". In: *Federal Register* 61.127 (Feb. 2018). URL: https://ferc.gov/sites/default/files/2020-06/Order-841.pdf.

[83] Donohoo-Vallett, Paul. *Revolution... now the future arrives for five clean energy technologies–2016 update*. Technical report. DOE, EERE, 2016.

[84] Bloomberg, New Energy Finance. "New energy outlook 2019". In: *Bloomberg New Energy Finance: New York, NY, USA* (2019).

[85] Milligan, Michael, Frew, Bethany A, Bloom, Aaron, Ela, Erik, Botterud, Audun, Townsend, Aaron, and Levin, Todd. "Wholesale electricity market design with increasing levels of renewable generation: Revenue sufficiency and long-term reliability". In: *The Electricity Journal* 29.2 (2016), pages 26–38.

[86] Auffhammer, Maximilian, Baylis, Patrick, and Hausman, Catherine H. "Climate change is projected to have severe impacts on the frequency and intensity of peak electricity demand across the United States". In: *Proceedings of the National Academy of Sciences* 114.8 (2017), pages 1886–1891.

[87] Seel, Joachim, Mills, Andrew D, and Wiser, Ryan H. "Impacts of high variable renewable energy futures on wholesale electricity prices, and on electric-sector decision making". In: *Lawrence Berkeley National Laboratory. Report LBNL-2001163* (2018). URL: https://escholarship.org/uc/item/2xq5d6c9.

[88] Prabavathi, M and Gnanadass, R. "Energy bidding strategies for restructured electricity market". In: *International Journal of Electrical Power & Energy Systems* 64 (2015), pages 956–966.

[89] Weron, Rafał. "Heavy-tails and regime-switching in electricity prices". In: *Mathematical Methods of Operations Research* 69.3 (2009), pages 457–473.

[90] Dickey, David A and Fuller, Wayne A. "Distribution of the estimators for autoregressive time series with a unit root". In: *Journal of the American statistical association* 74.366a (1979), pages 427–431.

[91] ERCOT. *Historical DAM Load Zone and Hub Prices*. URL: http://www.ercot.com/mktinfo/prices.

[92] Lucia, Julio J and Schwartz, Eduardo S. "Electricity prices and power derivatives: Evidence from the nordic power exchange". In: *Review of derivatives research* 5.1 (2002), pages 5–50.

[93] Smith, T. G. *pmdarima: ARIMA estimators for Python*. URL: http://www.alkaline-ml.com/pmdarima (visited on 2017).

[94] Johnson, Don H. "Point process models of single-neuron discharges". In: *Journal of computational neuroscience* 3.4 (1996), pages 275–299.

[95] Daley, Daryl J and Vere-Jones, David. *An introduction to the theory of point processes: volume I: elementary theory and methods*. Springer, 2003.

[96] Krishnamurthy, Dheepak, Uckun, Canan, Zhou, Zhi, Thimmapuram, Prakash R, and Botterud, Audun. "Energy storage arbitrage under day-ahead and real-

time price uncertainty". In: *IEEE Transactions on Power Systems* 33.1 (2017), pages 84–93.

[97] Shapiro, Alexander, Dentcheva, Darinka, and Ruszczyński, Andrzej. *Lectures on stochastic programming: modeling and theory*. SIAM, 2014.

[98] Hartigan, John A and Wong, Manchek A. "Algorithm AS 136: A k-means clustering algorithm". In: *Journal of the royal statistical society. series c (applied statistics)* 28.1 (1979), pages 100–108.

[106] *ERCOT Real Time Market*. 2021. URL: https://www.ercot.com/mktinfo/rtm.